

ROLE OF CENTRAL CANNABINOID RECEPTOR GPR18 IN CARDIOVASCULAR REGULATION

By

Anusha Penumarti

April 2014

Director of Dissertation: Dr. Abdel A. Abdel Rahman

Department of Pharmacology and Toxicology, Brody School of Medicine, East Carolina
University

The primary goal of this study was to characterize the role of GPR18 in the rostral ventrolateral medulla (RVLM) in blood pressure (BP) regulation and elucidate the mechanisms involved in central GPR18 mediated hypotensive response. The central hypothesis of this study was “central GPR18 signaling exerts a tonic sympathoinhibitory effect”. The data provide the first evidence for expression of GPR18 in the RVLM, the cardiovascular regulatory nuclei of the brainstem and its co-localization in tyrosine hydroxylase (TH)-expressing neurons as well as in RVLM neurons expressing cannabinoid₁ receptors (CB₁R). Also intra-RVLM activation of GPR18 receptors with abnormal cannabidiol (Abn CBD) produced a dose-dependent reduction in BP in conscious male Sprague Dawley rats whereas blockade of those receptors with 1, 3-dimethoxy-5-methyl-2-[(1*R*, 6*R*)-3-methyl-6-(1-methylethenyl)-2-cyclohexen-1-yl] benzene (O-1918) increased BP and abrogated the Abn CBD-evoked reduction in BP. Additional studies tested the hypothesis that the negligible hypotensive effect caused by the endogenous GPR18 ligand n-arachidonoyl glycine

(NAGly) could be due to concurrent activation of CB₁R in the RVLM. Our findings supported this hypothesis because NAGly-evoked hypotension was doubled following RVLM CB₁R blockade (SR141716). Ex-vivo studies revealed that intra-RVLM GPR18 activation (Abn CBD; 0.4 μg) enhanced RVLM Akt, ERK1/2 and nNOS phosphorylation and increased adiponectin (ADN) levels, during the hypotensive response. In contrast, prior GPR18 receptor blockade (O-1918) produced the opposite effects, and abrogated Abn CBD-evoked responses in conscious Sprague Dawley rats. Inhibition of RVLM PI3K/Akt (wortmannin), ERK1/2 (PD98059) or nNOS (N^ω-propyl-L-arginine, NPLA) or activation of adenylyl cyclase (forskolin) virtually abolished the intra-RVLM Abn CBD-evoked hypotension. Further, wortmannin, PD98059, NPLA or forskolin abrogated the GPR18-mediated increases in RVLM Akt, ERK1/2, nNOS phosphorylation and ADN levels, along with increased ROS generation. Our in-vitro studies show that GPR18 is co-expressed with CB₁R in nPC12 cells. Our in-vitro studies are in line with our in-vivo findings in normotensive rats indicating that GPR18 signals through the PI3K/Akt-ERK1/2-nNOS/ADN pathway. Additionally, our confocal imaging findings show that GPR18 is associated with lipid rafts (LRs). Furthermore, activation of GPR18 (Abn CBD/ NAGly) displaces it from the LRs and this response was abrogated by prior GPR18 blockade (O-1918). Furthermore, cholesterol depletion by methyl-β-cyclodextrin (MβCD) enhanced GPR18 signaling and uncovered O-1918 blockade in nPC12 cells. Collectively, these studies provide insight into identifying the potential signaling pathway(s) triggered by central GPR18 activation in conscious animals and the potential role of lipid rafts in modulating GPR18 signaling in-vitro.

**ROLE OF CENTRAL CANNABINOID RECEPTOR GPR18 IN CARDIOVASCULAR
REGULATION**

A Dissertation

Presented To

The Faculty of the Department of Pharmacology and Toxicology

The Brody School of Medicine at East Carolina University

In Partial Fulfillment

of the Requirements for the Degree

Doctor of Philosophy in Pharmacology and Toxicology

By

Anusha Penumarti

April 2014

© Anusha Penumarti, 2014

**ROLE OF CENTRAL CANNABINOID RECEPTOR GPR18 IN CARDIOVASCULAR
REGULATION**

By

Anusha Penumarti

APPROVED BY:

DIRECTOR OF

DISSERTATION: _____

Abdel A. Abdel-Rahman, PhD

COMMITTEE MEMBER AND CHAIR OF THE DEPARTMENT

OF PHARMACOLOGY & TOXICOLOGY: _____

David Taylor, PhD

COMMITTEE MEMBER: _____

Rukiyah Van Dross-Anderson, PhD

COMMITTEE MEMBER: _____

Ethan J. Anderson, PhD

COMMITTEE MEMBER: _____

Saame Raza Shaikh, PhD

DEAN OF THE

GRADUATE SCHOOL: _____

Paul J. Gemperline, PhD

This work is dedicated to my parents, Penumarti Venugopal and Penumarti Radha. Your immeasurable love, encouragement and constant support are the keys to my success.

ACKNOWLEDGEMENTS

When I look back on the journey that I have taken, I am completely humbled by the number of incredible people who played a vital role in helping me realize my dream of becoming a scientist. I would like to express my heartfelt thanks to some of the extraordinary people who were instrumental in shaping my graduate career into a fun and exciting journey.

First, I would like to express my gratitude to my dissertation advisor Dr. Abdel A. Abdel Rahman whom I had the immense honor and privilege to work with. Thank you Dr. Rahman for your trust in me and for unhesitatingly giving your precious time and invaluable advice. Your ability to quickly resolve research related problems and your knowledge of the current literature in the field has been inspirational. Working with you has greatly improved my ability to design experiments, interpret results, greatly improved my writing skills and helped me gain experience in the peer review system. Thank you for your constant encouragement, challenge, and confidence in my abilities that helped me to succeed during my Ph.D. training.

I would also like to thank the members of my committee: Dr. Rukiyah Van Dross, Dr. Saame Raza Shaikh, Dr. Ethan Anderson, and Dr. David Taylor. Thank you for always having an open door policy. Your valuable suggestions and input into this research project are much appreciated. Special thanks to Dr. Shaikh and his lab members for their help with confocal microscopy.

I would also like to thank all the current and former fellow lab members for their support, help, and encouragement. Special thanks to Mrs. Kui Sun who has been a wonderful lab

manager, technical guide and personal advisor. I would also like to thank Dr. Ming Fan, Jeannie Register, Dr. Badr Ibrahim and Dr. Marie McGee for their guidance and willingness to help in any way possible.

Thanks to my fellow graduate students and the faculty and staff in the department of Pharmacology and Toxicology for their recommendations and use of laboratory equipment. I would like to thank Kathleen and Mrs. Jackie for their help with cell culture and technical advice. Special thanks to Pam and Jackie for their administrative help. I would like to thank Dr. Douglas Weidner for teaching me how to acquire confocal images.

Last but not the least I want to thank my parents and my dearest friends: Amber, Taylor, Pranita, Praveen and Prudhvi who are like family and continue to support and inspire me. Your presence in my life is dearly cherished. Special thanks to Dr. Katwa's family who have embraced me like their daughter. Your love and guidance made my stay in the United States a pleasure. I feel very fortunate for having all of you in my life.

TABLE OF CONTENTS

LIST OF TABLES	i
LIST OF FIGURES	ii
LIST OF SYMBOLS OR ABBREVIATIONS	v
CHAPTER ONE-GENERAL INTRODUCTION	1
1.1. Evidence for the presence of Non CB ₁ /Non CB ₂ receptors	1
1.2. G-Protein Coupled Receptor 18	2
1.2.1. Expression and Distribution of GPR18.....	2
1.2.2. GPR18 ligands	3
1.2.3. Signal transduction following GPR18 activation	3
1.3. Oxidative Stress and Central Regulation of Cardiovascular Function.....	7
1.3.1. Rostral Ventrolateral Medulla (RVLM) in central cardiovascular regulation.....	7
1.3.2. Impact of Reactive Oxygen Species in the RVLM.....	8
1.4. Lipid Rafts.....	9
1.4.1. Lipid Rafts and GPCRs.....	9
1.4.2. Lipid Rafts and the Endocannabinoid System	9
1.5. Therapeutic Potentials of GPR18.....	11
1.6. Aims of Study.....	12
CHAPTER TWO- MATERIALS AND METHODS	18
2.1. Preparation of the Rats	18
2.1.1. Blood pressure (BP) and heart rate (HR) measurements.	19
2.2. Cell Culture	19
2.3. Immunohistochemistry.....	19

2.4.	Immunofluorescence	20
2.5.	Western Blot Analysis.....	22
2.6.	Dot Blotting.....	24
2.7.	Quantification of Reactive Oxygen Species.....	25
2.7.1.	Dihydroethidium (DHE) Staining for ROS Detection.....	25
2.7.2.	Measurement of Reactive Oxygen Species by DCFH-DA.....	26
2.8.	Measurement of Nitrate/Nitrite Level	26
2.9.	Measurement of cAMP	27
2.10.	Quantification of Catalase Activity	27
2.11.	Quantification of NADPH oxidase Activity.....	28
2.12.	Quantification of Aldehyde Dehydrogenase (ALDH) Activity	28
2.13.	Lipid Raft Labeling	29
CHAPTER THREE - THE NOVEL ENDOCANNABINOID RECEPTOR GPR18 IS EXPRESSED IN THE ROSTRAL VENTROLATERAL MEDULLA AND EXERTS A TONIC RESTRAINING INFLUENCE ON BLOOD PRESSURE		30
3.1.	Abstract	30
3.2.	Introduction	31
3.3.	Materials and Methods.....	34
3.3.1.	Preparation of the Rats.....	34
3.3.2.	Western Blot and Neurochemical Studies	34
3.3.3.	Immunohistochemistry.	35
3.3.4.	Immunofluorescence.....	35
3.3.5.	Measurement of Nitrate/Nitrite.....	35
3.3.6.	Dihydroethidium (DHE) Staining for ROS Detection.....	35
3.3.7.	Measurement of Reactive Oxygen Species by DCFH-DA.....	36

3.4.	Experimental Groups and Protocol	37
3.4.1	Experiment 1: Anatomical expression of GPR18 in the RVLM	37
3.4.2.	Experiment 2: Functional role of RVLM GPR18 in BP and HR regulation	37
3.4.3.	Experiment 3: Effect of O-1918 on the BP and neurochemical responses elicited by intra-RVLM Abn CBD.....	38
3.4.4.	Experiment 4: Effect of microinjecting ADN into the RVLM on BP, NO and ROS levels.....	39
3.4.5.	Experiment 5: Effect of RVLM CB1R blockade on the cardiovascular effects of NAGly... ..	39
3.4.6.	Drugs.....	40
3.5.	Data Analysis and Statistics.....	40
3.6.	Results	41
3.6.1.	Expression of GPR18 in tyrosine hydroxylase immunoreactive neurons in the RVLM.....	41
3.6.2.	Activation of RVLM GPR18 causes a hypotensive response.	41
3.6.3.	Intra-RVLM ADN reduces BP and lowers ROS and elevates NO levels in RVLM	42
3.6.4.	RVLM CB1R blockade unmasks NAGly-evoked hypotension.	42
3.6.5.	O-1918 abrogated Abn CBD evoked hypotension and neurochemical responses .	43
3.6.6.	GPR18 activation reduces ROS generation in the RVLM.....	43
3.7.	Discussion	72
CHAPTER FOUR - MOLECULAR MECHANISMS UNDERLYING ROSTRAL VENTROLATERAL MEDULLA GPR18-MEDIATED HYPOTENSION IN CONSCIOUS NORMOTENSIVE RATS.....		78
4.1.	Abstract	78
4.2.	Introduction	79
4.3.	Materials and Methods.....	81

4.3.1.	Intravascular Catheterization and Intra-RVLM Cannulations	81
4.3.2.	Western Blotting	82
4.3.3.	Dot Blotting	83
4.3.4.	Measurement of Reactive Oxygen Species by DCFH-DA.....	84
4.4.	Experimental Groups and Protocols.....	84
4.4.1.	Experiment 1: Effect of RVLM GPR18 activation or blockade on ERK1/2, Akt and nNOS phosphorylation in conscious male SD rats.....	84
4.4.2.	Experiment 2: Effect of intra-RVLM inhibition of ERK1/2, PI3K/Akt or NOS inhibition on Abn CBD-mediated hypotensive response.	85
4.4.3.	Experiment 3: Effect of intra-RVLM activation of adenylyl cyclase on Abn CBD-mediated hypotensive response.	86
4.4.4.	Experiment 4: Effect of Akt-ERK1/2-nNOS inhibition or increased cAMP on GPR18-mediated molecular events in the RVLM.....	87
4.4.5.	Drugs.....	87
4.5.	Data Analysis and Statistics	87
4.6.	Results	88
4.6.1.	Intra-RVLM Abn CBD Increased RVLM ERK1/2, Akt and nNOS phosphorylation.	88
4.6.2.	Intra-RVLM PI3K/Akt, ERK1/2 or nNOS Inhibition Attenuated Abn CBD evoked Hypotensive Response.....	88
4.6.3.	Increased RVLM cAMP levels abrogate GPR18-mediated Hypotension.....	89
4.6.4.	Akt-ERK1/2-nNOS inhibition or Increased cAMP Abrogates GPR18-mediated molecular events in the RVLM.	89
4.7.	Discussion	109
CHAPTER FIVE - GPR18 SIGNALING AND ITS INTERACTION WITH LIPID RAFTS IN DIFFERENTIATED PC12 CELLS.....		114
5.1.	Abstract	114
5.2.	Introduction	115

5.3.	Materials and Methods	118
5.3.1.	Cell Culture and Treatment	118
5.3.2.	Immunofluorescence	119
5.3.3.	Western Blotting	119
5.3.4.	Measurement of ROS (DCFH-DA)	120
5.3.5.	Nitrate/Nitrite Assay	120
5.3.6.	Measurement of cAMP	121
5.3.7.	Quantification of Catalase Activity	121
5.3.8.	Quantification of NADPH oxidase Activity	121
5.3.9.	Quantification of ALDH Activity	122
5.3.10.	Lipid Raft Labeling	123
5.3.11.	Drugs	123
5.4.	Data Analysis and Statistics	124
5.5.	Results	124
5.5.1.	Co-expression of GPR18 with CB ₁ R in nPC12 cell	124
5.5.2.	GPR18 modulates Akt-ERK1/2-nNOS-ADN signaling and cAMP level in nPC12 cells	125
5.5.3.	GPR18 Activation Reduces ROS Generation in nPC12 cells	125
5.5.4.	Interaction of GPR18 with Lipid Rafts Following Ligand Binding in nPC12 cells	126
5.5.5.	Effect of M β CD on GPR18-dependent Signaling Pathways	126
5.6.	Discussion	146
CHAPTER SIX-GENERAL DISCUSSION AND SUMMARY		151
LIMITATIONS		158
FUTURE DIRECTIONS		162

LIST OF TABLES

Table 1.1. Ligands of GPR18.....	5
Table 3.1. MAP (mmHg) and HR (beats/min) values immediately before intra-RVLM administration of the GPR18 agonists or their vehicles.....	54
Table 4.1. MAP (mmHg) and HR (beats/min) values before pharmacological intervention.	92

LIST OF FIGURES

Figure 3.1. Timeline for surgical procedures and experimental protocols for experiment 3.2....	44
Figure 3.2. Timeline for surgical procedures and experimental protocols for experiment 3.2.	Error! Bookmark not defined.
Figure 3.3. Time line for surgical procedures and experimental protocols for experiment 3.3.	Error! Bookmark not defined.
Figure 3.4. Time line for surgical procedures and experimental protocols for experiment 3.4... 50	
Figure 3.5. Time line for surgical procedures and experimental protocols for experiment 3.5... 52	
Figure 3.6. Expression of GPR18 in the rat RVLM.....	56
Figure 3.7. Effect of intra-RVLM Abn CBD or O-1918 on MAP and HR in conscious male rats	58
Figure 3.8. Effect of GPR18 activation and blockade on ADN and NOx levels.....	60
Figure 3.9. Effect of intra-RVLM adiponectin on MAP and HR	62
Figure 3.10. Co-expression of GPR18 with CB ₁ R and time course changes in MAP and HR caused by NAGly in the presence of SR141716.....	64
Figure 3.11. Time course of changes in MAP and HR following intra-RVLM microinjection of Abn CBD or O-1918.....	66

Figure 3.12. Time course changes in MAP and HR caused by intra-RVLM Abn CBD or O-1918 using 1-min time intervals	68
Figure 3.13. Effect of GPR18 activation or blockade on RVLM ROS levels	70
Figure 4.1. Time line for surgical procedures and experimental protocols for cardiovascular measurements.....	91
Figure 4.2. Effect of GPR18 ligands on pERK1/2, pAkt and p-nNOS levels	95
Figure 4.3. Effect of intra-RVLM wortmannin on GPR18 mediated sympathoinhibition	97
Figure 4.4. Effect of intra-RVLM PD98059 on GPR18 mediated sympathoinhibition	98
Figure 4.5. Effect of intra-RVLM nNOS and eNOS inhibition on GPR18 mediated hypotension	101
Figure 4.6. Effect of intra-RVLM adenylyl cyclase activation on GPR18 mediated sympathoinhibition	103
Figure 4.7. Effects of forskolin, NPLA, PD98059 or wortmannin pretreatments on pERK1/2, pAkt, p-nNOS, ADN and ROS levels in the RVLM	105
Figure 4.8. Proposed GPR18 signaling in the RVLM	107
Figure 5.1. GPR18 expression in nPC12 cells.....	Error! Bookmark not defined.
Figure 5.2. Effect of the different ligands on GPR18 signaling in nPC12 cells	129

Figure 5.3. Effect of GPR18 activation or blockade on ROS levels in nPC12 cells	131
Figure 5.4. Effect of GPR18 activation or blockade on catalase and ALDH activity in nPC12 cells	133
Figure 5.5. Effect of GPR18 activation or blockade on NADPH oxidase activity in nPC12 cells	135
Figure 5.6. Effect of drug treatment on association of GPR18 with lipid rafts in nPC12 cells.	137
Figure 5.7. Effect of lipid raft disruption and drug treatment on association of GPR18 with lipid rafts in nPC12 cells	140
Figure 5.8. Effect of lipid raft disruption on GPR18 signaling in nPC12 cells	142
Figure 5.9. Schematic representation of the biochemical responses elicited by activating GPR18 in nPC12 cells	144
Figure 6.1. Schematic presentation of the major findings of the study and proposed future studies. See details in the text.	160

LIST OF SYMBOLS OR ABBREVIATIONS

Abn CBD: Abnormal cannabidiol; (Trans-4-[3-methyl-6-(1-methylethenyl) -2-cyclohexen-1-yl]-5- Pentyl-1, 3-benzenediol)

AC: Adenylyl cyclase

ACSF: Artificial cerebrospinal fluid

ADN: Adiponectin

AEA: *N*-arachidonylethanolamine

BP: Blood pressure

cAMP: Cyclic adenosine monophosphate

CBD: Cannabidiol

CB₁R: Cannabinoid receptor 1

CB₂R: Cannabinoid receptor 2

CNS: Central nervous system

DCFH-DA: 2', 7'-dichlorofluorescein diacetate

DHE: Dihydroethidium

DMSO: Dimethyl sulfoxide

eNOS: Endothelial nitric oxide synthase

GPCR: G-protein coupled receptor

GPR18: G-protein coupled receptor 18

HR: Heart rate

iNOS: Inducible nitric oxide synthase

i.p.: Intraperitoneal

ir: Immunoreactive

i.v.: Intravenous

L-NIO: N^5 -(1-Iminoethyl)-L-ornithine

LR: Lipid raft

MAP: Mean arterial pressure

MAPK: Mitogen activated protein kinase

M β CD: Methyl beta cyclodextrin

NAGly: N-Arachidonoyl glycine

nNOS: Neuronal nitric oxide synthase

NO: Nitric Oxide

Nox: NADPH oxidase

NPLA: N^0 -Propyl-L-arginine hydrochloride

O-1918: 1, 3-Dimethoxy-5-methyl-2-[(1R, 6R)-3-methyl-6-(1-methylethenyl)-2-

cyclohexen-1-yl] benzene

PD98059: 2'-Amino-3'-methoxyflavone

pERK: Phosphorylated extracellular signal-regulated kinase

RVLM: Rostral ventrolateral medulla

SR141716: Rimonabant

TH: Tyrosine hydroxylase

CHAPTER ONE-GENERAL INTRODUCTION

1.1. Evidence for the presence of Non CB₁/Non CB₂ receptors

Cannabinoids elicit complex cardiovascular responses involving both peripheral and central sites (Randall et al., 2002; Randall et al., 2004). Cannabinoids cause vasorelaxation in vitro (Mason and Matthews, 2012). In anesthetized animals, cannabinoids reduce blood pressure and heart rate (Varga et al., 1995), but produce a long lasting pressor response along with bradycardia in conscious rats (Stein et al., 1996). Hence, the cardiovascular effects of cannabinoids are complex, and depend on the animal model used, experimental conditions and whether the cannabinoids are synthetic or endogenous (Randall et al., 2004). In terms of cardiovascular effects produced by cannabinoids, many studies have shown the involvement of several novel receptors in mediating the cardiovascular effects of several synthetic and natural cannabinoids (Pratt et al., 1998; Jarai et al., 1999; Offertáler et al., 2003; Begg et al., 2005; Mackie and Stella, 2006). The synthetic cannabinoid abnormal cannabidiol (Abn CBD), which is inactive at CB₁/CB₂ receptors, causes significant hypotension that is blocked by 1, 3-dimethoxy-5-methyl-2-[(1*R*, 6*R*)-3-methyl-6-(1-methylethenyl)-2-cyclohexen-1-yl] benzene (O-1918) (Offertáler et al., 2003). Also Abn CBD elicits endothelial-dependent vasodilation even in CBD receptor (CB₁ and CB₂) knockout mice (Jarai et al., 1999). This new receptor has been termed the ‘Abn CBD’ receptor and has been implicated in the endothelial-dependent vasodilation, hemodynamic responses and in the modulation of microglial and endothelial cell migration (Jarai et al., 1999; Offertáler et al., 2003; Mo et al., 2004; McCollum et al., 2007; McHugh et al., 2012). One such putative cannabinoid receptor, which is thought to be the Abn CBD receptor, is GPR18 (McHugh et al., 2010). There are studies showing that Abn CBD and O-1918 also serve as ligands to GPR55 (Johns et al., 2007;

Godlewski et al., 2009). However, more recent studies have shown that although GPR18 and GPR55 share the same ligands, they do not respond to these ligands in the same manner or with the same efficacy and have confirmed GPR18 as the “Abn CBD” receptor (McHugh et al., 2010; Okuno and Yokomizo, 2011).

1.2. G-Protein Coupled Receptor 18

Cannabinoids are a group of heterogeneous compounds that are either natural (isolated from *Cannabis sativa* (marijuana)) or synthetic in origin. CB₁ and CB₂ receptors are two subtypes of G protein coupled receptors (GPCRs) that have been well characterized as the cannabinoid receptors. GPR18 is a GPCR, which is the site of action of several natural and synthetic cannabinoids and has been recognized as a putative cannabinoid receptor as discussed above.

1.2.1. Expression and Distribution of GPR18

GPR18 is localized to human chromosome 13q32 (Gantz et al., 1997). Northern blot analysis of human tissues showed that GPR18 transcripts are most abundant in the testis and spleen and moderately expressed in brain and lungs (Gantz et al., 1997). Examination of GPCR repertoires in human and mouse tissues using real-time PCR showed strong expression of GPR18 in hypothalamus, thyroid, peripheral blood leucocytes, cerebellum and brainstem (Vassilatis et al., 2003). On the other hand, the liver, kidney, heart and lungs seem to lack GPR18 mRNA (Gantz et al., 1997).

1.2.2. GPR18 ligands

Although GPR18 seems to share homology with the μ opioid receptor, it does not bind opiate ligands (Gantz et al., 1997). N-arachidonoyl glycine (NAGly), which is an endogenous lipid highly expressed in the mammalian nervous system, exhibits high affinity for GPR18 (Huang et al., 2001). NAGly is produced by both oxidative metabolism of the ethanolamine moiety of anandamide (AEA) and through the conjugation of glycine to arachidonic acid (AA) that is released during the AEA hydrolysis by fatty acid amyl hydrolase (FAAH) (Bradshaw et al., 2009). While Abn CBD, O-1602, Δ^9 -THC and AEA are reported as full agonists at GPR18, AM251 is a partial agonist, and O-1918 and cannabidiol (CBD) are antagonists of GPR18 (McHugh et al., 2010; McHugh et al., 2011; McHugh, 2012). Other typical cannabinoid ligands like WIN55212-2, CP55940, JWH-133 and JWH-105 have no effect at GPR18 (McHugh, 2012).

1.2.3. Signal transduction following GPR18 activation

As discussed below, several downstream signaling molecules are either activated or inhibited upon GPR18 activation. For example, cAMP synthesis is reduced via inhibition of adenylyl cyclase activity, stimulation of phosphorylation of ERK1/2 and Akt (Fig. 1.1).

1.2.3.1. Inhibition of adenylyl cyclase.

GPR18 is a *Gai/o* coupled receptor that has been demonstrated to be negatively coupled to adenylyl cyclase (Kohno et al., 2006). Studies on GPR18 in different model systems have shown that activation of GPR18 inhibits adenylyl cyclase activity, resulting in the reduction of cAMP

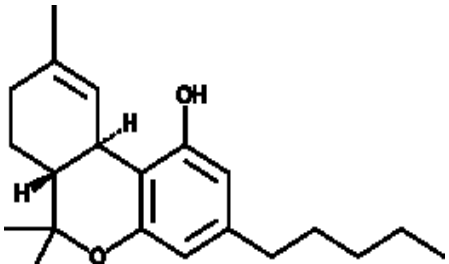
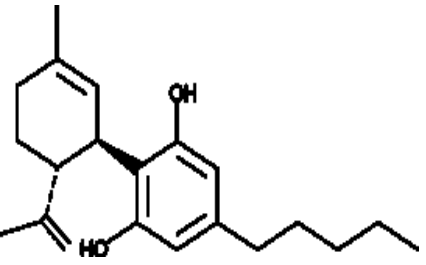
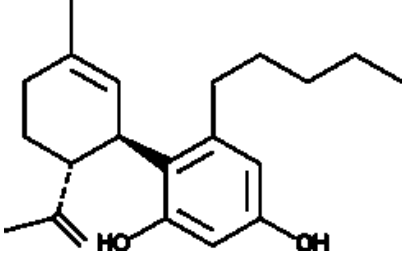
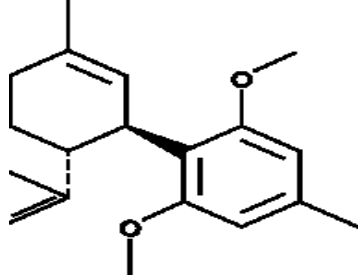
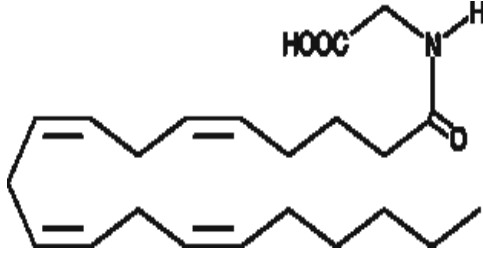
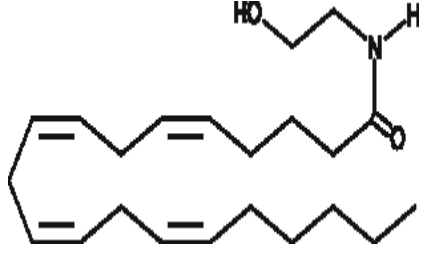
production in a pertussis toxin-sensitive manner (Kohno et al., 2006; McHugh et al., 2010; Carbone, 2012).

1.2.3.2. Modulation of ERK1/2 and PI3K/Akt signaling.

GPR18 signaling has been linked to activation of extracellular-signal regulated kinases1/2 (ERK1/2) in several model systems. Importantly, GPR18 activation by NAGly or Abn CBD in BV-2 microglial and HEK 293 cells potently drives cellular migration through, ERK1/2 phosphorylation, which was significantly inhibited by O-1918 (McHugh et al., 2010). Abn CBD induced phosphorylation of ERK1/2 and Akt in HUVEC cells is sensitive to pertussis toxin treatment (indicating the association with a G α i/o coupled receptor) and is antagonized by O-1918 (Offertáler et al., 2003). Also, NAGly, Abn CBD, AEA and THC activated GPR18 to cause cell migration in HEC-1B cells via phosphorylating ERK1/2 (McHugh et al., 2011). NAGly also causes apoptosis in mouse macrophage cell line through GPR18 by activating ERK1/2, p38 MAPK and JNK pathway (Carbone, 2012). Whether ERK1/2 and/or PI3K/Akt signaling pathways are involved in central GPR18-elicited sympathoinhibition has yet to be elucidated.

Table. 1.1. Ligands of GPR18

Representative structures of phyto-, synthetic, and endogenous cannabinoid compounds active at GPR18. The compounds NAGly, Abn CBD and O-1918 were used in these studies.

Phytocannabinoids	Δ^9 -tetra-hydrocannabinol (Δ^9 -THC) 	Cannabidiol (CBD) 
Synthetic cannabinoids	Abnormal cannabidiol (Abn CBD) 	O-1918 
Endogenous cannabinoids	N-Arachidonoylglycine (NAGly) 	Anandamide (AEA) 

1.3. Oxidative Stress and Central Regulation of Cardiovascular Function

Recent studies strongly suggest that increased reactive oxygen species (ROS) generation in the brainstem contributes to the neural mechanism underlying the development of hypertension in hypertensive rats (Pilowsky and Goodchild, 2002; Kishi et al., 2004; Yoshitaka, 2008). The RVLM is the major neural pool that determines basal sympathetic activity and is essential for the maintenance of basal vasomotor tone (Dampney, 1994; Sved et al., 2003; Kishi et al., 2004; Guyenet, 2006; Ribeiro de Campos and Bergamaschi, 2006).

1.3.1. Rostral Ventrolateral Medulla (RVLM) in central cardiovascular regulation

Several brainstem nuclei are implicated in the central regulation of cardiovascular functions including blood pressure (BP). In this study, attention has been focused on the rostral ventrolateral medulla (RVLM), which plays a pivotal role in central control of sympathetic outflow and cardiovascular function (Kishi et al., 2001; Institute for Laboratory Animal Research, 2011; Worlein et al., 2011). The RVLM is located in the ventral part of the brainstem, lateral to the inferior olive, caudal to the facial nucleus, and ventral to the nucleus ambiguus (Farlow et al., 1984; Dampney et al., 1987). It controls BP by integrating a variety of signals originating in other regions of the brain like the periaqueductal gray, the paraventricular nucleus and/or the lateral hypothalamus (Guyenet et al., 1989; Kishi et al., 2001). The RVLM contains both adrenergic and noradrenergic groups of neurons (Hokfelt T. et al., 1984) in addition to neurons containing several other neurotransmitters (Pilowsky et al., 1986), and receptors like Angiotensin II AT₁ receptors (Potts et al., 2000), mu-opioid receptors (Aicher et al., 2001; Drake et al., 2005), imidazoline I₁ receptors (Zhang and Abdel-Rahman, 2002; Zhang and Abdel-

Rahman, 2005), α_{2A} adrenergic receptors (El-Mas and Abdel-Rahman, 2004; Li et al., 2005), adenosine receptors (A_{2A}) (Nassar and Abdel-Rahman, 2008), cannabinoid CB_1 receptors (Herkenham et al., 1991; Padley et al., 2003) and CB_2 receptors (Van Sickle et al., 2005). Evidence has implicated the RVLM C1 neurons in the modulation of sympathetic activity and regulation of BP (Dampney, 1994; Sved et al., 2003; Guyenet, 2006). Other physiological processes like breathing and nociception are also regulated by the RVLM (Nattie and Li, 1990; Javanmardi et al., 2005; Karlsson et al., 2006).

1.3.2. Impact of Reactive Oxygen Species in the RVLM

Oxidative stress in the RVLM has been shown to be one of the major contributing factors for the high BP in hypertensive rats (Pilowsky and Goodchild, 2002; Kishi et al., 2004). ROS levels are higher (Fridovich, 1978; Yoshitaka, 2008) and superoxide dismutase (a ROS scavenging enzyme) expression and activity are lower (Chan et al., 2006; Yoshitaka, 2008) in the RVLM of SHR rats when compared with that of WKY rats. Further, NADPH Oxidase is a major source of ROS production in CNS (Griendling et al., 2000; Bedard and Krause, 2007; Akki et al., 2009; Frey et al., 2009). It has also been demonstrated that expression of inducible nitric oxide synthase (iNOS) in the NTS and RVLM decreases blood pressure and heart rate by inhibiting sympathetic nervous system activity (Kimura et al., 2009) and may be linked to reduced ROS generation. However, the rapid (10-15 min) onset of the GPR18-mediated hypotension in the preliminary study precludes a major role for iNOS in the hypotensive response. Therefore, the present study dealt with the role of constitutive NOS isoforms, particularly nNOS and eNOS in GPR18 signaling.

1.4. Lipid Rafts

The plasma membrane is a phospholipid bilayer that is highly organized and is composed of microdomains called Lipid Rafts (LRs) (Herkenham et al., 1991). These lateral platforms enriched in cholesterol, sphingolipids are resistant to solubilization with non-ionic detergents (Herkenham et al., 1991; Pike, 2003). Caveolae are funnel shaped invaginations of membrane proteins called caveolins and are a subtype of lipid raft (Fielding and Fielding, 1997; Czarny et al., 1999). These LR microdomains participate in a number of cellular functions including cell signaling, cell trafficking and membrane transport (Moffett et al., 2000; Gaus et al., 2003; Wilson et al., 2004) and play a very important role in health and disease (Jin et al., 2011).

1.4.1. Lipid Rafts and GPCRs

Lipid rafts/caveolae are the microdomain regions of localization of several physiologically important GPCRs (Becher et al., 2004; Chini and Parenti, 2004; Insel et al., 2005) and it is well known that the activity of several GPCRs is modulated by lipid rafts (Dainese et al., 2007). Many studies indicate that LRs and caveolae participate in the regulation of GPCR signaling by affecting both signaling selectivity and coupling efficacy (Chini and Parenti, 2004).

1.4.2. Lipid Rafts and the Endocannabinoid System

There is growing evidence suggesting that the endocannabinoid uptake and signaling through the cannabinoid receptors are highly dependent on the composition and integrity of lipid rafts (Biswas et al., 2003; Bari et al., 2005b; Bari et al., 2006; Rimmerman et al., 2008b). Recent studies suggest that anandamide (a precursor of NAGly) and its metabolites accumulate into lipid

rafts and these microdomains play important role in the cellular processing and regulation of AEA (Sarker and Maruyama, 2003; McFarland et al., 2004; Bari et al., 2005a). NAGly is synthesized from AEA and serves as endogenous GPR18 ligand (Huang et al., 2001). Additionally, AEA is a common endocannabinoid for both GPR18 and CB₁R (Bradshaw et al., 2009). There is also evidence that CB₁R binding/signaling, as well as anandamide (AEA) transport is controlled by LRs and caveolin-1 (Dainese et al., 2007; Bari et al., 2008). CB₁R signaling through AC and MAPK is reduced by half following disruption of LRs indicating the importance of the integrity of LRs in CB₁R signaling (Bari et al., 2005b; Bari et al., 2006). Interestingly, in the case of CB₁R, agonist-induced endocytosis is dependent on LRs/caveolae and it is this process that counteracts desensitization of the receptor by facilitating its recycling and reactivation (Wu et al., 2008). In contrast, raft disruption does not influence CB₂R signaling or binding (Bari et al., 2005a; Sarnataro et al., 2005; Bari et al., 2006). One recent publication on the interaction of GPR55 (a putative cannabinoid receptor) with lipid rafts showed that activation of GPR55 leads to localization of the receptor in the LRs and that this association is essential for proper GPR55 signaling (Li et al., 2005). Taken together these findings suggest the important role for LRs in modulating the endocannabinoid system and that the cannabinoid receptor subtypes are differentially modulated by LRs.

1.5. Therapeutic Potentials of GPR18

The endocannabinoid system with its several endogenous and exogenous modulators plays a very important role in impacting human health and disease. Its therapeutic potential seems to encompass mental illness, pain management, cardiovascular disorders, metabolic disorders, obesity, osteoporosis, and liver disease and nicotine addiction. Abn CBD (a GPR18 agonist) was shown to produce peripheral vasodilation independent of both CB₁R and CB₂R involvement (Offertáler et al., 2003). Also the fact that GPR18 does not modulate the psychoactive effects of marijuana makes it a promising therapeutic target (Caldwell et al., 2013). An understanding of the physiology and pharmacology of GPR18 and its association with the well characterized cannabinoid receptors and ligands is vital to assess and manipulate the cannabinoid signaling system for the development of new therapeutics that will benefit human health.

1.6. Aims of Study

Previous studies have provided substantial evidence for the existence of novel cannabinoid (CBD) receptors influencing the cardiovascular system (Offertáler et al., 2003). One such group of GPCRs, which is considered as putative CBD receptors, is the GPR18 (Kohno et al., 2006). No studies have examined the expression and function of centrally located GPR18 within central cardiovascular regulating nuclei and whether GPR18 is associated with lipid rafts in those areas. Also several studies have shown that reactive oxygen species (ROS) are produced endogenously in response to several stimuli and that excess amounts of ROS contributes to various pathologies like hypertension (Pilowsky and Goodchild, 2002; Kishi et al., 2004; Yoshitaka, 2008). Recently, it has been shown that GPR18 ligands possess antioxidant properties (Rimmerman et al., 2008a; Carroll et al., 2012). Therefore, the present studies tested the central hypothesis that **activation of GPR18 by its lipid ligands in the rostral ventrolateral medulla (RVLM) of the brainstem elicits sympathoinhibition and hypotension by circumventing oxidative stress**. Additionally, the current study tested the corollary hypothesis that **enhancement of ERK1/2-Akt-neuronal nitric oxide synthase signaling and inhibition of cAMP in the RVLM constitute the molecular mechanisms for the GPR18-mediated hypotension**. Finally, we complemented the in vivo findings with additional molecular studies by evaluating the **potential role of lipid rafts in GPR18 signaling in nPC12 cells**. The pharmacological, and subsequent ex vivo signal transduction and biochemical studies, were undertaken in conscious normotensive rats.

Specific Aim 1 experiments first examined the expression of GPR18 in the RVLM and its spatial distribution within tyrosine hydroxylase immunoreactive (TH-ir) (pre-sympathetic) neurons.

Second, the studies under this aim evaluated the function of RVLM GPR18 and subsequently tested the hypothesis that the Abn CBD-evoked hypotensive response involves activation of rat RVLM GPR18. Studies under this aim also evaluated the spatial and functional crosstalk between GPR18 and CB₁R in the RVLM.

Rationale: There are no reports on the presence of GPR18 protein in the brainstem and specifically in the cardiovascular regulating nuclei like the RVLM. Therefore, the first objective of the studies outlined under this aim was to determine whether GPR18 is expressed in the RVLM. The preliminary hemodynamic studies have shown that activation of RVLM GPR18 leads to hypotension, while its blockade led to a hypertensive response indicating that GPR18 influences sympathetic tone. Also, we hypothesized that the negligible hypotensive effect caused by the endogenous GPR18 ligand NAGly in our preliminary studies could be due to concurrent activation of CB₁R in the RVLM because the latter mediates sympathoexcitation (Ibrahim and Abdel-Rahman, 2011). Therefore the studies under this aim investigated the possible influence of CB₁R in GPR18-mediated hypotension following microinjection of NAGly. Experiments performed under this aim extended the preliminary protein expression and cardiovascular responses, discussed above, using highly selective lipid ligands and addressing the following questions:

1- Is GPR18 expressed within the RVLM and is it spatially localized within TH-ir neurons?

2- Does intra-RVLM administration of GPR18 ligands produce dose-dependent cardiovascular effects?

3- What are the cardiovascular effects caused by intra-RVLM GPR18 activation (Abn CBD) in the presence or absence of the GPR18 antagonist, O-1918?

4- Is GPR18 co-expressed with CB₁R in the RVLM?

5- Does prior blockade of RVLM CB₁R (SR141716a) enhance the hypotensive effect caused by the endogenous GPR18 agonist NAGly?

Specific Aim 2 studies tested the hypothesis that cAMP/Akt/ERK1/2/nNOS-dependent reduction in ROS generation in the RVLM underlies the GPR18 mediated sympathoinhibition and hypotension.

Rationale: Activation of the peripheral ‘Abn-CBD’ receptor leads to vasodilation and hypotension through a Gi/o coupled receptor (Jarai et al., 1999; Kohno et al., 2006; McHugh et al., 2010). GPR18 belongs to the Gi/o coupled family of GPCRs, and NAGly or Abn CBD activation of GPR18, which is coupled to the Gi/o family (Kohno et al., 2006), enhances ERK1/2 phosphorylation and PI3K/Akt signaling (Offertáler et al., 2003; Mo et al., 2004). Reported studies including studies from this laboratory suggested a causal role for nitric oxide (NO) generation in the RVLM in hypotensive responses triggered by the activation of other receptors (Chan et al., 2001; Nassar and Abdel-Rahman, 2008). While there are no reports that implicated GPR18 signaling in adiponectin (ADN) release, we reasoned such a link exists because an anti-inflammatory role is a common denominator between GPR18 (Vuong et al., 2008) and ADN (Nanayakkara et al., 2012) signaling. More pertinent to the present study are the findings that ADN serves an antioxidant role in the RVLM (see below), which explains its sympathoinhibitory

role (Chan et al., 2001; Konno et al., 2012; Nanayakkara et al., 2012). Together, these findings implicate RVLM NO and ADN in the GPR18-mediated hypotensive response, at least partly, via a reduction in neuronal oxidative stress (ROS) in the RVLM. The experiments under this aim determined, for the first time, if cAMP/Akt/ERK1/2/nNOS-dependent reduction in ROS generation in the RVLM is implicated in GPR18-mediated hypotension and elucidated the downstream signaling of GPR18 that led to a decrease in blood pressure by addressing the following questions:

- 1- Does intra-RVLM GPR18 activation and inhibition increase and decrease ERK1/2, Akt and nNOS phosphorylation, respectively?
- 2- What is the effect of ERK1/2 or Akt inhibition on the cardiovascular effects produced by intra-RVLM Abn CBD?
- 3- What is the effect of nNOS/eNOS inhibition or adenylyl cyclase (AC) activation on the cardiovascular effects produced by intra-RVLM Abn CBD?
- 4- What are the effects of intra-RVLM Abn CBD on ERK1/2, Akt and nNOS phosphorylation and adiponectin levels in the RVLM of rats pretreated with ERK1/2 inhibitor, PD98059 or the PI3K inhibitor, wortmannin or nNOS inhibitor, *N*^ω-Propyl-L-arginine hydrochloride (NPLA) or the AC activator, forskolin?
- 5- What is the effect of intra-RVLM administration of GPR18 ligands on RVLM NO and ADN levels?

6- Does RVLM GPR18 activation reduce neuronal oxidative stress?

Specific Aim 3 studies elucidated the role of lipid rafts (LR) in GPR18 signaling in nPC12 cells.

Rationale: There is growing evidence that LRs and caveolae participate in the regulation of GPCR signaling by affecting both signaling selectivity and coupling efficacy (Chini and Parenti, 2004). There is also evidence that CB₁R binding/signaling, as well as anandamide (AEA) transport is controlled by LRs and caveolin-1 (Dainese et al., 2007; Bari et al., 2008). NAGly is synthesized from AEA and serves as an endogenous GPR18 ligand (Huang et al., 2001; Kohno et al., 2006). Additionally, AEA is a common endocannabinoid for both GPR18 and CB₁R (Bradshaw et al., 2009). Based on these findings, we hypothesized that activation of GPR18 causes receptor dissociation from (LR), which consequently leads to activation of PI3K/Akt-ERK1/2-NOS pathway and inhibition of ROS signaling. However, as the methods for detecting lipid rafts are technically difficult to conduct in tissues, we used nPC12 cells, which are rat pheochromocytoma cells that are capable of differentiating into a neuronal phenotype (Okouchi et al., 2005). Another reason for conducting signaling studies in nPC12 cells is the limited tissue amounts obtained from the RVLM of treated and control rats, which made conducting some neurochemical studies difficult. For example, the GPR18 antagonist cannabidiol inhibited catalase activity in the liver (Usami et al., 2008). Such changes in major enzymes that control the oxidative state of the RVLM neurons might explain the expected reduced and enhanced ROS generation in the RVLM neurons following selective GPR18 activation and blockade, respectively. These and similar neurochemical studies could be conducted in drug or vehicle treated nPC12 cells. Nonetheless, it was imperative to conduct preliminary studies to ensure that

GPR18 is expressed in nPC12 cells and that signaling products of GPR18 activation are similar in nPC12 cells and RVLM. The association of GPR18 with LRs and the signaling pathways of the receptor in this model system were elucidated by addressing the following questions:

1- Is GPR18 expressed in nPC12 cells?

2- Is GPR18 co-expressed with CB₁R in nPC12 cells?

3- Does GPR18 associate with LRs or does it interact with these membrane microdomains only upon activation?

4- What is the effect of LR disruption on GPR18 signaling in nPC12 cells?

5- Does GPR18 activation enhance antioxidant (catalase and ALDH) and inhibit pro-oxidant (NADPH Oxidase) enzyme activity in nPC12 cells?

The findings of the present study provide the first comprehensive *in vivo* and *ex vivo* evidence of the role of central GPR18 on the cardiovascular system in conscious normotensive rats, elucidating its role in central regulation of blood pressure. Further, our *in vitro* studies help to understand the role of lipid rafts in the signaling of the putative cannabinoid (CB) receptor GPR18.

CHAPTER TWO- MATERIALS AND METHODS

2.1. Preparation of the Rats

Male Sprague-Dawley rats (300-350 g; Charles River Laboratories, Raleigh, NC) were used in the present study. Animals received buprenorphine (0.03 mg/kg) 30 min prior to anesthesia with i.p. ketamine (9 mg/100g) and xylazine (1 mg/100g). A 5-cm PE-10 tube connected to PE-50 tubing filled with heparinized saline (heparin 200 units/ml) was placed in the abdominal aorta via the left femoral artery for measurement of blood pressure (BP) and heart rate (HR) as in our previous studies (Zhang and Abdel-Rahman, 2002). The catheter was tunneled subcutaneously and exteriorized at the back of the neck between the scapulae, and plugged with stainless steel pins. Wounds were closed by surgical clips and swabbed with povidone-iodine solution.

The implantation of the guide cannula into the RVLM was performed as described in our previous studies (Mao and Abdel-Rahman, 1995). Briefly, following anesthesia, the head of the animal was placed in stereotaxic frame (David Kopf Instruments, Tujunga, CA), and a 23-gauge stainless steel guide cannula (Small Parts, Miami, FL, USA) was implanted unilaterally such that the tip of the guide cannula was positioned 2 mm above the RVLM (posterior -2.8 mm, lateral \pm 2.0 mm, dorsoventral -0.5 mm) (Paxinos and Watson, 2005). The cannula was secured to the skull with dental cement (Durelon; Thompson Dental Supply, Raleigh, NC, USA). Each rat received buprenorphine (0.05 mg/kg s.c.) to control pain and penicillin G procaine (100,000 U/kg i.p.). Animals were housed 5 days in separate cages to allow for recovery before conducting experiments.

2.1.1. Blood pressure (BP) and heart rate (HR) measurements.

On the day of the experiment, the arterial catheter was flushed with heparinized saline (100 IU/ml) and connected to a Gould-Statham (Oxnard, CA) pressure transducer. BP was recorded by ML870 (PowerLab 8/30) and analyzed by LabChart (v.6) pro software (ADInstruments, Colorado Springs, CO). Heart rate was computed from BP recording by the LabChart (v.6) blood pressure analysis module, and both variables were continuously recorded and stored for offline analysis. BP and HR were allowed to stabilize for at least 30 min. Microinjections of a constant volume (80nl) were made directly into the RVLM of unrestrained rats through a 30-gauge stainless steel injector as described in our previous studies (Mao and Abdel-Rahman, 1994; Zhang and Abdel-Rahman, 2002).

2.2. Cell Culture

Rat pheochromocytoma cells (PC12 cells) (ATCC, Rockville, MD) were cultured, at 37°C with saturated air containing 5% CO₂, on Corning CellBind flasks in ATCC-formulated F-12K medium supplemented with horse serum (15%), fetal bovine serum (2.5%), penicillin (100U/ml) and streptomycin (100U/ml). Cells were treated with NGF (50ng/ml) for 48hrs to initiate neuronal differentiation. Culture media was changed every 2 days.

2.3. Immunohistochemistry

The procedure reported in Current Protocols in Neuroscience for immunohistochemistry for light microscopy (Ince et al., 1997) was followed. Briefly, brains were fixed by transcardiac perfusion with 4% paraformaldehyde in phosphate-buffered saline (PBS) following a lethal dose

of ketamine-xylazine mixture. Brains were then transferred into 30% sucrose in PBS for infiltration until they sank. Brain sections that contained the RVLM (-12.8 to -11.8 mm relative to bregma) were cut serially at -24°C with a microtome cryostat (HM 505 E; Microm International GmbH, Walldorf, Germany) (Paxinos and Watson, 2005) as in a previous study from this laboratory (Zhang and Abdel-Rahman, 2005). Six to eight sections of the brain ($20\ \mu\text{m}$) were collected in each well of a cell culture plate (12 wells; BD Biosciences, San Jose, CA) containing ice-cold PBS. The avidin-biotin complex method was used according to the manufacturer's instruction (Vectastain ABC kit; Vector Laboratories, Burlingame, CA) with minor modification (Ince et al., 1997). For immunohistochemical detection of GPR18, the RVLM sections of naïve rats were incubated with goat anti-GPR18 primary antibody (1:200; Santa Cruz; Dallas, TX). After rinsing with Tris-buffered saline (TBS), 3'-diaminobenzidine (in H_2O) solution was added, and the sections were examined under a microscope (Nikon Diaphot 300; Nikon, Tokyo, Japan) for the appearance of reddish brown staining. After dehydration the sections were sealed with Permount (Fisher Scientific Co., Pittsburgh, PA) and observed under the microscope. For GPR18, the immunoreactive neurons (brown stain) were identified in the RVLM.

2.4. Immunofluorescence

Colocalization studies were conducted according to the protocol used in previous reports (Wang and Abdel-Rahman, 2005; Matias et al., 2008; Worlein et al., 2011). Brains were fixed by transcardiac perfusion with 4% paraformaldehyde in Phosphate-buffered saline (PBS) following a lethal dose of ketamine-xylazine mixture. Brains were then transferred into 30% sucrose in

PBS for infiltration until they sank. Brain sections that contained the RVLM (-12.8 to -11.8 mm relative to bregma) were cut serially using vibrotome in to ice cold PBS. Free floating sections, prepared as above, were then washed with TBS for 15 min, and incubated for 3 hr in blocking buffer (1% bovine serum albumin, 5% normal donkey serum in TBS containing 0.1% Triton X-100; TBST) at room temperature (RT) with continuous shaking. The sections were then incubated 48 hr at 4°C with shaking in goat anti-GPR18 (1:200; Santa Cruz; Dallas, TX) and mouse anti-tyrosine hydroxylase (1:500; Abcam; Cambridge, MA) or mouse anti CB₁R (1:200; Santa Cruz; Dallas, TX) mixture diluted in blocking buffer. After being washed 3X in TBST, immunofluorescence was revealed by incubation for 2 hr in Cy-3 conjugated donkey anti-goat and fluorescein isothiocyanate-conjugated donkey anti-mouse (1:200; Jackson Immunoresearch Laboratories Inc., West Grove, PA). Sections were washed in TBS in the dark and mounted on slides and cover slipped with Vectashield mounting medium containing DAPI as counterstain (Vector Laboratories, Burlingame, CA) and left in the dark overnight to harden. Images were acquired by multi-track acquisition mode to eliminate channels-cross talk using confocal laser microscopy (Carl Zeiss LSM 510, Thornwood, New York). Six sections per animal at the level of the RVLM were examined and representative images were edited by the Zeiss LSM Image Browser software (v 4.2) and Adobe Photoshop (v. CS4, Adobe Systems, San Jose, CA), where only image brightness and contrast were adjusted for clarity. Co-localization analysis was performed using Pearson's correlation coefficient of the JACoP plugin in ImageJ. Negative controls (absence of primary or secondary antibody) were run simultaneously.

nPC12 cells were cultured on Lab-Tek Chamber slides coated with poly-L-lysine, washed with cold PBS and fixed with 4% paraformaldehyde for 30min. The cell membranes were permeabilized with 0.1% triton X-100 and non-specific binding was blocked by 1% bovine serum albumin and 5% normal donkey serum. The cells were incubated for 2.5 hrs with the respective primary antibody. The cells were then incubated with the corresponding secondary antibody (1:200; Jackson Immunoresearch Laboratories Inc., West Grove, PA) for 1 hr, mounted with Vectashield mounting medium containing DAPI as the counterstain (Vector Laboratories, Burlingame, CA) and left in the dark overnight to harden. Images were acquired using confocal laser microscopy (Carl Zeiss LSM 510, Thornwood, New York). Representative images were analyzed using the JACoP plugin in ImageJ software.

2.5. Western Blot Analysis

Animals received a lethal dose of ketamine-xylazine mixture (i.p.), and following decapitation, brains were removed, flash frozen in 2-methylbutane on dry ice, and stored at -80°C until use. Brains were equilibrated to -20°C and coronal sections containing the RVLM were obtained with a cryostat (HM 505E; Microm International GmbH, Waldorf, Germany) according to atlas coordinates (Paxinos and Watson, 2005). Tissue from the RVLM was collected bilaterally using a 0.75 mm punch instrument as described in other studies (Ibrahim and Abdel-Rahman, 2011) from approximately -12.8 to -11.8 mm relative to bregma (Paxinos and Watson, 2005). Tissue was homogenized on ice by sonication in cell lysis buffer (20 mM Tris pH 7.5, 150 mM NaCl, 1 mM EDTA, 1 mM EGTA, 1% Triton X-100, 2.5 mM sodium pyrophosphate, 1 mM β -glycerolphosphate, 1 mM activated sodium orthovanadate) containing a

protease inhibitor cocktail (Roche Diagnostics, Indianapolis, IN). Protein concentration in samples was quantified using a standard Bio-Rad protein assay system (Bio-Rad Laboratories, Hercules, CA). Protein extracts (20 µg per lane) were denatured at 97°C for 5 minutes, separated on NuPAGE Novex Bis-Tris 4 to 12% SDS-PAGE gels (Invitrogen, Carlsbad, CA) using MOPS NuPAGE running buffer, and electroblotted to nitrocellulose membranes using standard procedures. Nonspecific binding sites on the membranes were blocked at room temperature in wash buffer (10 mM Tris, 150 mM NaCl, 0.2% 0.5 M EDTA pH 8.0, 0.01% Triton X-100) containing 5% nonfat milk for 1 to 2 hours. The membranes were then incubated overnight at 4°C with goat anti-GPR18 primary antibody (1:200; Santa Cruz; Dallas, TX) diluted in blocking solution. The blots were washed twice and then incubated for 60 min at room temperature with anti-rabbit IgG horseradish peroxidase-linked secondary antibody (1:2,000; GE Healthcare, Piscataway, NJ). After 4 more washes, protein was detected on the blots by enhanced chemiluminescence. Consistency in sample loading was confirmed by stripping the membranes with Blot Fresh Stripping Reagent (SignaGen, Gaithersburg, MD) and reprobing with rabbit anti-actin antibody (1:2,000; Sigma; St. Louis, MO); all data were expressed as values normalized to actin.

For adiponectin measurements, RVLM punches obtained from treatment or control groups, were simultaneously blocked (1 hr) with Odyssey blocking buffer (LICOR Biosciences; Lincoln, NE) and incubated with a mixture of mouse monoclonal anti-actin antibody (1:1000) and rabbit polyclonal anti-adiponectin antibody (1:1000) overnight. All antibodies were purchased from Cell Signaling Technology (Danvers, MA). After washing with PBS, the membranes were

incubated for 1 hr with a mixture of IRDye680-conjugated goat anti-rabbit and IRDye800-conjugated goat anti-mouse (1:10,000; LICOR Biosciences; Lincoln, NE). Membranes were washed with PBS containing 0.1% Tween 20 and bands representing adiponectin and actin were visualized simultaneously using an Odyssey Infrared Imager and analyzed with Odyssey application software v.3 (LICOR Biosciences; Lincoln, NE). All data are presented as mean values of integrated density ratio of adiponectin normalized to actin (Komura et al., 2013).

Freshly subcultured nPC12 cells were processed with or without drug treatment and total cell lysates were used to evaluate the expression of ERK1/2 and pERK1/2 or Akt and pAkt using western blot analysis. Homogenized protein extracts were run on 12% SDS-PAGE gel (Invitrogen, Carlsbad, CA) and electroblotted to nitrocellulose membranes. Blots were blocked with Odyssey blocking buffer and incubated overnight at 4°C with rabbit anti-ERK1/2 or rabbit anti-Akt and mouse anti-pERK1/2 or mouse anti-pAkt (1:500). The blots were then washed with rinse buffer and incubated at room temperature with donkey anti-rabbit and donkey anti-mouse IgG secondary antibody (1:10,000). Following additional washes the blots were detected using an Odyssey Infrared Imaging system and analyzed with Odyssey application software v.3 (LICOR Biosciences). All data are presented as mean values of integrated density ratio of phosphorylated protein normalized to its corresponding total protein.

2.6. Dot Blotting

The dot blot technique was employed to detect and analyze the proteins present in the sample. It differs from the western blot in that the protein samples are spotted through circular templates directly onto the nitrocellulose membrane instead of being separated

electrophoretically. This technique was preferred over western blotting because the amount of protein required is much smaller given the small size of the RVLM tissue. A 96 well Bio-dot Microfiltration Apparatus (Bio-Rad Laboratories, Inc., Hercules, CA) was used and the samples were loaded in the wells and directly separated by vacuum filtration on to nitrocellulose membrane. The membrane was then washed with 1x PBS and allowed to dry. The membranes were blocked for 1 hr with Odyssey blocking buffer (LICOR Biosciences Lincoln, NE), and incubated with primary and secondary antibodies according to the experimental design (see Methods under individual experiments) and visualized simultaneously using an Odyssey Infrared Imager and analyzed with Odyssey application software v.3 (LICOR Biosciences). All data are presented as mean values of the integrated density ratio of phosphorylated protein normalized to its corresponding total protein or to actin.

2.7. Quantification of Reactive Oxygen Species

2.7.1. *Dihydroethidium (DHE) Staining for ROS Detection.*

For measurement of ROS, fresh unfixed brainstem sections (20 μm) were incubated with 10 μM dihydroethidium (DHE) (Molecular Probes, Grand Island, NY) at 37°C in the presence of 5% CO₂ in a moist chamber for 30 min. Positive and negative controls were used to validate the assay (see experimental groups and protocols). Images were visualized with a Zeiss LSM 510 microscope. Three-five images were acquired from each of the 5-6 brainstem sections for each experimental condition. Quantification was conducted using Image J software (NIH) and changes in total fluorescence intensity, normalized to control, were calculated as reported (Collin et al., 2007).

2.7.2. Measurement of Reactive Oxygen Species by DCFH-DA.

RVLM specimens from treated and control groups were homogenized in PBS. The homogenate was centrifuged (14,000 rpm) for 20 min. Protein in the supernatant was quantified using a Bio-Rad protein assay system. 2', 7'-dichlorofluorescein diacetate (DCFH-DA) (Molecular Probes) was dissolved in DMSO (12.5 mM) and kept at -80°C in the dark. It was freshly diluted with 50 mM phosphate buffer (pH 7.4) to 125 µM before the experiment. DCFH-DA was added to the RVLM homogenate supernatant (10 µl) in a 96-well microtiter plate for a final concentration (25 µM). 2', 7'-Dichlorofluorescein (DCF) was used for a 6-point standard curve. Quantification was conducted by examining fluorescence intensity using a microplate fluorescence reader at excitation 485 nm/emission 530 nm. Kinetic readings were recorded for 30 min at 37°C. ROS level was calculated by relative DCF fluorescence per µg protein. Positive and negative controls were used to validate the assay as in previous studies from this laboratory (McGee and Abdel-Rahman, 2012).

Freshly sub-cultured cells were exposed to 5µM DCFH-DA for 30min after which they were subjected to appropriate drug treatment for 2hrs. The cells were washed with PBS, trypsinized and collected in Eppendorf tubes. The fluorescence was measured using a flow cytometer.

2.8. Measurement of Nitrate/Nitrite Level

RVLM punches were obtained from the rats of different experimental groups and homogenized in 300 µl phosphate buffered saline (PBS). The homogenate was centrifuged (14,000 rpm) for 20 min and the protein in the supernatant was quantified using a Bio-Rad

protein assay system. The supernatant, 140 μ l, was ultra-filtered using Amicon Centrifugal Filter Units (10 kDa) and centrifuged (14,000 rpm) for 1 hour. The NO_x content was measured using a Nitrate colorimetric assay kit (Catalog # 780001) according to manufacturer's instructions (Cayman Chemical Company; Ann Arbor, MI) and as detailed in reported studies (Misko et al., 1993; El-Mas et al., 2009).

2.9. Measurement of cAMP

cAMP-Glo Max Assay kit (Promega V1681) was used to measure cAMP in treated nPC12 cells. Cell lysates were subjected to the assay as per the manufacturer's instructions (Promega, Madison, WI) and luminescence was determined with a luminometer and used as a measure of cAMP produced. For each sample: the change in relative luminescence units (Δ RLU) = RLU (untreated sample) – RLU (treated sample) was calculated. Using this Δ RLU value and the linear equation generated from the standard curve, the cAMP concentration was calculated from the linear formula from the graph.

2.10. Quantification of Catalase Activity

Colorimetric measurement of catalase generated as a result of drug treatment was measured following instructions for the Catalase assay kit obtained from Sigma Aldrich (St. Louis, MO). One RVLN punch from the rat brain was sonicated in 25 μ l PBS. For cells, 1ml of PBS was added to 100 cm² Petri dish and the cells were gently scraped and collected into centrifuge tubes after drug treatment for 30 min. The tissue/cell suspension was centrifuged at 4°C, 5000 rpm for 5 min. The supernatant was collected, the amount of the protein in the sample was quantified

using a Bio-Rad protein assay (Bio-Rad Laboratories, Hercules, CA) and catalase activity was measured as per the manufacturer's instructions (Sigma Aldrich; St. Louis, MO). The absorbance of the samples was measured at 520nm.

2.11. Quantification of NADPH oxidase Activity

NADPH oxidase activity was measured by a fluorescence assay using Amplex Red (Molecular Probes, OR) dissolved in buffer, pH 7.4 (105 mM K-MES, 30 mM KCl, 10 mM KH₂PO₄, 5 mM MgCl₂-6H₂O, 0.5 g/L BSA), Superoxide dismutase (7500 U/ml), Horseradish peroxidase (300 U/ml) and the addition of NADPH (10 mM). Hydrogen peroxide was used to generate a 7-point standard curve. Quantification was conducted by examining fluorescence intensity using the Fluoromax-3 spectrofluorometer (Horiba Jobin Yvon, Edison, NJ) at excitation (530 nm)/emission (590 nm). Cell suspension samples (50 µg/25 µl) were added to 200 µl Amplex Red, 2 µl Superoxide dismutase and 2 µl horseradish peroxidase. Baseline measurements were taken for five minutes and NADPH (10 µl) was added and readings were recorded for an additional 5 minutes.

2.12. Quantification of Aldehyde Dehydrogenase (ALDH) Activity

Freshly sub-cultured nPC12 cells were scraped in 1xPBS and homogenized using a syringe. The cell suspension was centrifuged at 4°C and 5000rpm for 4min. The supernatant was collected for protein assay and ALDH activity measurement. The final volume of the assay mixture (200 µl) comprised of 50 µg/25 µl protein or 25 µl of 1xPBS (Blank), 4 µl of 300 µM 6-Methoxy-2-naphthaldehyde in 166.4 µl of 1xPBS. The fluorescence of this mixture was read at

excitation 310nm and emission 360nm for 7min before adding 1.3 μ l of 11.4 mM NAD. After this addition the fluorescence of this assay mixture was read at 310nm/360nm every 5 min for 45 min and ALDH activity was calculated from the fluorescence values.

2.13. Lipid Raft Labeling

nPC12 cells were cultured on Lab-Tek Chamber slides coated with poly-L-lysine, washed with cold PBS and fixed with 4% paraformaldehyde for 30 min. The cell membranes were permeabilized with 0.1% triton X-100 and non-specific binding was blocked using 1% bovine serum albumin and 5% normal donkey serum. The cells were incubated for 2.5 hr with goat anti-GPR18 (1:200). The cells were then incubated with fluorescein isothiocyanate-conjugated donkey anti-goat (1:200; Jackson ImmunoResearch Laboratories Inc., West Grove, PA) for 1 hr, mounted with Vectashield mounting medium containing DAPI as counterstain (Vector Laboratories, Burlingame, CA) and left in dark overnight to harden. Vybrant Alexa Fluor 488 lipid raft labeling kit (Molecular Probes, Eugene, OR) was used to label lipid rafts in accordance with the manufacturer's instructions. Images were acquired using confocal laser microscopy (Carl Zeiss LSM 510, Thornwood, New York). Representative images were analyzed using JACoP plugin in ImageJ software.

CHAPTER THREE - THE NOVEL ENDOCANNABINOID RECEPTOR GPR18 IS EXPRESSED IN THE ROSTRAL VENTROLATERAL MEDULLA AND EXERTS A TONIC RESTRAINING INFLUENCE ON BLOOD PRESSURE

3.1. Abstract

Systemic administration of the GPR18 agonist, abnormal cannabidiol (Abn CBD), lowers blood pressure (BP). Whether GPR18 is expressed in the CNS and plays a role in BP control is not known despite the presence of an abundance of the GPR18 ligand N-arachidonoyl glycine (NAGly) in the CNS. Therefore, we first determined if GPR18 is expressed in the presympathetic tyrosine hydroxylase (TH) immunoreactive (ir) neurons of the brainstem cardiovascular regulatory nuclei. Second, we investigated the impact of GPR18 activation and/or blockade on BP and heart rate (HR) and neurochemical modulators of sympathetic activity/BP. Immunofluorescence findings revealed GPR18 expression in TH-ir neurons in the rostral ventrolateral medulla (RVLM). Intra-RVLM GPR18 activation (Abn CBD) and blockade (O-1918) elicited dose-dependent reductions and elevations in BP, respectively, along with respective increases and decreases in HR in conscious male Sprague-Dawley rats. RVLM GPR18 activation increased neuronal adiponectin (ADN) and NO and reduced reactive oxygen species (ROS) levels while GPR18 blockade reduced neuronal ADN and increased oxidative stress (ROS) in the RVLM. Finally, we hypothesized that the negligible hypotensive effect caused by the endogenous GPR18 ligand NAGly could be due to concurrent activation of CB₁R in the RVLM. Our findings supported this hypothesis because NAGly-evoked hypotension was doubled following RVLM CB₁R blockade (SR141716). These findings are the first to demonstrate GPR18 expression in the RVLM, and to suggest a sympathoinhibitory role for this

receptor. The findings yield new insight into the role of a novel cannabinoid receptor (GPR18) in central BP control.

3.2. Introduction

Endogenous and exogenous cannabinoids exert complex cardiovascular effects due, at least partly, to their activation of diverse cannabinoid receptors (CBR) and their location within the cardiovascular system and different brain nuclei (Randall et al., 2004). The two classical CBRs (CB₁R and CB₂R) are implicated in behavior and cardiovascular regulation (Randall et al., 2002). However, the cardiovascular responses might be confounded by the use of anesthetics because cannabinoids (CBDs) produce hypotension in anesthetized animals (Varga et al., 1995), which is consistent with vasorelaxation in vitro (Jarai et al., 1999), but produce pressor responses in conscious rats (Gardiner et al., 2002; Ibrahim and Abdel-Rahman, 2011). Further, many studies implicated several novel receptors in the diverse cardiovascular effects of synthetic and natural cannabinoids (Offertáler et al., 2003). For example, abnormal cannabidiol (Abn CBD) caused mesenteric vasodilation and hypotension in mice lacking CB₁/CB₂ receptors via the activation of a novel CB receptor (Jarai et al., 1999). This new Gi/Go coupled receptor, which mediates endothelium-dependent vasodilation (Begg et al., 2005; Mackie and Stella, 2006), has been named the endothelial ‘anandamide receptor’ or the ‘Abn CBD’ receptor. Recent findings indicate that N-arachidonoyl glycine (NAGly), Abn CBD and Δ^9 tetrahydrocannabinol (THC) (McHugh et al., 2011) act as selective agonists while O-1918, an analog of cannabidiol (CBD), acts as an antagonist at this receptor (Offertáler et al., 2003; McHugh et al., 2010).

Recent studies have identified the orphan G protein-coupled receptor GPR18 as the 'Abn CBD' receptor and NAGly as its endogenous ligand (Kohno et al., 2006; McHugh et al., 2010; McHugh, 2012). It is possible that Abn CBD and O-1918 might act via another putative cannabinoid receptor, GPR55 (Johns et al., 2007; Godlewski et al., 2009). However, more recent studies showed that although GPR18 and GPR55 share some ligands, they do not respond to them in the same manner or with the same efficacy (McHugh et al., 2010; Okuno and Yokomizo, 2011).

GPR18 is found in humans, rodents and canine (Gantz et al., 1997), and its mRNA is most abundantly expressed in testis, spleen and brain stem among other tissues (Vassilatis et al., 2003). Although GPR18 mRNA is expressed in human and rodent brainstem (Vassilatis et al., 2003) and NAGly is abundant in the brain (Huang et al., 2001), there are no studies on the expression and function of GPR18 in brainstem cardiovascular/sympathetic activity regulating nuclei. Notably, NAGly or Abn CBD activation of GPR18, which is coupled to the Gi/o family (Kohno et al., 2006), enhances ERK1/2 phosphorylation and PI3K/Akt signaling (Offertáler et al., 2003) as well as glycinergic transmission in the nervous system (Jeong et al., 2010). Further, NAGly causes vasorelaxation via NO release in rat small mesenteric arteries (Kishi et al., 2001) and N-palmitoyl glycine (a palmitic acid conjugate of NAGly) increases the levels of NO (Rimmerman et al., 2008a). Whether these signaling effects result in functional changes in sympathetic activity and ultimately in BP has not been investigated. Notably, the findings that the endogenous GPR18 ligand, NAGly, has the potential to increase anandamide (AEA) (an endogenous CB₁R agonist) (Burstein et al., 2002), and that central CB₁R activation increases BP

(Ibrahim and Abdel-Rahman, 2012a) might influence the final BP response mediated by NAGly activation of RVLM GPR18.

The main objectives of the present study were to determine if GPR18 is expressed in RVLM presympathetic neurons, and to elucidate its role in central control of BP. To achieve these goals, we conducted integrative dose-response studies that permitted measurements of BP and HR responses caused by direct activation and/or blockade of the RVLM GPR18 in conscious rats. We also investigated the possibility that concurrent activation of RVLM CB₁R, which mediates sympathoexcitation, might explain the dampened hypotensive response produced by the endogenous GPR18 ligand NAGly. Finally, the integrative pharmacological studies were complemented with *ex vivo* neurochemical studies to elucidate the molecular mechanisms implicated in the central GPR18-mediated hypotensive response.

3.3. Materials and Methods

3.3.1. Preparation of the Rats.

Male Sprague-Dawley rats (300-350 g; Charles River Laboratories, Raleigh, NC) were used in the present study. All rats were housed two per cage in a room with controlled environment at a constant temperature of $23 \pm 1^{\circ}\text{C}$, humidity of $50 \pm 10\%$, and a 12 hr light/dark cycle. Food (Prolab Rodent Chow, Prolab RMH 3000; Granville Milling, Creedmoor, NC) and water were provided ad libitum. All surgical, postoperative care and experimental procedures were performed in accordance with, and approved by, the Institutional Animal Care and Use Committee and in accordance with the Guide for the Care and Use of Laboratory Animals (Institute for Laboratory Animal Research, 2011). Arterial catheterization, intra-RVLM cannulation and blood pressure measurements were performed as reported in previous studies from this laboratory (Mao and Abdel-Rahman, 1995; Zhang and Abdel-Rahman, 2002).

3.3.2. Western Blot and Neurochemical Studies.

Animals received a lethal dose of ketamine/xylazine mixture (i.p.), and following decapitation, brains were removed, flash frozen in 2-methylbutane on dry ice, and stored at -80°C until use as detailed in chapter 2.

3.3.3. *Immunohistochemistry.*

The procedure reported in Current Protocols in Neuroscience for immunohistochemistry for light microscopy (Ince et al., 1997) was followed as detailed in chapter 2.

3.3.4. *Immunofluorescence.*

Co-localization studies were conducted according to the protocol used in previous reports (Wang and Abdel-Rahman, 2005; Matias et al., 2008) and as detailed in chapter 2.

3.3.5. *Measurement of Nitrate/Nitrite.*

RVLM punches were obtained from the rats of different experimental groups and homogenized in 300 μ l phosphate buffered saline (PBS). The homogenate was centrifuged (14,000 rpm) for 20 min and the protein in the supernatant was quantified using Bio-Rad protein assay system. The supernatant, 140 μ l, was ultra-filtered using Amicon Centrifugal Filter Units (10 kDa) and centrifuged (14,000 rpm) for 1 hour. The NO_x content was measured using a Nitrate colorimetric assay kit (Catalog # 780001) according to manufacturer's instructions (Cayman Chemical Company; Ann Arbor, MI) and as detailed in reported studies (Misko et al., 1993; El-Mas et al., 2009).

3.3.6. *Dihydroethidium (DHE) Staining for ROS Detection.*

For measurement of ROS, fresh unfixed brainstem sections (20 μ m) were incubated with 10 μ M dihydroethidium (DHE) (Molecular Probes, Grand Island, NY) at 37°C in the presence of 5% CO₂ in a moist chamber for 30 min. Positive and negative controls were used to validate the

assay (see experimental groups and protocols). Images were visualized with a Zeiss LSM 510 microscope. Three-five images were acquired from each of the 4 brainstem sections/RVLM for each experimental condition. Quantification was conducted using Image J software (NIH) and changes in total fluorescence intensity, normalized to control, were calculated as reported (Collin et al., 2007).

3.3.7. Measurement of Reactive Oxygen Species by DCFH-DA.

RVLM specimens from treated and control groups were homogenized in PBS. The homogenate was centrifuged (14,000 rpm) for 20 min. Protein in the supernatant was quantified using a Bio-Rad protein assay system. 2', 7'-dichlorofluorescein diacetate (DCFH-DA) (Molecular Probes) was dissolved in DMSO (12.5 mM) and kept at -80°C in the dark. It was freshly diluted with 50 mM phosphate buffer (pH 7.4) to 125 µM before experiment. DCFH-DA was added to RVLM homogenate supernatant (10 µl) in a 96-well microtiter plate for a final concentration (25 µM). 2', 7'-Dichlorofluorescein (DCF) was used for a 6-point standard curve. Quantification was conducted by examining fluorescence intensity using a microplate fluorescence reader at excitation 485 nm/emission 530 nm. Kinetic readings were recorded for 30 min at 37°C. ROS level was calculated by relative DCF fluorescence per µg protein. Positive and negative controls were used to validate the assay as in previous studies from this laboratory (McGee and Abdel-Rahman, 2012).

3.4. Experimental Groups and Protocol

3.4.1 *Experiment 1: Anatomical expression of GPR18 in the RVLM.*

Coronal sections were obtained from naïve rats (n=5) and used for detecting GPR18 protein by immunohistochemistry and by Western blotting as described under methods. Positive (testis and spleen) and negative (liver) controls, based on reported studies (Gantz et al., 1997), were simultaneously run with RVLM GPR18 to confirm the Western blot findings. Further, we used the GPR18 blocking peptide, recommended by the manufacturer, to verify the GPR18 antibody specificity. Spatial distribution of GPR18, in relation to tyrosine hydroxylase (TH)-ir neurons, in the RVLM was investigated using dual labeling immunofluorescence in brainstem sections containing the RVLM as described in the methods and in previous studies from this laboratory to verify the co-localization of the c-Fos immuno-reactive cell nucleus and TH-ir neurons in the RVLM (Ibrahim and Abdel-Rahman, 2011).

3.4.2 *Experiment 2: Functional role of RVLM GPR18 in BP and HR regulation.*

There are no reported studies on the effect of the activation or blockade of RVLM GPR18 on blood pressure in conscious or even anesthetized rats. Therefore, we conducted preliminary studies in conscious instrumented rats to identify a dose range for the effect of microinjected GPR18 agonist Abn CBD on BP. Thereafter, 4 groups of conscious unrestrained rats (n=5-6) were employed for investigating the dose-BP/HR responses elicited by intra-RVLM microinjections of the GPR18 agonists NAGly (0.5, 1, 2 or 4 µg) or Abn CBD (0.2, 0.4 or 0.8 µg) or the antagonist O-1918 (0.2, 0.4, 0.8 µg); control rats received an equal volume (80 nl) of

vehicle (methyl acetate). Following stabilization of BP and HR at baseline, the rats in a particular group received intra-RVLM microinjections of only the GPR18 agonist or antagonist, and control rats received equal amount of the vehicle (Fig.3.1). Three additional groups of rats (n=6 each) were included to determine the involvement of baroreflexes in the tachycardic and bradycardic response observed following Abn CBD and O-1918 microinjection, respectively. Vagal (atropine 1 mg/kg; i.v.) and β -adrenergic receptor blockade (propranolol 1 mg/kg; i.v.), which abolishes baroreflex mediated bradycardia and tachycardia, according to an established protocol (Coleman, 1980), was induced in all rats. Thirty min after atropine and propranolol administration, the rats in a particular group received intra-RVLM Abn CBD (0.2, 0.4 or 0.8 μ g), O-1918 (0.2, 0.4, 0.8 μ g) or an equal volume of vehicle (Fig. 3.1).

3.4.3. Experiment 3: Effect of O-1918 on the BP and neurochemical responses elicited by intra-RVLM Abn CBD.

Based on the dose-response findings of experiment 2, 0.4 μ g of Abn CBD or O-1918 (80 nl) was utilized in this experiment to test the hypothesis that enhancement of adiponectin and NO generation in the RVLM underlie the GPR18-mediated hypotensive response. The effects of RVLM GPR18 activation (Abn CBD) on BP and neurochemical responses were investigated in the absence or presence of the selective GPR18 blockade (O-1918) in four groups of conscious male rats (n=5-6 each). After stabilization of BP and HR at baseline, the rats in a particular group received intra- RVLM vehicle or Abn CBD (0.4 μ g) 30 min after methyl acetate (vehicle) or O-1918 (0.4 μ g). BP and HR were monitored after Abn CBD administration and the animals were euthanized during the hypotensive response in the Abn CBD group and the corresponding time

in the O-1918 + Abn CBD group (Fig.3.3). The brains were collected and processed for neurochemical studies.

3.4.4. Experiment 4: Effect of microinjecting ADN into the RVLM on BP, NO and ROS levels.

In this experiment, we investigated the impact of microinjecting ADN into the RVLM, on mean arterial pressure and heart rate. Animals in this experiment received increasing doses of adiponectin (0.25, 0.5, 1, 2, 4 pmol); (Fig. 3.4) the doses were based on adding two lower and two higher doses than the reported 1 pmol ADN microinjected into the area postrema (Fry et al., 2006). Neurochemical effects of ADN were investigated in the brains collected after the conclusion of the cardiovascular studies; the contralateral (untreated) RVLM tissues were used as controls.

3.4.5. Experiment 5: Effect of RVLM CB₁R blockade on the cardiovascular effects of NAGly.

In this experiment, we investigated the impact of CB₁R blockade, with the selective blocker SR141716, (Hohmann et al., 2005), on the BP response elicited by intra-RVLM NAGly because NAGly regulates AEA (CB₁R agonist) levels (Huang et al., 2001; Burstein et al., 2002). Four groups of conscious rats (n = 5-6 each) received one of the following intra-RVLM treatment combination: (i) DMSO (solvent for SR141716) + Vehicle; (ii) SR141716 (0.1 µg) + Vehicle; (iii) DMSO + NAGly (1 µg) or (iv) SR141716 + NAGly. SR141716 or DMSO was administered into the RVLM 30 min before NAGly or vehicle (Fig. 3.5) and the dose of SR141716 was based

on reported studies (Hohmann et al., 2005). DMSO was diluted in ACSF (1:16) and this DMSO/ACSF mixture had no effect on BP, which is consistent with our previous findings (Nassar et al., 2011). The BP and HR measurements continued for 30 min after which the rats were euthanized and the brains were collected and stored at -80°C for subsequent biochemical studies.

3.4.6. Drugs.

Abn CBD, NAGly, O-1918 and SR141716 were purchased from Cayman Chemical (Ann Arbor, MI). Methyl acetate, propranolol hydrochloride, atropine sulfate and dimethyl sulfoxide were purchased from Sigma Aldrich (St. Louis, MO). Adiponectin was purchased from Phoenix Pharmaceuticals (Burlingame, CA). Sterile saline was purchased from B. Braun Medical (Irvine, CA). DMSO was used as the vehicle for SR141716. Methyl acetate was used as the vehicle for Abn CBD, O-1918, and NAGly and was tested in at least three animals without any significant changes in MAP and HR from the basal levels.

3.5. Data Analysis and Statistics

All values were expressed as mean \pm S.E.M change from their respective baselines. The dose response curves were analyzed using repeated measures ANOVA using SPSS 16.0 statistical package for Windows (SPSS Inc., Chicago, IL) for differences in treatment trends. All other statistical analyses were done using a one-way or repeated-measures ANOVA with Bonferroni post hoc test and Student's t test, Prism 5.0 software (GraphPad Software Inc., San Diego, CA) was used to perform statistical analysis and $P < 0.05$ was considered significant.

3.6. Results

3.6.1. Expression of GPR18 in tyrosine hydroxylase immunoreactive neurons in the RVLM. Western blot (Fig. 3.6A) and immunohistochemical (Fig. 3.6B) findings revealed the expression of GPR18 in RVLM neuronal tissues. Positive and negative controls using tissues rich in (testis and spleen), or devoid of (liver), GPR18 verified the GPR18 findings (Fig. 3.6A). Further, dual labeled immunofluorescence findings revealed the localization of GPR18 in tyrosine hydroxylase-ir neurons of the RVLM (Fig. 3.6C).

3.6.2. Activation of RVLM GPR18 causes a hypotensive response. These studies were conducted to elucidate the functional role of RVLM GPR18 in BP control. Compared with the vehicle (methyl acetate), intra-RVLM microinjection of the GPR18 agonist Abn-CBD caused dose-related reductions in BP along with tachycardic responses (Figs. 3.7A, B). On the other hand, microinjection of the GPR18 antagonist O-1918 caused dose-dependent increases in BP along with bradycardic responses (Figs. 3.7A, B). Prior autonomic blockade with atropine and propranolol (1 mg/kg each) had no significant effect on the dose-related reductions and elevations in BP caused by Abn CBD and O-1918, respectively, but fully abrogated the associated HR responses (Figs. 3.7 C, D). Notably, however, intra-RVLM microinjection of the endogenous GPR18 agonist NAGly caused small ($P>0.05$) hypotensive (-5 ± 1 mmHg; $n=6$) and inconsistent HR responses (Figs. 3.7E, F). BP and HR values prior to Abn CBD or NAGly were not significantly different (Table 3.1). Compared to the vehicle control, RVLM GPR18 activation (Abn CBD) increased ADN and NO levels while blockade (O-1918) reduced ADN level (Figs. 3.7A, B) in the RVLM.

3.6.3. Intra-RVLM ADN reduces BP and lowers ROS and elevates NO levels in RVLM. ADN caused dose-dependent reductions (-2 ± 2 to -12 ± 1 mmHg; $n=4$) in BP (Fig. 3.9 A), but not in HR; however, slight increases in HR of the control group resulted in significant differences in HR at the 0.25 and 1 pmol doses (Fig. 3.9 B). Compared to the control, ADN increased NO_x (Fig. 3.9 C) and reduced ROS (Fig. 3.9 D) levels in the RVLM.

3.6.4. RVLM CB₁R blockade unmasks NAGly-evoked hypotension. This experiment was conducted to determine if concomitant NAGly (indirect) activation of RVLM CB₁R masks the GPR18-mediated hypotensive response. Fig. 3.10A shows co-localization of GPR18 and CB₁R in the presympathetic neurons of the RVLM of naïve rats inferring a potential interaction between the two receptors. Pharmacologic studies showed that selective RVLM CB₁R blockade with SR141716 (0.1 µg) caused a modest but significant ($P<0.05$) BP reduction (-8 ± 2 mmHg; $n=6$) while HR was not significantly changed (Figs. 3.10 B and C). Further, despite gradual return of BP to baseline level within 30 min of SR141716 administration, prior CB₁R blockade significantly ($P<0.05$) enhanced the hypotensive response (-11 ± 1 mmHg; $n=6$) caused by intra-RVLM NAGly (Fig. 5B). The effect of SR141716 at CB₁R lasts at least 2hrs as reported in a different model system (Jarbe et al., 2010). Therefore, NAGly-evoked hypotension was not a result of the additive hypotensive responses caused by NAGly and SR141716 (Fig. 3.10 B). HR was not influenced by any of the treatments (Fig. 3.10C). Neurochemical findings showed that SR141716/NAGly treatment significantly increased ADN and NO levels (Figs. 3.8 A, B) and reduced ROS levels (Fig. 3.13 A) in the RVLM compared to NAGly alone.

3.6.5. O-1918 abrogated Abn CBD evoked hypotension and neurochemical responses.

To confirm the involvement of GPR18 in Abn CBD evoked BP and RVLM neurochemical responses, Abn CBD was microinjected after the GPR18 antagonist O-1918. Intra-RVLM O-1918 (0.4 μ g) abrogated ($P < 0.05$) the reduction in BP (Figs. 3.11A, B) and the increases in RVLM ADN (Fig. 3.8A) and NO levels (Fig. 3.8B) caused by intra-RVLM Abn CBD (0.4 μ g). The selected Abn CBD and O-1918 doses were based on the dose-response curves for these drugs (Figs. 3.7A, B). Notably, at the time of Abn CBD or its vehicle administration, the BP of O-1918 pretreated rats had declined towards pretreatment level (Fig. 3.11A), which rules out functional antagonism as a potential reason for O-1918 abrogation of the hypotensive effect of Abn CBD. Importantly, O-1918 blockade of GPR18 (Abn CBD)-mediated responses was evident for at least 1 hr (Caldwell et al., 2013). The HR responses were not significantly different among the different treatment groups during the observation period (Fig. 3.11B).

3.6.6. GPR18 activation reduces ROS generation in the RVLM. Given the established link between ROS generation in the RVLM and sympathoexcitation/pressor response (Kishi et al., 2004), this experiment was conducted to determine the impact of GPR18 activation (Abn CBD) or blockade (O-1918) on RVLM ROS level in neuronal tissues collected during the BP responses caused by these interventions. Compared with vehicle, Abn CBD significantly ($P < 0.05$) reduced (Fig. 3.13A) while O-1918 significantly ($P < 0.05$) increased ROS levels in the RVLM (Figs. 3.13A, B). Further, O-1918 abrogated the reduction in RVLM ROS caused by Abn CBD (Figs. 3.13A); these neurochemical responses paralleled the BP responses described above (Figs. 3.11A, B).

Figure 3.1. Timeline for surgical procedures and experimental protocols for experiment 3.2.

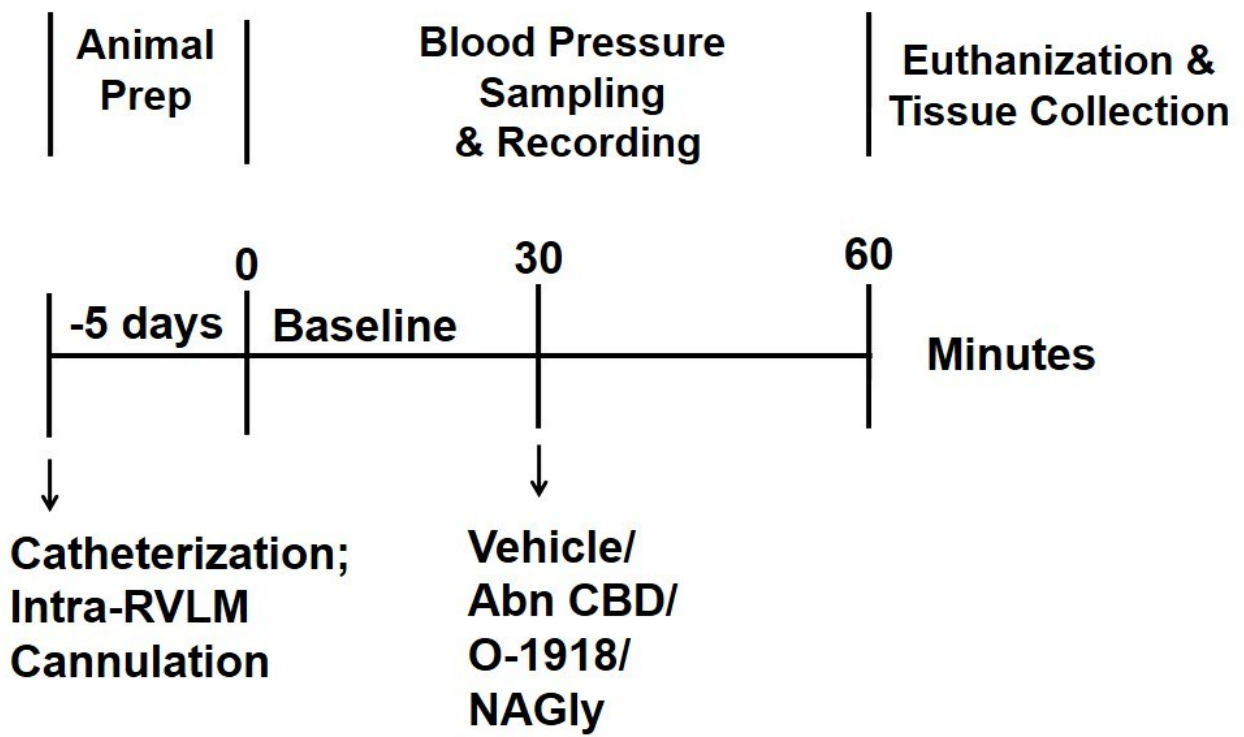


Figure 3.2. Timeline for surgical procedures and experimental protocols for experiment 3.2.

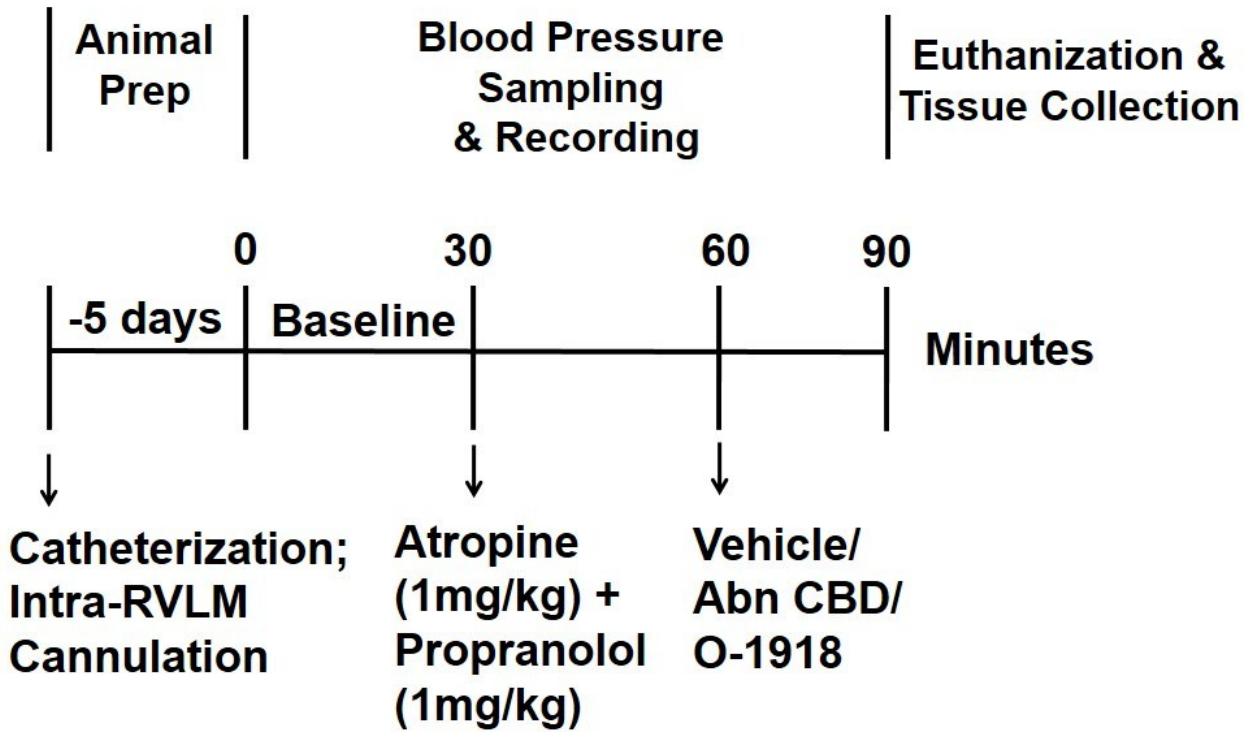


Figure. 3.3. Time line for surgical procedures and experimental protocols for experiment 3.3.

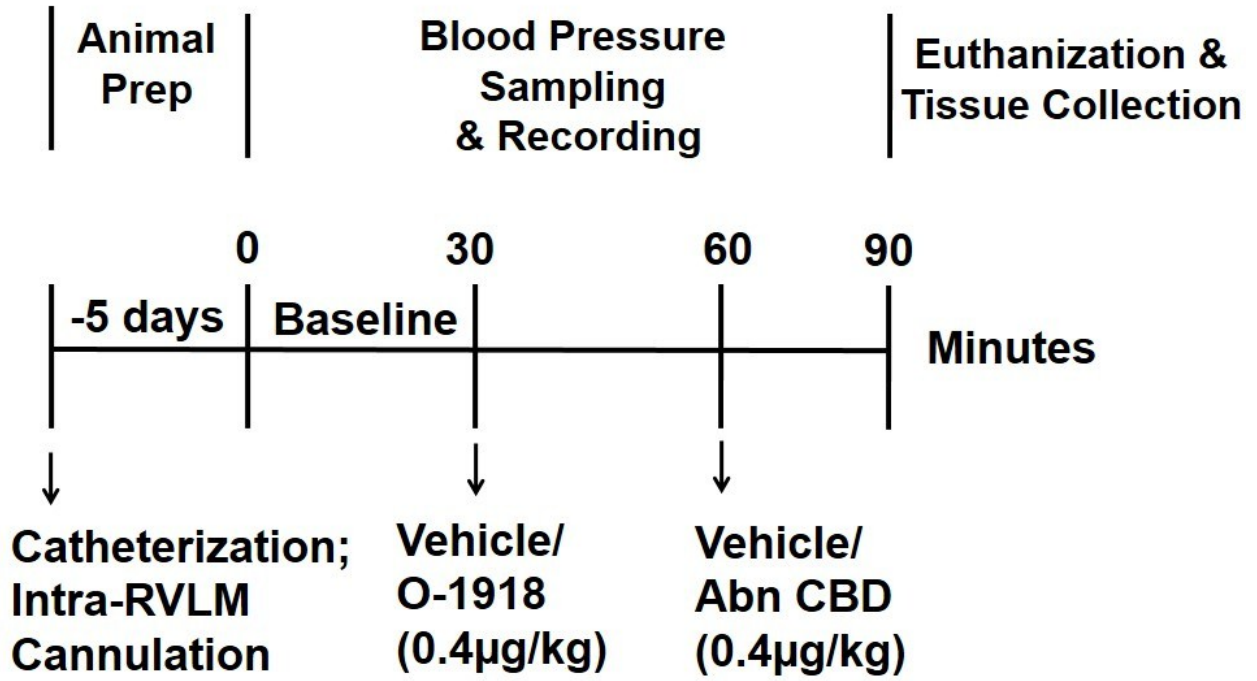


Figure 3.4. Time line for surgical procedures and experimental protocols for experiment 3.4.

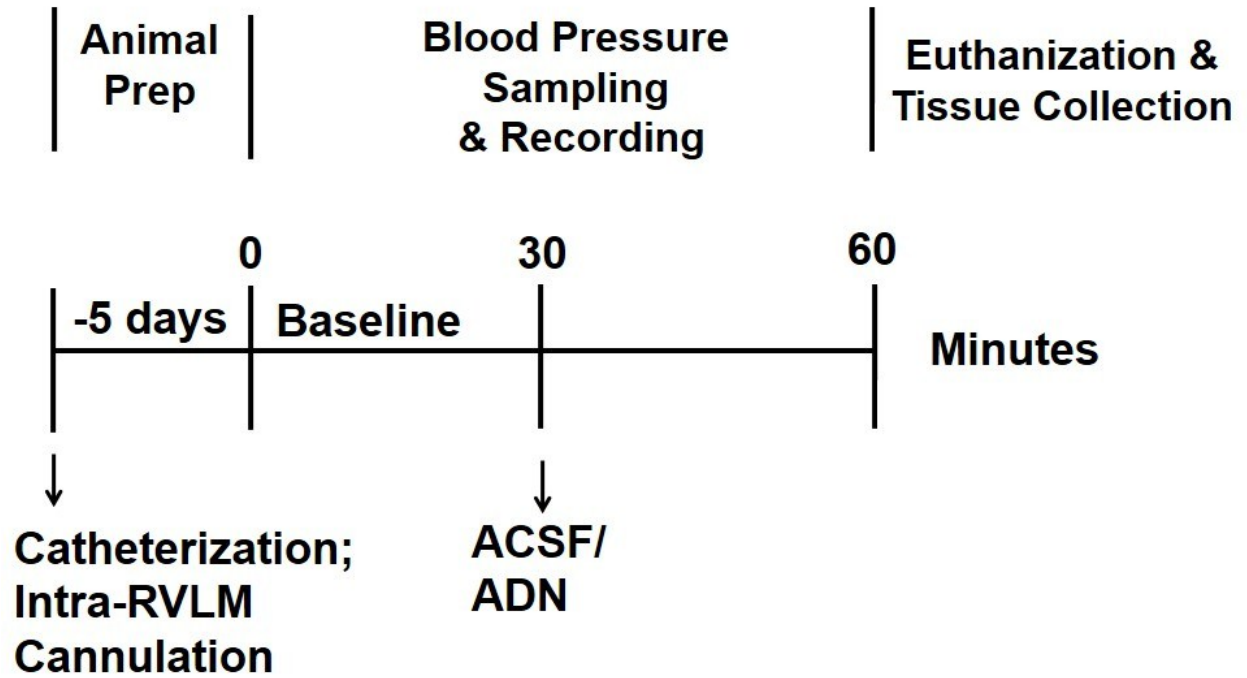


Figure. 3.5. Time line for surgical procedures and experimental protocols for experiment 3.5.

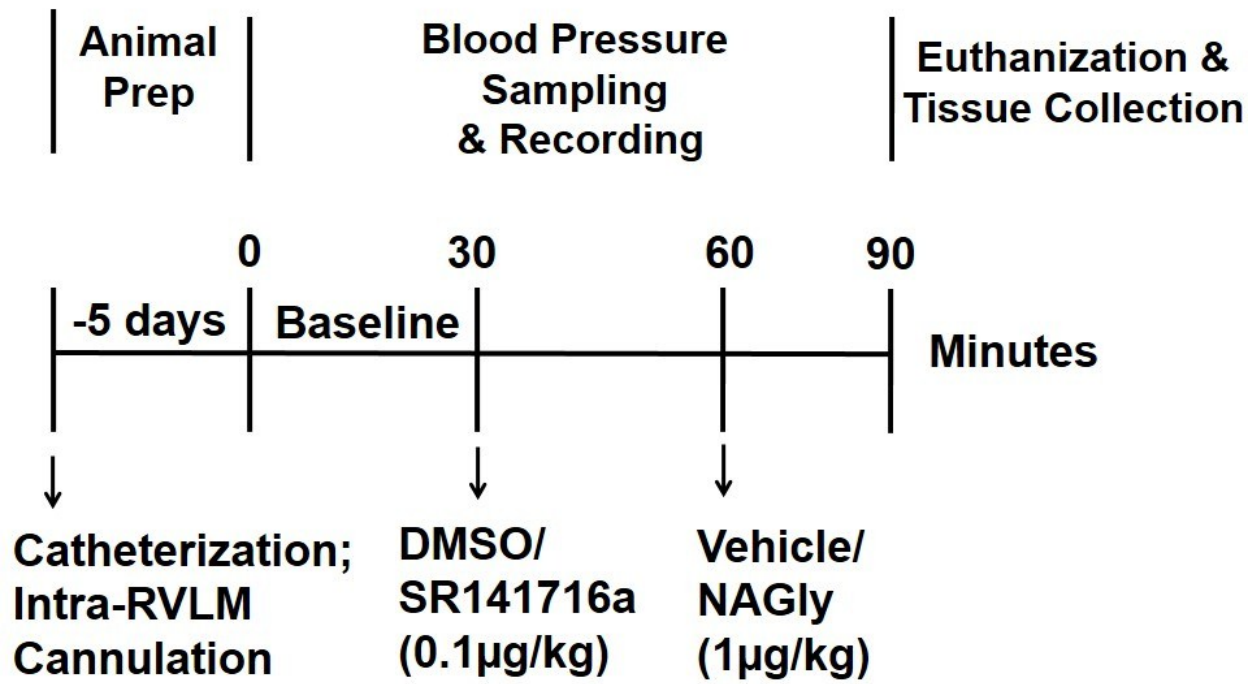


Table 3.1. MAP (mmHg) and HR (beats/min) values immediately before intra-RVLM administration of the GPR18 agonists or their vehicles.

Group	n	MAP	HR
Vehicle	5	110 ± 5	364 ± 12
Abn CBD	6	100 ± 8	376 ± 9
NAGly	6	113 ± 2	327 ± 20
O-1918	6	108 ± 3	343 ± 7
Atropine/Propranolol + Vehicle	6	120 ± 5	353 ± 8
Atropine/Propranolol + Abn CBD	6	120 ± 11	342 ± 24
Atropine/Propranolol + O-1918	6	113 ± 5	340 ± 16
ADN	4	111 ± 5	336 ± 17
DMSO/Vehicle	5	109 ± 7	325 ± 24
DMSO/NAGly	6	115 ± 5	356 ± 17
SR141716/Vehicle	6	107 ± 6	352 ± 12
SR141716/NAGly	6	110 ± 8	360 ± 22
Vehicle/Vehicle	5	108 ± 5	351 ± 9
Vehicle/Abn CBD	6	113 ± 4	362 ± 13
O-1918/Vehicle	6	117 ± 6	345 ± 18
O-1918/Abn CBD	6	112 ± 7	366 ± 12

Figure 3.6. Expression of GPR18 in the rat RVLM

(A) Expression of GPR18 (38kDa) in the rat RVLM compared with testes and spleen (positive controls) and liver (negative control). **(B)** Immunohistochemical staining showing the expression of GPR18 in the RVLM of perfused naïve rat brains. **(C)** Dual labeled immunofluorescence of perfused naïve rat brains showing co-expression of GPR18 and Tyrosine Hydroxylase (TH) expressing neurons in the RVLM.

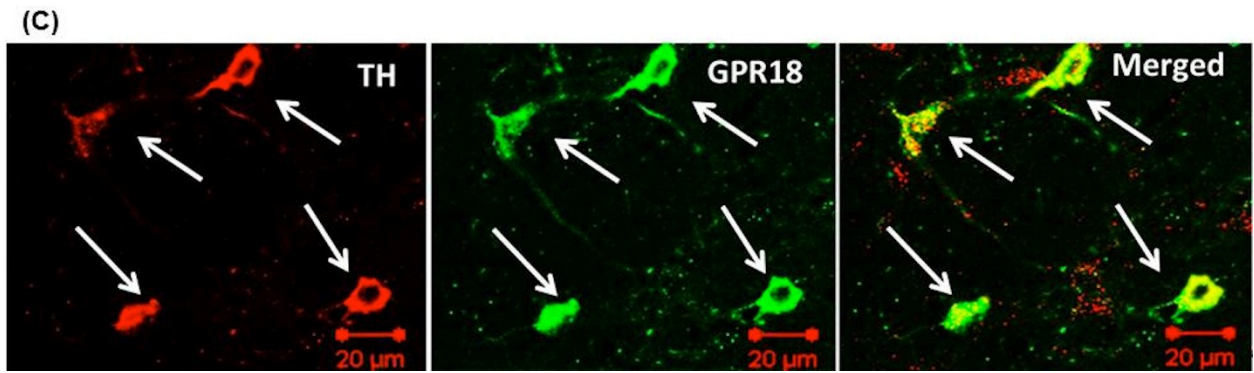
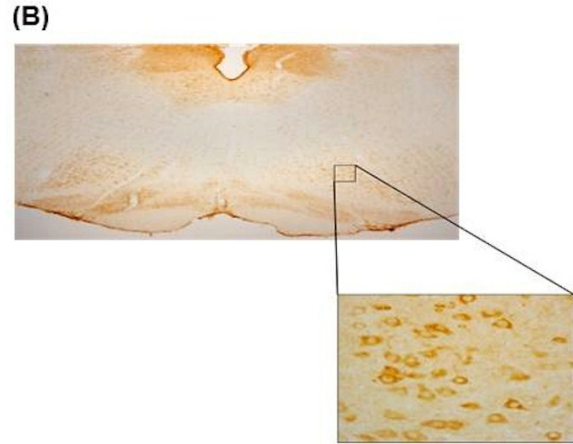
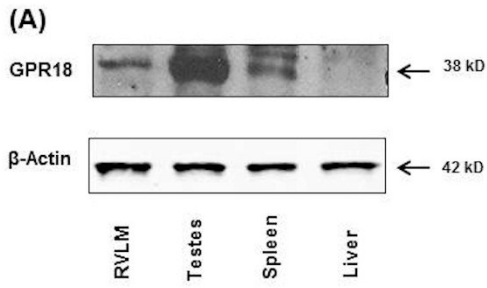


Figure 3.7. Effect of intra-RVLM Abn CBD or O-1918 on MAP and HR in conscious male rats

Effect of intra-RVLM Abn CBD or O-1918 (0.2, 0.4 or 0.8 μg) (**A, B**) on mean arterial pressure (MAP) and heart rate (HR) in conscious male rats. (**C, D**) Effect of vagal and beta adrenergic blockade with atropine (1mg/kg) and propranolol (1mg/kg), respectively, on the MAP and HR elicited by intra-RVLM Abn CBD or O-1918 (0.2, 0.4 or 0.8 μg). Effect of the endogenous ligand of GPR18, NAGly (0.5, 1, 2 or 4 μg) (**E, F**) on the MAP and HR. Values are mean \pm S.E.M. of 5-6 observations. * $P < 0.05$ vs. control (Vehicle).

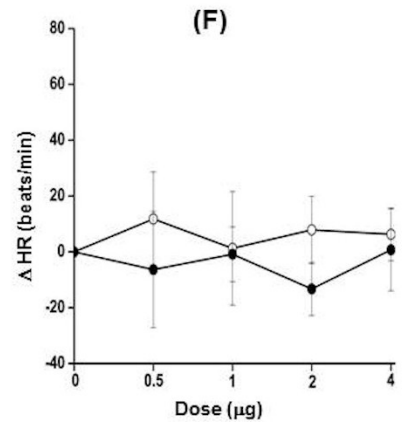
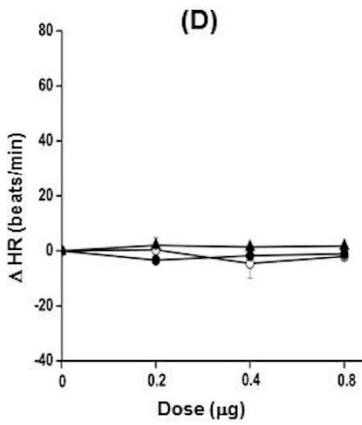
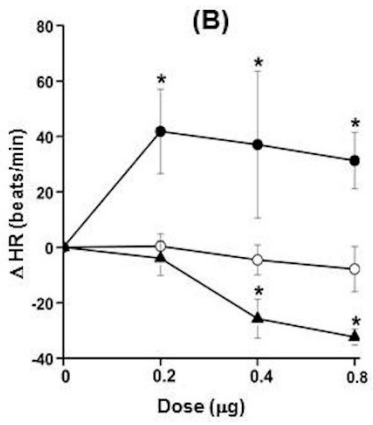
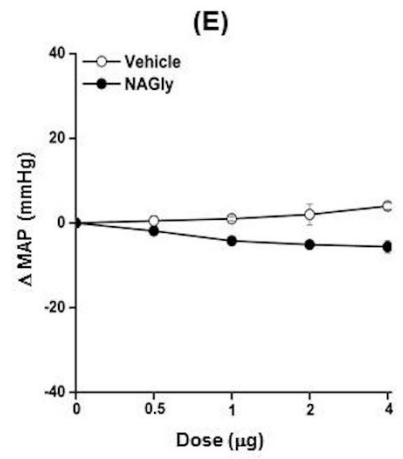
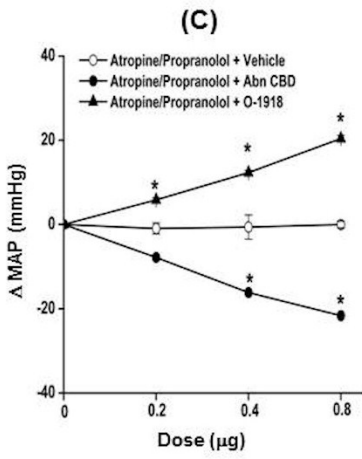
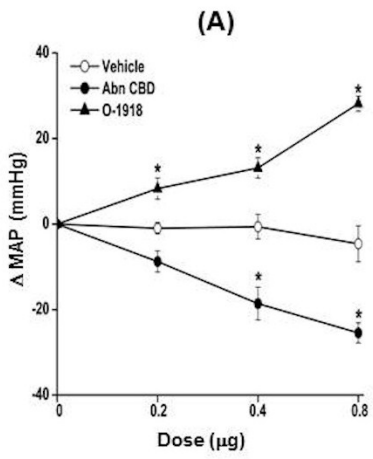


Figure 3.8. Effect of GPR18 activation and blockade on ADN and NOx levels

Western blots and total nitrate/nitrite levels in the RVLM (NOx content; index of NO) showing the effects of NAGly (1 μ g), Abn CBD (0.4 μ g), O-1918 (0.4 μ g), or O-1918 (0.4 μ g)/Abn CBD (0.4 μ g) or SR141716 (0.1 μ g)/NAGly (1 μ g) treatment on adiponectin (ADN) expression (**A**) and nitrate/nitrite (NOx) level (**B**) in the RVLM. Values are mean \pm S.E.M. of 5-6 observations.

* $P < 0.05$ vs. vehicle; # $P < 0.05$ vs. Abn CBD; ^ $P < 0.05$ vs. NAGly values.

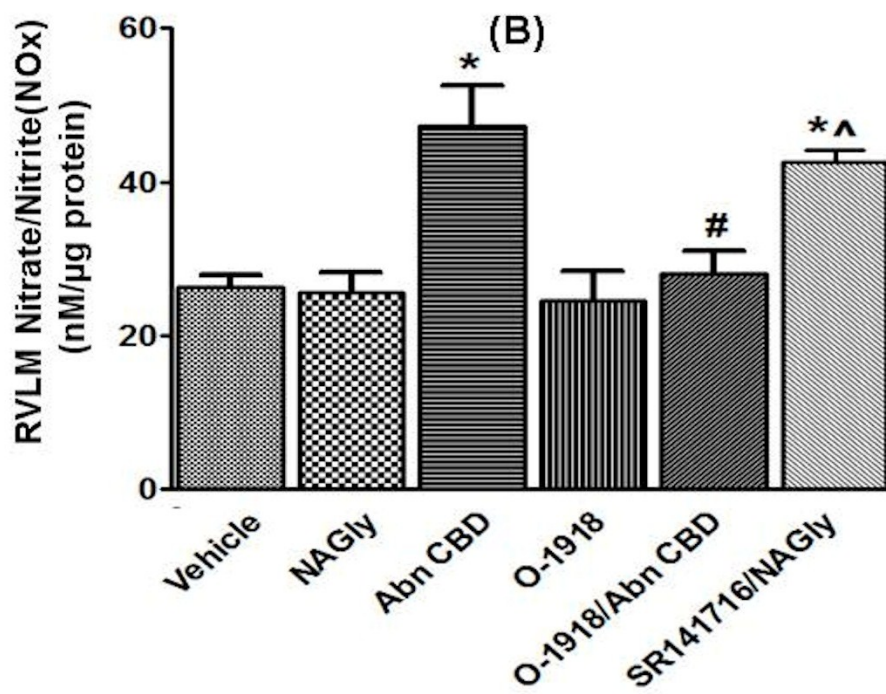
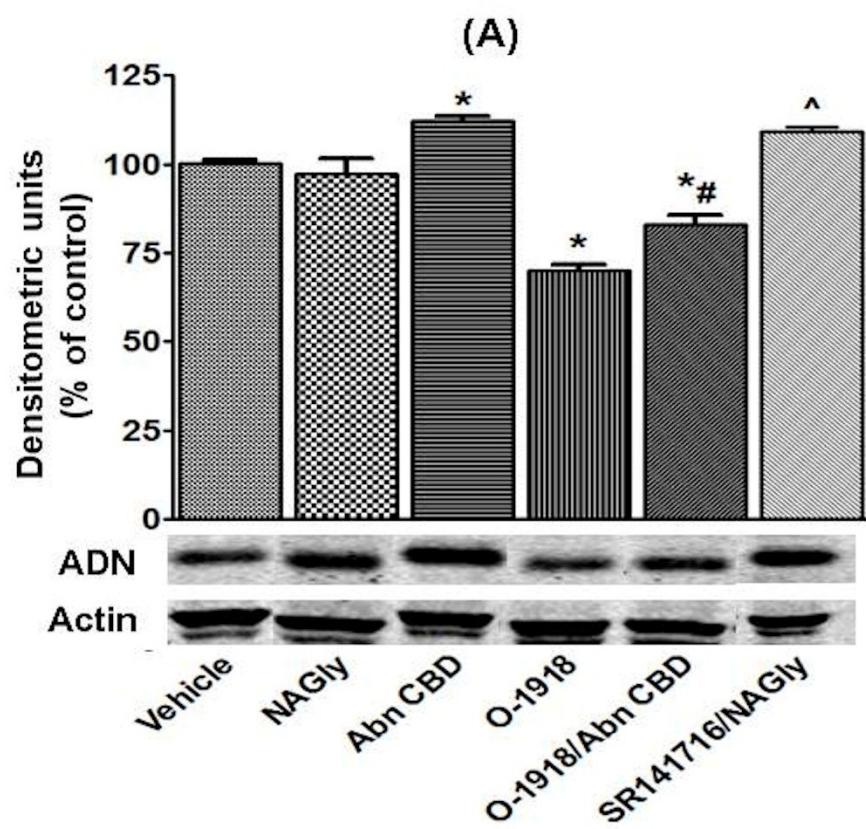


Figure 3.9. Effect of intra-RVLM adiponectin on MAP and HR

Effect of intra-RVLM adiponectin, ADN (0.25, 0.5, 1, 2 and 4 pmol) (**A, B**) on mean arterial pressure and heart rate in conscious male rats (n=4), compared with values obtained from vehicle (ACSF)-treated rats (n=3). Total nitrate/nitrite levels (NO_x; index of NO) (**C**) and DCFH-DA measured ROS (**D**) in the RVLM following ADN microinjection, compared with the corresponding values in the contralateral (control) RVLM. **P* < 0.05 vs. contralateral RVLM levels.

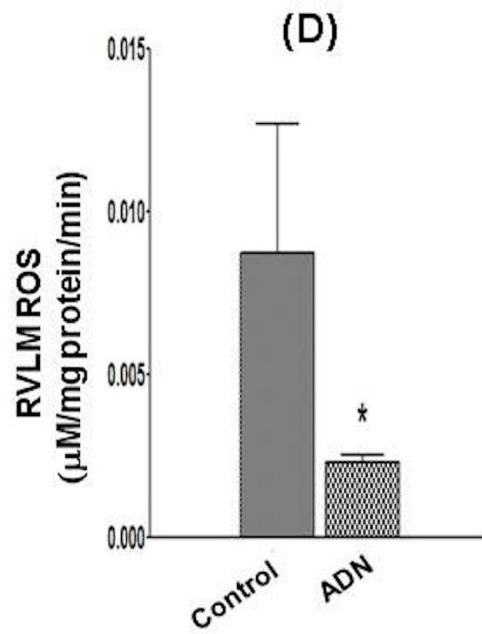
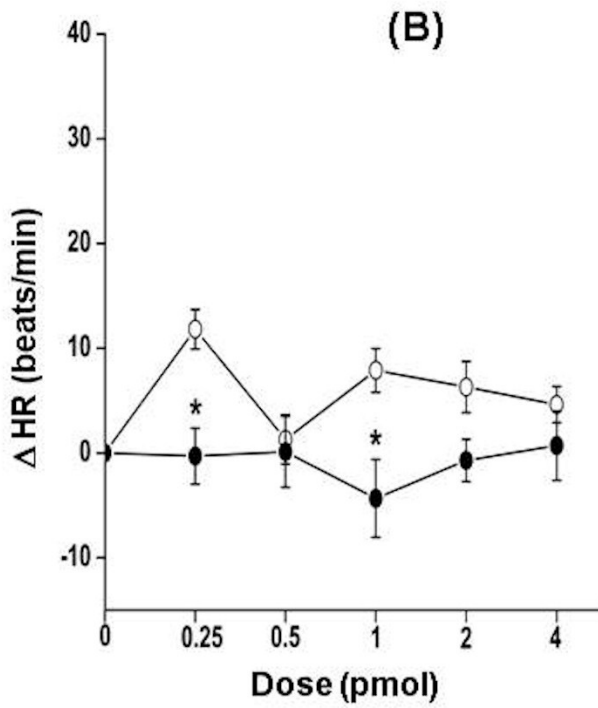
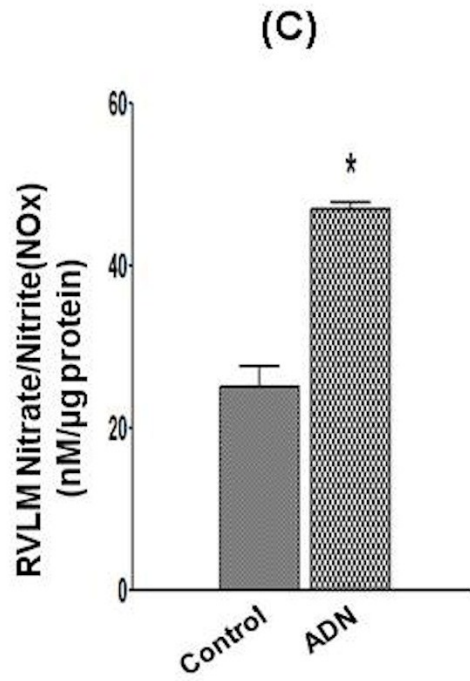
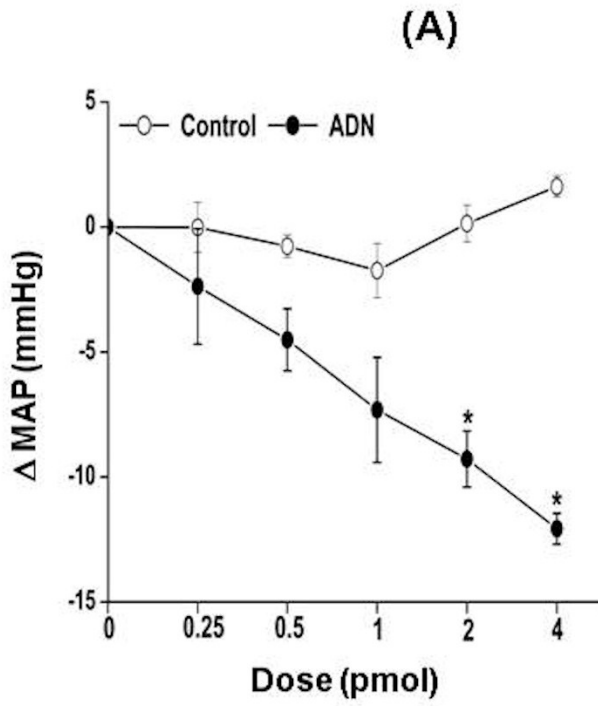


Figure 3.10. Co-expression of GPR18 with CB₁R and time course changes in MAP and HR caused by NAGly in the presence of SR141716

(A) Dual labeled immunofluorescence of perfused naïve rat brains showing co-expression of GPR18 and CB₁R in the RVLM neurons. Time course changes in Δ MAP (B) and Δ HR (C) caused by intra-RVLM microinjection of DMSO/Vehicle, DMSO/NAGly (1 μ g), SR141716 (0.1 μ g)/Vehicle and SR141716 (0.1 μ g)/NAGly (1 μ g). The animals in each group received intra-RVLM microinjections of either DMSO (diluted 1:16 in ACSF) or SR141716 (0.1 μ g) at -30 min followed by vehicle (methyl acetate) or NAGly (1 μ g) at time “0”. Pretreatment with SR141716 (CB₁R blockade) uncovered NAGly (GPR18)-mediated hypotension. Values are means \pm S.E.M. of 5 observations. * $P < 0.05$ compared with the corresponding control value.

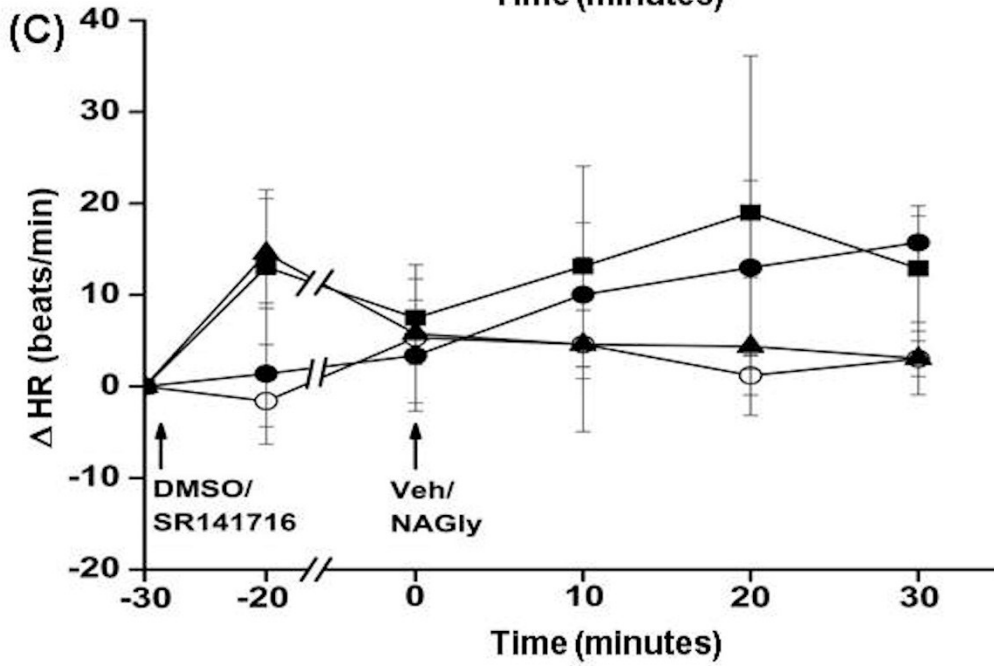
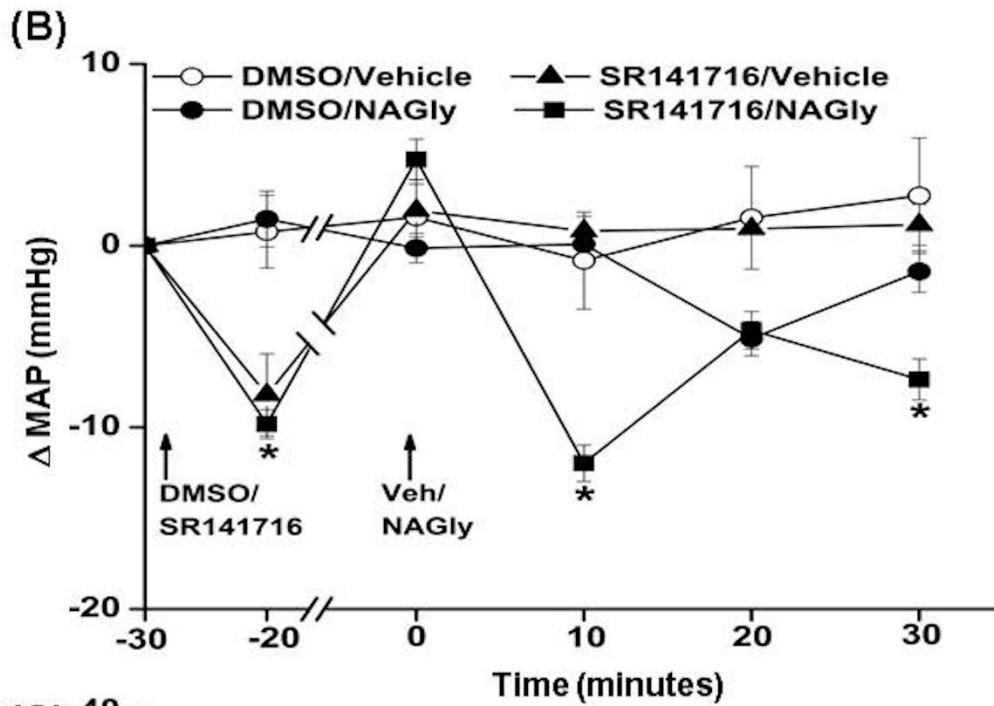
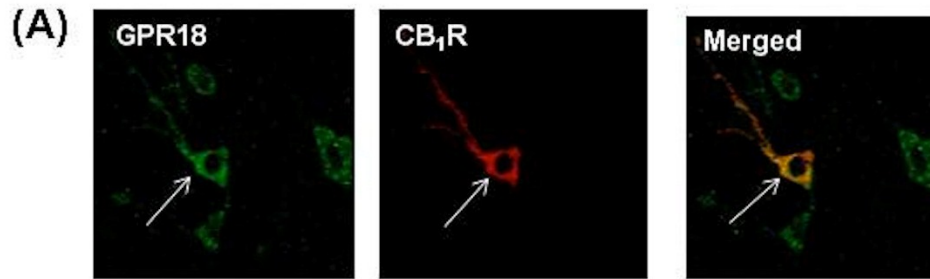


Figure 3.11. Time course of changes in MAP and HR following intra-RVLM microinjection of Abn CBD or O-1918

(A, B) Time course of changes in MAP and HR following intra-RVLM microinjection of vehicle/Abn CBD (0.4 μ g), O-1918 (0.4 μ g)/vehicle or O-1918 (0.4 μ g)/Abn CBD (0.4 μ g), compared with corresponding vehicle/vehicle values. The animals in each group received intra-RVLM microinjections of either vehicle (methyl acetate) or O-1918 (0.4 μ g) at -30 min followed by vehicle (methyl acetate) or Abn CBD (0.4 μ g) at time "0". Pretreatment with O-1918 abrogated the hypotensive effect produced by Abn CBD and the associated tachycardic response. The bar graphs (C-F) depict the area under the curve (AUC) data generated from the time-course values over the pretreatment (-30 to 0 min) and treatment (0-30 min) period. Compared with vehicle, the two groups that were pretreated with O-1918 exhibited significant elevations in BP and reductions in HR. Treatment with Abn CBD caused significant reduction in BP and increase in HR, and these responses were abrogated in O-1918 pretreated rats. Values are mean \pm S.E.M. of 5-6 observations. * $P < 0.05$ vs. vehicle.

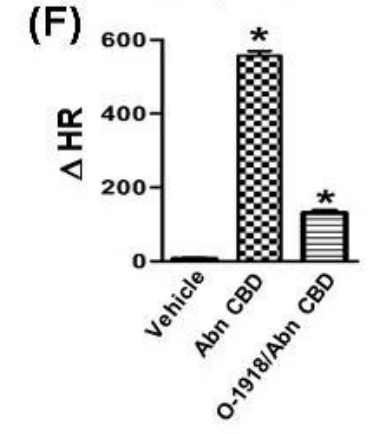
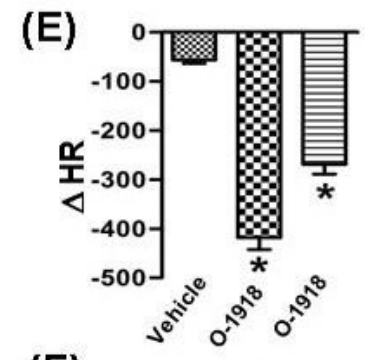
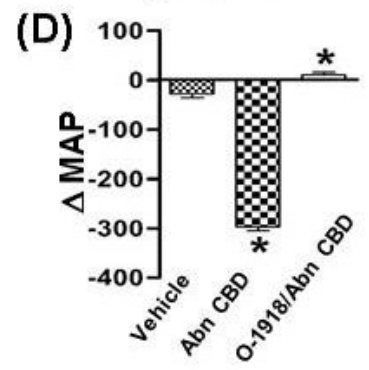
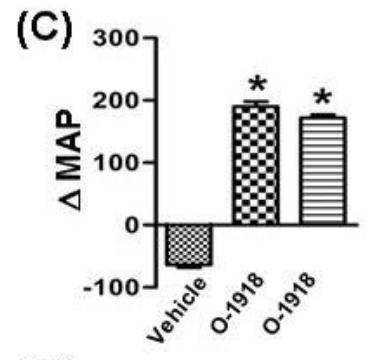
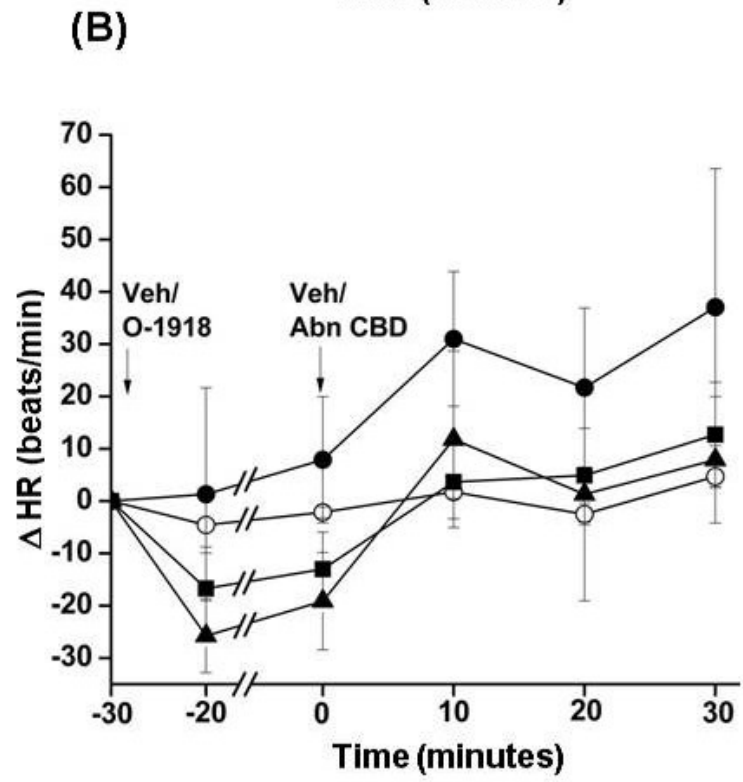
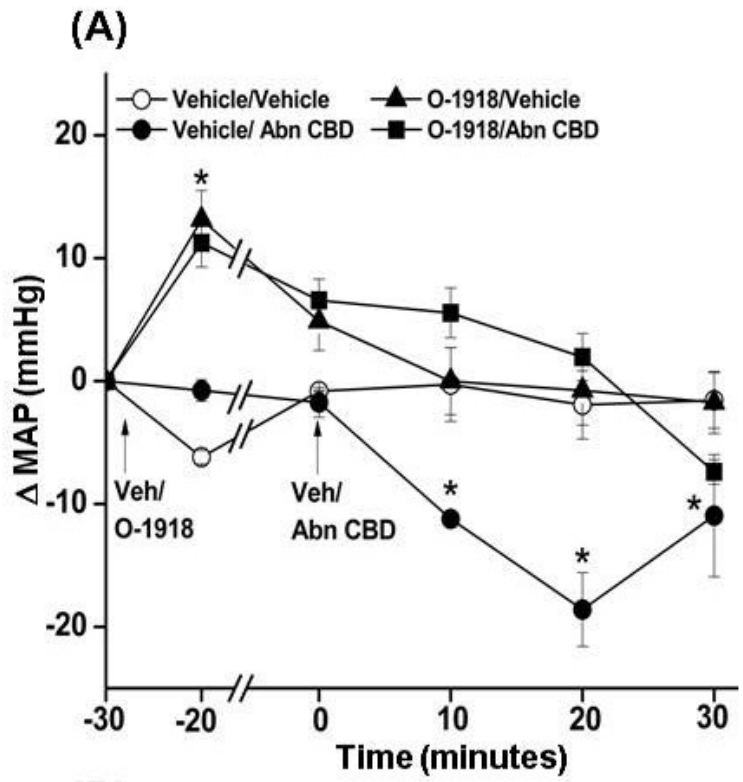
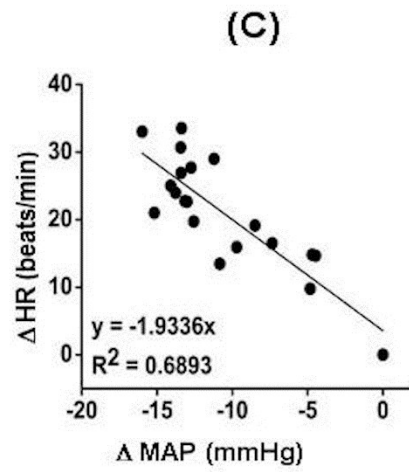
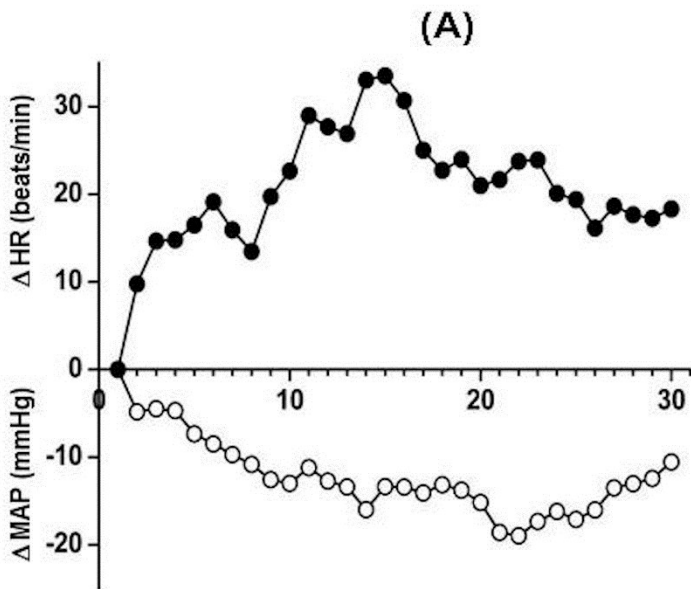


Figure 3.12. Time course changes in MAP and HR caused by intra-RVLM Abn CBD or O-1918 using 1-min time intervals

The time course changes in BP and HR caused by intra-RVLM Abn CBD (**A, C**) or O-1918 (**B and D**) microinjection (0.4 μ g), presented in Figure 3.11, have been reanalyzed using 1-min time intervals during the 30 min observation period. Abn CBD caused a hypotensive response that started within 2-3 min, and reached its nadir at approx. 20 min before it started to recover. The reduction in BP was associated with increases in HR with a maximum response achieved at approx. 15 min. Regression analysis was conducted to determine if the increases in the HR (independent variable) are inversely related to the decreases in BP, which is expected if the HR response is mediated, at least partly, via the baroreflex response. The significant inverse relationship (**C**) is consistent with the involvement of a baroreflex component in the tachycardic response that accompanied the hypotensive response caused by intra-RVLM Abn CBD (**A**). Notably, however, the tachycardic response started to dissipate before the hypotensive response reached its nadir (**A**), which contradicts a “purely” baroreflex mediated tachycardia. This finding might infer a counterbalancing effect of the central sympathoinhibitory effect of Abn CBD against the baroreflex mediated tachycardia. More studies are needed to investigate this possibility. Applying the same time-course and regression analysis criteria to data generated with O-1918 (0.4 μ g) revealed a pressor response that started within 2-3 min, and reached its peak at approx. 20 min (**B**). A bradycardic response was closely associated with (**B**), and inversely related to (**D**), the pressor response. S.E bars are omitted in A and B for clarity.

Intra-RVLM Abn CBD (0.4 μ g)



Intra-RVLM O-1918 (0.4 μ g)

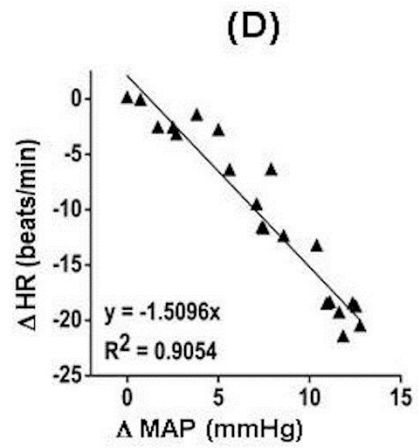
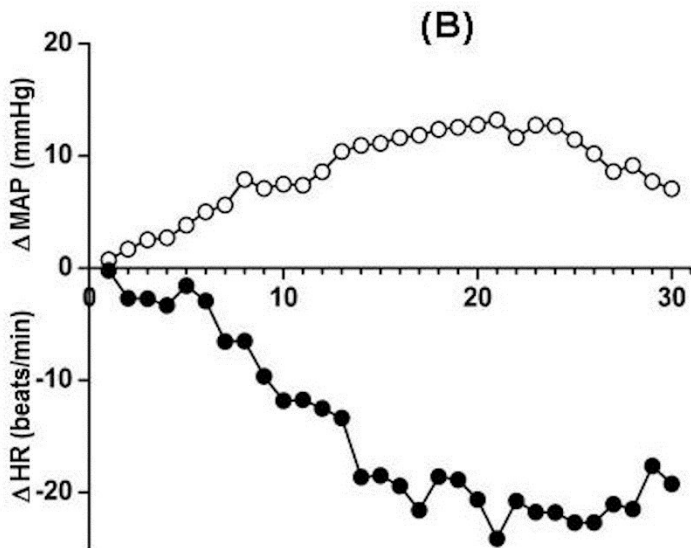
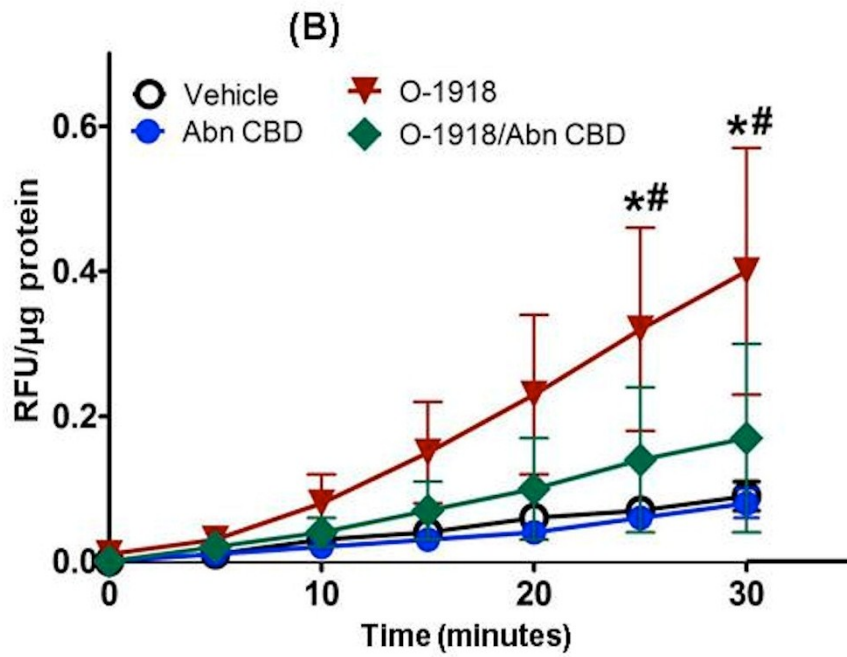
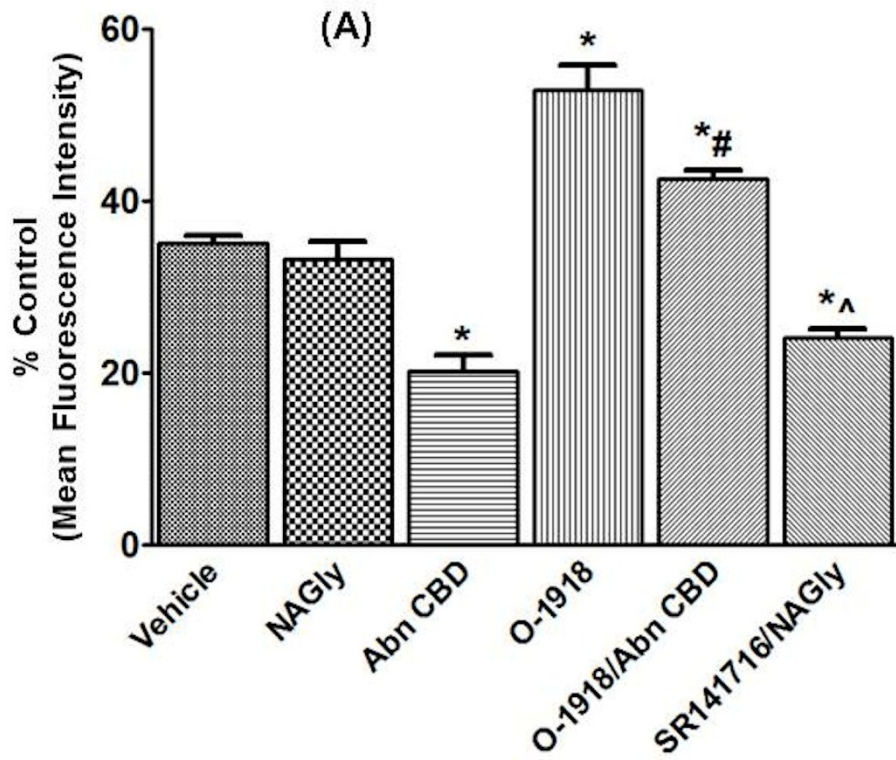


Figure 3.13. Effect of GPR18 activation or blockade on RVLM ROS levels

(A) Effect of vehicle, NAGly (1 μ g), Abn CBD (0.4 μ g), O-1918 (0.4 μ g), O-1918 (0.4 μ g)/Abn CBD (0.4 μ g) and SR141716 (0.1 μ g)/NAGly (1 μ g) on RVLM ROS levels shown by Dihydroethidium (DHE) staining visualized with confocal microscopy. Values are mean \pm S.E.M (n=5-6 rats). * P < 0.05 vs. vehicle values; # P < 0.05 vs. Abn CBD; ^ P < 0.05 vs. NAGly values.

(B) DCFH-DA measured ROS levels in terms of relative fluorescence units (RFU) in the RVLM following treatment with vehicle, Abn CBD (0.4 μ g), O-1918 (0.4 μ g) and O-1918 (0.4 μ g) /Abn CBD (0.4 μ g). The values of NAGly (1 μ g) were not significantly different from the control and are not shown for clarity. Values are mean \pm S.E.M (n=5-6 rats). * P < 0.05 vs. vehicle values; # P < 0.05 vs. Abn CBD.



3.7. Discussion

The following are the most important findings of the present study, which is the first to elucidate the function of RVLM GPR18 in conscious rats: (i) GPR18 is expressed in the TH-ir (presympathetic) neurons of the RVLM; (ii) activation and blockade of RVLM GPR18 causes dose-dependent reduction and elevation in MAP, respectively; (iii) GPR18 blockade (O-1918) abrogated Abn CBD-evoked hypotension; (iv) concomitant CB₁R activation dampens the hypotensive response caused by the endogenous GPR18 ligand NAGly; (v) RVLM GPR18 activation increases ADN and NO_x, and reduces ROS levels in the RVLM while its blockade produced the opposite neurochemical responses; (vi) Intra-RVLM ADN reduced BP and RVLM ROS, and increased RVLM NO_x. Collectively, the findings identify novel sympathoinhibitory role for RVLM GPR18 mediated, at least partly, by reducing oxidative stress in the RVLM.

While GPR18 mRNA is expressed in humans and mice (Vassilatis et al., 2003), these data are the first to demonstrate GPR18 protein expression in the RVLM of rats (Figs. 3.6A, B). Further, GPR18 is spatially located within the RVLM TH-ir neurons (Fig. 3.6C), which modulate sympathetic activity (Sved et al., 2003; Guyenet, 2006) inferring GPR18 involvement in central control of sympathetic tone and MAP. To elucidate the RVLM GPR18 functional role, we microinjected a selective GPR18 agonist or antagonist into the RVLM of conscious rats. Abn CBD causes CB₁R/CB₂R-independent peripheral vasodilation (Randall et al., 2004; Johns et al., 2007); in the latter study, Abn CBD was administered i.v. in anesthetized mice in much higher doses (30 mg/kg). Differences in the route of administration, dose, and anesthesia might explain the differences in the onsets and durations of the hypotensive responses and HR responses in the

two studies. Here, we report the first evidence that intra-RVLM Abn CBD caused dose-dependent hypotensive response (Fig. 3.7A). This response was GPR18-mediated because it was abrogated (Fig. 3.11A) by O-1918, a selective GPR18 antagonist (McHugh et al., 2010). Further, intra-RVLM O-1918 elicited dose-related pressor response (Fig. 3.7A). Prior cardiac vagal and adrenergic blockade virtually abolished the HR, but not the BP, responses caused by GPR18 activation or blockade (Figs. 3.7C, D), which suggest that the HR responses are mediated, at least partly, via cardiac baroreflex responses.

It is imperative to comment on the complexity of the observed HR responses. While the reciprocal relationships between HR and BP responses elicited by Abn CBD or O-1918 (Figs. 3.7 and 3.12) support the involvement of the baroreceptors in the HR responses, it is notable that atropine and propranolol also block baroreceptor-independent cardiac responses. It is highly unlikely that Abn CBD produced direct chronotropic effects because it was microinjected into the RVLM in substantially lower doses than those used systemically (Johns et al., 2007). Nonetheless, it is possible that the central sympathoinhibitory effect of intra-RVLM Abn CBD might have dampened the tachycardic response. This possibility might explain the plateaued tachycardic response despite the dose-dependent hypotensive response caused by Abn CBD (Fig. 3.7), and the decline of the tachycardic response from its peak before the hypotensive response reached its nadir (Fig. 3.12). Collectively, these findings suggest that RVLM GPR18 exerts a tonic restraining sympathoinhibitory influence on BP, and that such a central effect might contribute to the complexity of the observed HR responses.

The finding that intra-RVLM NAGly, the endogenous GPR18 ligand (Kohno et al., 2006), only modestly reduced BP (Fig. 3.7E) might: (i) cast doubt about the biological significance of RVLM GPR18, and (ii) infer that Abn CBD mediated hypotension was a consequence of local redox changes in the RVLM rather than direct agonism at RVLM GPR18. Notably, NAGly can inhibit the enzyme fatty acid amide hydrolase (FAAH) leading to increased AEA levels (Huang et al., 2001; Burstein et al., 2002). AEA may then activate central CB₁R, which mediate the sympathoexcitation/pressor response (Ibrahim and Abdel-Rahman, 2011), and ultimately counterbalance the GPR18-dependent reduction in BP caused by NAGly. In support of this notion are the following findings: (i) GPR18 and CB₁R are co-localized in RVLM neurons (Fig. 3.10A), which partly agrees with our findings that demonstrated CB₁R expression in RVLM TH-ir neurons (Ibrahim and Abdel-Rahman, 2011); (ii) the ability of intra-RVLM SR141716 (CB₁R blockade) to lower BP (Fig. 3.10B) is consistent with a sympathoexcitatory/pressor function for central CB₁R (Ibrahim and Abdel-Rahman, 2011); (iii) while NAGly alone had no effect on ADN, NO_x or ROS levels, prior CB₁R blockade (SR141716) uncovered the NAGly ability to increase ADN and NO (Figs. 3.8 A, B), and to reduce ROS levels (Fig. 3.13A) in the RVLM along with lowering BP (Fig. 3.10B). These novel findings replicated the redox and BP effects of Abn CBD (Figs. 3.8, 3.13A). Together, these data support the conclusion that the reductions in RVLM oxidative stress and BP are caused by Abn CBD direct agonism at GPR18 and suggest a functional role for GPR18-CB₁R interaction in the RVLM in modulating the local redox state and BP. It is imperative to comment on the pharmacological perspectives of our study because the endogenous GPR18 ligand NAGly lowered BP only following blockade of CB₁R, which might infer that CB₁R blockade is required for uncovering the GPR18-mediated responses. Our

present findings argue against generalizing this notion because the GPR18 agonist Abn CBD, which does not interact with CB₁R directly or indirectly (Jarai et al., 1999; Offertáler et al., 2003), lowered BP without prior CB₁R blockade.

It is important to comment on the complexity of RVLM NOS-derived NO in BP regulation because NO is implicated in GPR18-evoked hypotension (this study) and CB₁R-mediated hypertension (Ibrahim and Abdel-Rahman, 2012). Findings of the latter agree with a sympathoexcitatory role for RVLM NO (Chan et al., 2003). It is likely that the RVLM NO effect on BP depends on the source of NO, and its effect on local sympathoinhibitory (GABA) and sympathoexcitatory (L-glutamate) neuromodulators. For example, while GABA inhibition is implicated in the NO-dependent CB₁R-mediated pressor response (Ibrahim and Abdel-Rahman, 2012b), eNOS-derived NO mediates increases in RVLM GABA level, and hypotension (Kishi et al., 2001; Kishi et al., 2002). More studies are warranted to delineate the mechanisms of the differential role of RVLM NO in modulating sympathetic activity/BP, and to investigate the possibility that GPR18-dependent NO generation enhances RVLM GABA release/signaling in future studies.

A common anti-inflammatory role for ADN (Nanayakkara et al., 2012) and GPR18 (Vuong et al., 2008) infers a role for ADN in GPR18 signaling. We present the first evidence that GPR18 activation in the RVLM increases ADN (Figs. 3.8A) along with findings that support a functional role for ADN in GPR18 signaling because RVLM GPR18 blockade (O-1918): (i) reduced RVLM ADN (Fig. 3.8A) and elevated BP; (ii) abrogated the GPR18 (Abn CBD)-mediated BP and neurochemical responses (Figs. 3.8, 3.11). Next, we show, for the first time,

that ADN produced dose-dependent reductions in BP (Fig. 3.9A), increased RVLM NO_x (Fig. 3.9C), and reduced RVLM ROS levels (Fig. 3.9D). The ADN doses were based on a reported microinjected dose of ADN in area postrema (Fry et al., 2006). In the latter study, ADN caused modest pressor response and inconsistent changes in HR. Differences in the neuroanatomical targets, and use of anesthesia in the reported study might account for the differences in BP responses. Further, a very recent study (Song et al., 2013) showed that the active (globular) ADN fraction replicates ADN-evoked neuroprotection via a reduction in oxidative stress. Together, these findings implicate RVLM ADN in the GPR18-mediated reductions in neuronal oxidative stress (ROS) in the RVLM and BP.

We reasoned that the GPR18-mediated neurochemical responses, discussed above, would ultimately reduce BP via ROS reduction in RVLM because enhanced and suppressed ROS production in the RVLM leads to elevation and reduction in BP, respectively (Kishi et al., 2004; Yoshitaka, 2008). Using two different methods, we showed that activation of RVLM GPR18 reduced neuronal ROS while its blockade increased neuronal ROS and abrogated the GPR18-mediated ROS reduction (Fig. 3.13). These redox findings, which paralleled the ADN (Fig. 3.8A) and BP (Figs. 3.11A, B) responses, reinforce a well-established role for oxidative stress in RVLM neurons in sympathoexcitation and BP elevation. Further, the findings lend credence to our conclusion that ADN-dependent reduction in RVLM ROS plays a crucial role in GPR18-mediated hypotension.

In summary, the present study yields new insight into the role of the novel cannabinoid receptor GPR18 in central (RVLM) control of BP. We present the first evidence that RVLM

GPR18 mediates reductions in oxidative stress and BP in conscious rats. The neurochemical findings suggest that increases in ADN and NO and reduced ROS production in the RVLM play significant role in GPR18-mediated hypotension. In the RVLM, CB₁R serves a counterbalancing role against GPR18, which explains the negligible hypotensive response caused by the endogenous GPR18 ligand NAGly in our model system. Future studies are warranted to delineate the GPR18 signaling implicated in the neurochemical effects described in this study, and to investigate the role of GPR18 signaling in hypertension. Such studies will advance our knowledge of the role of endocannabinoids in the neural control of BP and might lead to the development of novel antihypertensive drugs.

CHAPTER FOUR - MOLECULAR MECHANISMS UNDERLYING ROSTRAL VENTROLATERAL MEDULLA GPR18-MEDIATED HYPOTENSION IN CONSCIOUS NORMOTENSIVE RATS

4.1. Abstract

The endocannabinoid receptor GPR18 is expressed in tyrosine hydroxylase-immunoreactive (TH-ir) neurons in the rostral ventrolateral medulla (RVLM), and its direct activation (abnormal cannabidiol; Abn CBD) and blockade (O-1918) lowers and elevates blood pressure (BP), respectively, in conscious rats. However, the molecular mechanisms for GPR18 regulation of BP are not fully understood. We hypothesized that the RVLM PI3K/Akt-ERK1/2-nNOS and adenylyl cyclase-cAMP networks play pivotal roles in GPR18 modulation of oxidative stress and BP via local adiponectin (ADN). Intra-RVLM GPR18 activation (Abn CBD; 0.4 µg) enhanced RVLM Akt, ERK1/2 and nNOS phosphorylation and ADN level, during the hypotensive response, and prior GPR18 blockade (O-1918) produced the opposite effects, and abrogated Abn CBD-evoked responses in conscious Sprague Dawley rats. Inhibition of RVLM PI3K/Akt (wortmannin), ERK1/2 (PD98059) or nNOS (N^ω-propyl-L-arginine, NPLA) or activation of adenylyl cyclase (forskolin) virtually abolished the intra-RVLM Abn CBD-evoked hypotension. Further, wortmannin, PD98059, NPLA or forskolin abrogated GPR18-mediated increases in RVLM Akt, ERK1/2, nNOS phosphorylation and ADN levels, along with increased ROS generation. Our integrative and neurochemical findings implicate the RVLM PI3K/Akt-ERK1/2-nNOS/ADN and cAMP in GPR18 modulation of RVLM redox state and BP in conscious rats.

4.2. Introduction

Several novel cannabinoid (CB) receptors mediate the diverse cardiovascular effects of synthetic and natural cannabinoids (Offertáler et al., 2003). One putative cannabinoid receptor, the “Abnormal Cannabidiol” (Abn CBD) receptor, is GPR18 (Kohno et al., 2006; McHugh et al., 2010). This novel G-protein coupled CB receptor is distinct from the typical CB₁R and CB₂R because: 1) N-arachidonoyl glycine (NAGly), an endogenous metabolite of the endocannabinoid, anandamide, acts as a selective agonist at GPR18 (McHugh et al., 2010); 2) Abn CBD, a synthetic isomer of the phytocannabinoid, cannabidiol (CBD), causes GPR18-dependent vasorelaxation of isolated mesenteric arteries (McHugh et al., 2010); 3) the GPR18 antagonist O-1918 attenuates Abn CBD-mediated vasorelaxation in a CB₁R/CB₂R-independent manner (Offertáler et al., 2003; McHugh et al., 2010). Although GPR18 mRNA is detected in human and mice brainstem (Vassilatis et al., 2003), and NAGly is abundant in the brain (Huang et al., 2001), our recent findings (Penumarti and Abdel-Rahman, 2014) are the first to demonstrate: (i) GPR18 protein expression in TH-ir RVLM neurons, which modulate the sympathetic activity (Sved et al., 2003; Kishi et al., 2004; Guyenet, 2006); (ii) activation and blockade of intra-RVLM GPR18 lowers and elevates BP, respectively, suggesting a restraining influence for RVLM GPR18 on sympathetic tone and BP.

The molecular mechanisms of the RVLM GPR18 modulation of central sympathetic tone and BP are not known. Activation of GPR18 (Abn CBD) in the periphery leads to vasodilation and a decrease in BP (Offertáler et al., 2003) and the endogenous GPR18 agonist, NAGly, causes vasodilation via NO release (Kishi et al., 2001). GPR18 belongs to the Gi/o coupled GPCRs

family, and its activation *in vitro* causes inhibition of cAMP production (Kohno et al., 2006), activation of ERK1/2 (Alexander, 2012) and Akt (McCollum et al., 2007). Notably, the role of the PI3K-Akt-ERK1/2 pathway in modulating the redox state in the RVLM and subsequently BP remains controversial because enhanced ERK1/2 phosphorylation and elevated NO levels in the RVLM mediate the sympathoexcitation/pressor response (Ibrahim and Abdel-Rahman, 2012b; Ibrahim and Abdel-Rahman, 2012a; Chan and Chan, 2014) or sympathoinhibition/hypotension (Zhang and Abdel-Rahman, 2005; Nassar and Abdel-Rahman, 2008; Chan and Chan, 2014). These responses are ROS-dependent because brainstem ROS elevation (Kishi et al., 2004; Hirooka, 2008; Yoshitaka, 2008), and inhibition (Zanzinger and Czachurski, 2000; Campese et al., 2004) are implicated in elevation and reduction in BP, respectively. It is likely that downstream signaling molecules triggered by the activation of the PI3K-Akt-NOS pathway determine the final redox state and the ultimate BP response caused by the activation of different receptors in the RVLM. Here, we hypothesized that RVLM ADN generation, due to local PI3K-Akt-nNOS activation or cAMP inhibition, underlies GPR18-mediated hypotension. ADN confers neuroprotection via reduced oxidative stress (Song et al., 2013), and our preliminary findings showed that intra-RVLM ADN lowers BP and increases NO and decreases ROS levels in RVLM (Penumarti and Abdel-Rahman, 2014). Therefore, experiments undertaken in this study focus on elucidating the molecular mechanisms implicated in RVLM GPR18 modulation of local redox state and BP. Selective GPR18 agonists and antagonist along with other pharmacologic interventions were directly microinjected into the RVLM of conscious unrestrained rats, and molecular studies were conducted in RVLM tissues to complement the integrative findings.

4.3. Materials and Methods

Male Sprague-Dawley rats (Charles River Laboratories, Raleigh, NC), 11 to 12 weeks old, were used in this study. After vascular catheterization and intra-RVLM cannulation, the rats were housed individually in separate cages in a room with controlled environment. The temperature was maintained at $23 \pm 1^{\circ}\text{C}$, $50 \pm 10\%$ humidity and a 12 hr light/dark cycle. Food (Prolab Rodent Chow; Granville Milling, Creedmoor, NC) and water were provided ad libitum. All surgical and experimental procedures are detailed in the supplement and were conducted in accordance with and approved by the East Carolina University Institutional Animal Care and Use Committee and in accordance with the Guide for the Care and Use of Laboratory Animals (Institute for Laboratory Animal Research, 2011). These surgeries were performed as reported in our previous studies (Zhang and Abdel-Rahman, 2002; Penumarti and Abdel-Rahman, 2014). On the day of the experiment the arterial catheter was flushed with heparin in saline (200 U/ml) and connected to a Gould-Statham (Oxnard, CA) pressure transducer and BP of unrestrained rats was measured as mentioned in our previous studies (Nassar et al., 2011; Ibrahim and Abdel-Rahman, 2012a).

4.3.1. Intravascular Catheterization and Intra-RVLM Cannulations

These surgeries were performed as reported in previous studies (Zhang and Abdel-Rahman, 2002) and detailed in the Materials and Methods chapter.

4.3.2. Western Blotting

Animals were euthanized and following decapitation, brains were removed, flash frozen in 2-methylbutane on dry ice, and stored at -80°C until use. Brains were equilibrated to -20°C and sectioned with a cryostat (HM 505E; Microm International GmbH, Waldorf, Germany) to the rostral ventrolateral medulla (RVLM) according to atlas coordinates. Tissue from the RVLM was collected bilaterally using a 0.75 mm punch instrument as described in other studies (Ibrahim and Abdel-Rahman, 2011) from approximately -12.8 to -11.8 mm relative to bregma² from treatment and control groups. Tissue was homogenized on ice by sonication in cell lysis buffer (20 mM Tris pH 7.5, 150 mM NaCl, 1 mM EDTA, 1 mM EGTA, 1% Triton X-100, 2.5 mM sodium pyrophosphate, 1 mM β -glycerolphosphate, 1 mM activated sodium orthovanadate) containing a protease inhibitor cocktail (Roche Diagnostics, Indianapolis, IN). Protein concentration in samples was quantified using a standard Bio-Rad protein assay system (Bio-Rad Laboratories, Hercules, CA). Protein extracts (20 μg per lane) were denatured at 97°C for 5 minutes, separated on NuPAGE Novex Bis-Tris 4 to 12% SDS-PAGE gels (Invitrogen, Carlsbad, CA) using MOPS NuPAGE running buffer, and electroblotted to nitrocellulose membranes using standard procedures. The membranes were blocked for 1 hr with Odyssey blocking buffer (LICOR Biosciences Lincoln, NE) and incubated with a mixture of rabbit anti-ERK1/2 or rabbit anti-Akt and mouse anti-pERK1/2 or mouse anti-pAkt (1:500) overnight. All of the antibodies were purchased from Cell Signaling Technology (Danvers, MA). After washing the membranes with PBS, they were incubated for 1 hr with a mixture of IRDye680-conjugated goat anti-rabbit and IRDye800-conjugated goat anti-mouse (1:10,000; LICOR Biosciences).

Membranes were washed with PBS containing 0.1% Tween 20 and bands representing total and phosphorylated proteins were visualized simultaneously using an Odyssey Infrared Imager and analyzed with Odyssey application software v.3 (LICOR Biosciences). All data are presented as mean values of the integrated density ratio of phosphorylated protein normalized to its corresponding total protein.

4.3.3. Dot Blotting

The dot blot technique was employed to detect and analyze the proteins present in the sample. It differs from the western blot in that, the protein samples are spotted through circular templates directly on to the nitrocellulose membrane instead of being separated electrophoretically. This technique was employed to permit multiple protein level measurements in the limited amount of RVLM tissue in the groups that received pharmacologic interventions to inhibit local kinases of NOS. A 96 well Bio-dot Microfiltration Apparatus (Bio-Rad Laboratories, Inc., Hercules, CA) was used and the samples were loaded in the wells and directly separated by vacuum filtration on to nitrocellulose membrane. The membrane was then washed with PBS and allowed to dry. The membranes were blocked for 1 hr with Odyssey blocking buffer (LICOR Biosciences Lincoln, NE) and incubated with primary and secondary antibodies as described for Western Blotting and visualized simultaneously using an Odyssey Infrared Imager and analyzed with Odyssey application software v.3 (LICOR Biosciences). All data are expressed as mean values of the integrated density ratio of phosphorylated protein normalized to its corresponding total protein.

4.3.4. Measurement of Reactive Oxygen Species by DCFH-DA.

RVLM specimen from treated and control groups were homogenized in PBS. The homogenate was centrifuged (14,000 rpm) for 20 min. Protein in the supernatant was quantified using a standard Bio-Rad protein assay system. 2', 7'-dichlorofluorescein diacetate (DCFH-DA) (Molecular Probes) was dissolved in DMSO (12.5 mM) and kept at -80°C in the dark. It was freshly diluted with 50 mM phosphate buffer (pH 7.4) to 125 µM before experiment. DCFH-DA was added to RVLM homogenate supernatant (10 µl) in a 96-well microtiter plate for a final concentration (25 µM). 2', 7'-Dichlorofluorescein (DCF) was used for a 6-point standard curve. Quantification was conducted by examining fluorescence intensity using a microplate fluorescence reader at excitation 485 nm/emission 530 nm. Kinetic readings were recorded for 30 min at 37°C. ROS level was calculated by relative DCF fluorescence per µg protein. Positive and negative controls were used to validate the assay as in our previous studies (McGee and Abdel-Rahman, 2012).

4.4. Experimental Groups and Protocols

4.4.1. Experiment 1: Effect of RVLM GPR18 activation or blockade on ERK1/2, Akt and nNOS phosphorylation in conscious male SD rats.

Recent studies from this laboratory showed that activation (Abn CBD) of GPR18 produced a hypotensive response while blocking (O-1918) the receptor caused a pressor effect (Worlein et al., 2011). In the experiment reported herein, we used the tissues collected at the end of the cardiovascular studies in the recent study (Worlein et al., 2011) to test the hypothesis that an

enhanced phosphorylation of ERK1/2 (pERK1/2), Akt (pAKT), and nNOS (p-nNOS) in the RVLM contributes to the GPR18 (Abn CBD)-mediated hypotensive response. Five groups of rats (n=5-6 each) that received one of the following treatments – vehicle (methyl acetate), NAGly (1 µg), Abn CBD (0.4 µg), O-1918 (0.4 µg) or O-1918 (0.4 µg)/Abn CBD (0.4 µg) were used in this experiment. We measured the ratio of RVLM pERK1/2, pAKT, and p-nNOS to their corresponding total proteins in the RVLM of animals treated with intra-RVLM GPR18 ligands or vehicle as detailed under methods.

4.4.2. Experiment 2: Effect of intra-RVLM inhibition of ERK1/2, PI3K/Akt or NOS inhibition on Abn CBD-mediated hypotensive response.

The objective of these experiments, and the complementary ex vivo experiments (see below), was to support a causal role for the GPR18 (Abn CBD)-induced enhancement of the phosphorylation of Akt, ERK1/2 and nNOS in RVLM and the hypotensive response. Therefore, we investigated the BP and HR responses elicited by intra-RVLM Abn CBD in the absence or presence of pharmacologic inhibitors of PI3K/Akt (wortmannin; 100 nmol), ERK1/2 (PD98059; 50 µmol) (Alessi et al., 1995; Seyedabadi et al., 2001), eNOS (L-NIO; 100 pmol) (El-Mas et al., 2009) or nNOS (*N*^ω-Propyl-L-arginine hydrochloride NPLA); (250 pmol) (El-Mas et al., 2009). DMSO was used as the vehicle for all kinase inhibitors, while saline was the vehicle for NOS inhibitors. DMSO was diluted in ACSF (1:16) and this DMSO/ACSF mixture had no effect on BP, which is consistent with our previous findings (Nassar et al., 2011). The rats in each group (n=6 unless specified) received one of the following treatment combinations: DMSO + vehicle (n=3), DMSO + Abn CBD (n=3), saline + vehicle (n=3), saline + Abn CBD (n=3), wortmannin

+ vehicle, wortmannin + Abn CBD, PD98059 + vehicle, PD98059 + Abn CBD, L-NIO + vehicle, L-NIO + Abn CBD, NPLA + vehicle, NPLA + Abn CBD. The respective pretreatment (DMSO, saline, wortmannin, PD98059, L-NIO or NPLA) was microinjected into the RVLM 30 min prior to Abn CBD (0.4 µg) or vehicle injection. All intra-RVLM injections were of equal volume (80nl). At the end of 30 min cardiovascular measurements after Abn CBD or vehicle injection, the rats were euthanized and brains were collected and stored at -80°C for biochemical measurements.

4.4.3. Experiment 3: Effect of intra-RVLM activation of adenylyl cyclase on Abn CBD-mediated hypotensive response.

We investigated the effect of intra-RVLM adenylyl cyclase (AC) activation (forskolin; 50 µmol) (McHugh et al., 2010) on the GPR18-mediated hypotensive response in 4 groups of conscious male rats (n=3-6). The rats in each group received one of the following treatment combinations: DMSO + vehicle (n=3), DMSO + Abn CBD (n=3), forskolin + vehicle (n=6), forskolin + Abn CBD (n=6). Forskolin or an equal volume of DMSO (vehicle for forskolin) was administered 30 min prior to microinjection of Abn CBD (0.4 µg) or its vehicle (methyl acetate). At the end of 30 min cardiovascular measurements after Abn CBD or vehicle injection, the rats were euthanized and brains were collected and stored at -80°C for biochemical measurements.

4.4.4. Experiment 4: Effect of Akt-ERK1/2-nNOS inhibition or increased cAMP on GPR18-mediated molecular events in the RVLM.

Ex vivo biochemical studies were conducted in RVLM tissues collected from treatment and control animals employed in the integrative (in vivo) cardiovascular studies. In these studies, we investigated the changes in RVLM pERK1/2, pAKT, p-nNOS, ADN and ROS levels caused by intra-RVLM Abn CBD in the absence or presence of inhibitors of ERK1/2 (PD98059) or PI3K/Akt (Wortmannin), nNOS (NPLA) or activation of adenylyl cyclase (forskolin) using Dot Blot and DCFH-DA assay (ROS).

4.4.5. Drugs

Abn CBD, NAGly and O-1918 were purchased from Cayman Chemical (Ann Arbor, MI). Methyl acetate, wortmannin, PD98059, forskolin and dimethyl sulfoxide were purchased from Sigma Aldrich (St. Louis, MO). L-NIO and NPLA were purchased from Tocris Biosciences (Ellisville, MO) and dissolved in sterile saline. Sterile saline was purchased from B.Braun Medical (Irvine, CA). DMSO was used as the vehicle for PD98059, wortmannin and forskolin. Methyl acetate was used as the vehicle for Abn CBD, O-1918, NAGly. Methyl acetate and DMSO were tested in at least three animals without any significant changes in MAP and HR from the basal levels. All intra-RVLM injections were of equal volume (80nl).

4.5. Data Analysis and Statistics

All values were expressed as mean \pm S.E.M change from their respective baselines. All other statistical analyses were done using a one-way or repeated-measures ANOVA with

Bonferroni post hoc test and Student's t test, Prism 5.0 software (GraphPad Software Inc., San Diego, CA) was used to perform statistical analysis and $P < 0.05$ was considered significant.

4.6. Results

4.6.1. Intra-RVLM Abn CBD Increased RVLM ERK1/2, Akt and nNOS phosphorylation. Intra-RVLM GPR18 activation (Abn CBD; 0.4 $\mu\text{g}/\text{animal}$) increased ERK1/2, nNOS and Akt phosphorylation in the RVLM (Fig. 4.2). The endogenous GPR18 ligand, NAGly, only increased RVLM Akt phosphorylation, and the increase was much smaller than that caused by Abn CBD (Fig. 4.2). By contrast, RVLM GPR18 blockade (O-1918, 0.4 $\mu\text{g}/\text{animal}$) reduced RVLM Akt, ERK1/2 and nNOS phosphorylation, and abrogated Abn CBD enhancement of ERK1/2, nNOS and Akt phosphorylation (Fig. 4.2).

4.6.2. Intra-RVLM PI3K/Akt, ERK1/2 or nNOS Inhibition Attenuated Abn CBD evoked Hypotensive Response. Time-course (Figs. 4.3-4.5 A & B) and area under the curve (AUC) data (Figs. 4.3-4.5 C & D) showed that, compared to the DMSO/vehicle (methylacetate) or saline/vehicle, pretreatment with the PI3K/Akt inhibitor, wortmannin (100 nmol), the ERK1/2 inhibitor, PD98059 (50 μmol), or the nNOS inhibitor, NPLA (250 pmol), caused a significant elevation in BP (Figs. 4.3-4.5 A). The BP subsided toward control level before subsequent Abn CBD or vehicle administration (Figs. 4.3-4.5 A). Prior inhibition of RVLM PI3K/Akt (Figs. 4.3 A & C), ERK1/2 (Fig. 4.4 A & C) or nNOS (Fig. 4.5 A & C), but not eNOS (L-NIO; 100 pmol) (Fig. 4.5 A & C), attenuated ($P < 0.05$) Abn CBD (0.4 μg) mediated hypotensive response. RVLM eNOS inhibition (L-NIO) had no effect on BP or on the Abn CBD-evoked hypotension (Fig. 4.5 A & C). The changes in HR in the different treatment groups were not significantly different.

However, when the HR responses were expressed as AUC, a significant bradycardic response occurred when Abn CBD was administered following DMSO, but not following saline (Figs. 4.3-4.5 B).

4.6.3. Increased RVLM cAMP levels abrogate GPR18-mediated Hypotension. Intra-RVLM activation of adenylyl cyclase/elevation of cAMP levels by forskolin (50 μ mol) significantly increased BP (Figs. 4.6 A & C), but had no effect on HR (Figs. 4.6 B & D). Forskolin pretreatment abrogated central GPR18-mediated hypotensive (Figs. 4.6 A & C) and bradycardic (Fig. 4.6 D) responses.

4.6.4. Akt-ERK1/2-nNOS inhibition or Increased cAMP Abrogates GPR18-mediated molecular events in the RVLM. Dot blot analysis was used to permit multiple measurements of the targeted proteins as well as ADN and ROS levels in the limited amount of RVLM tissues collected from treatment and control groups. Importantly, this methodology was verified by the resemblance of the Western (Fig. 4.2) and dot (Fig. 4.7) blot data for Akt, ERK1/2 and nNOS. Intra-RVLM pretreatment with wortmannin, NPLA, PD98059 or forskolin significantly ($P < 0.05$) attenuated the GPR18 (Abn CBD)-mediated increases in ERK1/2, Akt, nNOS phosphorylation, and in ADN levels in the RVLM (Fig. 4.7 A-D). These neurochemical findings paralleled the BP responses (Figs. 4.3-4.6). While RVLM GPR18 activation had no effect on the low basal ROS levels (Fig. 4.7 E), RVLM GPR18 blockade significantly increased local ROS levels and abrogated the Abn CBD-mediated hypotension in our recent study (Penumarti and Abdel-Rahman, 2014). Similarly, inhibition of Akt, ERK1/2, or nNOS

phosphorylation or elevation of cAMP abrogated GPR18-mediated hypotension (Figs. 4.3-4.6), and resulted in significant elevation in ROS levels in the RVLM (Fig. 4.7 E).

Figure 4.1. Time line for surgical procedures and experimental protocols for cardiovascular measurements.

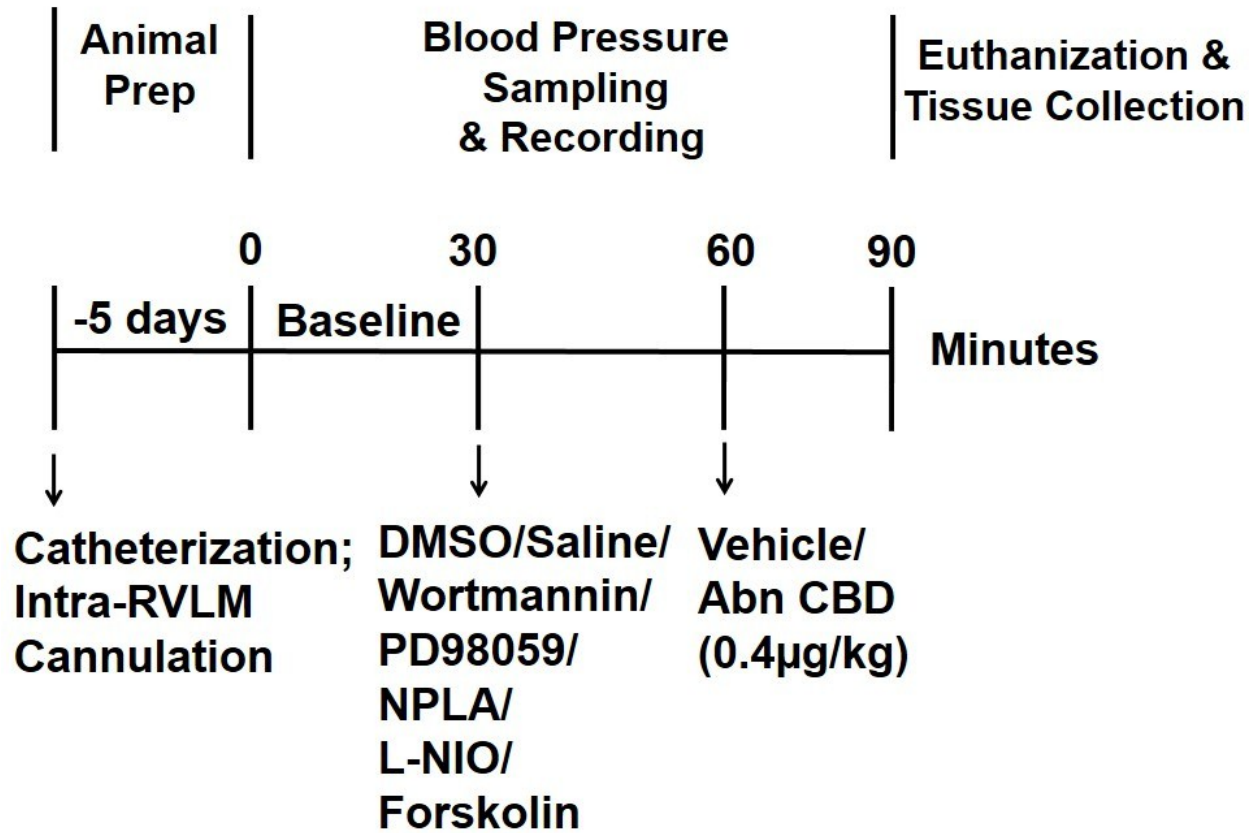


Table 4.1. MAP (mmHg) and HR (beats/min) values before pharmacological intervention.

Values of Mean Arterial Pressure (MAP, mmHg) and Heart Rate (HR, beats/min) at the end of pretreatment (time=30min) and immediately before treatment with the indicated intervention or its vehicle.

Pretreatment/Treatment	n	MAP	HR
DMSO/Vehicle	3	121 ± 3	359 ± 10
Saline/Vehicle	3	116 ± 5	372 ± 8
DMSO/Abn CBD	3	111 ± 8	363 ± 7
Saline/Abn CBD	3	113 ± 7	330 ± 18
PD98059/Vehicle	6	115 ± 3	324 ± 11
PD98059/Abn CBD	6	120 ± 1	367 ± 12
Wortmannin/Vehicle	6	118 ± 5	328 ± 14
Wortmannin/Abn CBD	6	117 ± 6	349 ± 16
NPLA/Vehicle	6	123 ± 5	342 ± 9
NPLA/Abn CBD	6	114 ± 5	361 ± 11
L-NIO/Vehicle	6	122 ± 9	335 ± 10
L-NIO/Abn CBD	6	119 ± 2	357 ± 13
Forskolin/Vehicle	6	112 ± 7	345 ± 17
Forskolin/Abn CBD	6	109 ± 8	376 ± 15

Figure 4.2. Effect of GPR18 ligands on pERK1/2, pAkt and p-nNOS levels

Effects of NAGly (1 μg), Abn CBD (0.4 μg), O-1918 (0.4 μg) or O-1918 (0.4 μg)/Abn CBD (0.4 μg) on ERK1/2 (**A**), nNOS (**B**) and Akt (**C**) phosphorylation compared to total protein. Data are presented as the integrated density ratio of the phosphorylated protein to its total protein and expressed as percent of control (vehicle). Values are mean \pm S.E.M. of 5-6 observations. * $P < 0.05$ vs. vehicle; # $P < 0.05$ vs. Abn CBD. Veh, vehicle (methylacetate); NAG, NAGly; AbC, Abn CBD.

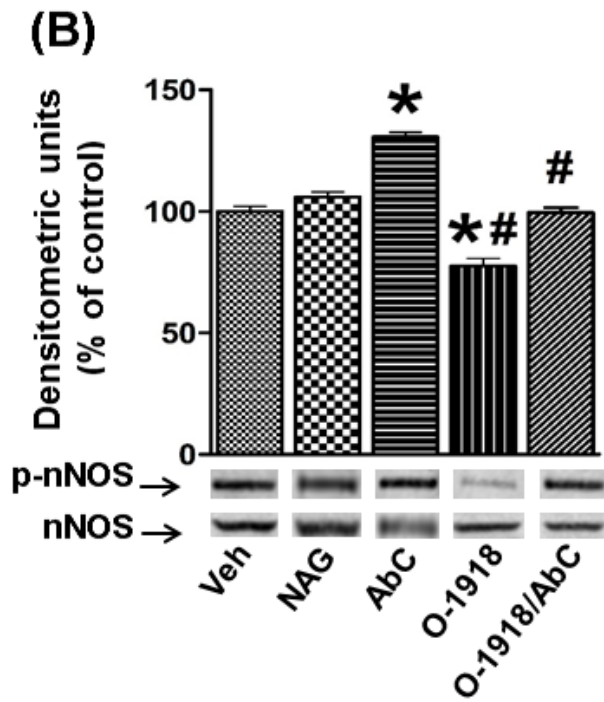
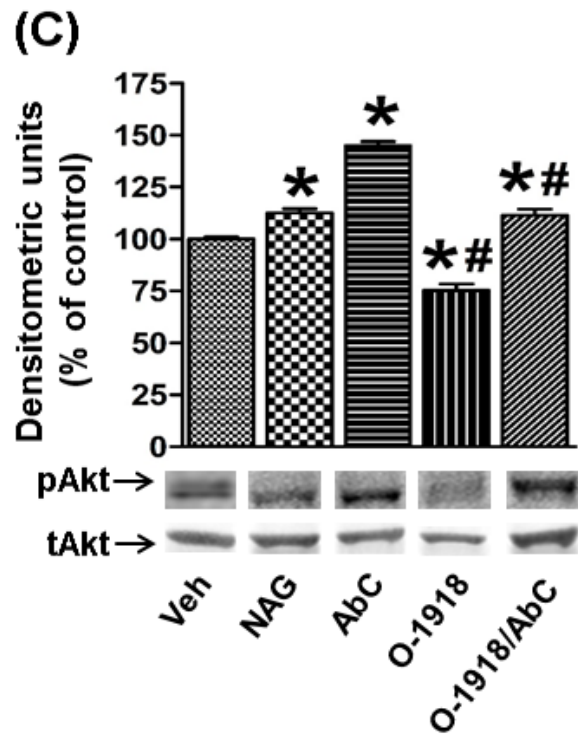
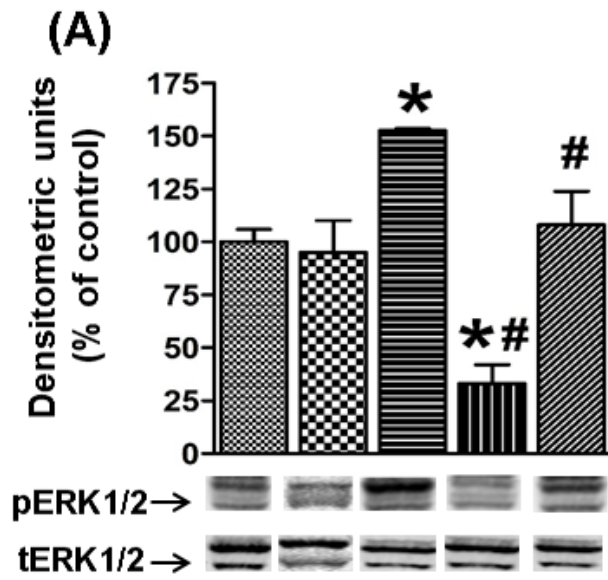


Figure 4.3. Effect of intra-RVLM wortmannin on GPR18 mediated sympathoinhibition

Time course changes in mean arterial pressure (Δ MAP) (**A**) and heart rate (Δ HR) (**B**) following intra-RVLM Abn CBD (0.4 μ g) or equal volume of vehicle in conscious rats pretreated, 30min earlier, with the PI3K/Akt inhibitor wortmannin (100 nmol) or equal volume of its vehicle (DMSO). **C** and **D**, area under the curve (AUC) values generated from the time course data, show that inhibition of Akt phosphorylation (wortmannin) abrogates the GPR18 (Abn CBD)-mediated hypotensive response. The values of the two groups that received the same pretreatment (DMSO or wortmannin) were combined for clarity; n = 6 for all groups except DMSO/Vehicle and DMSO/Abn CBD groups (n = 3, each). * $P < 0.05$ vs. control (vehicle); # $P < 0.05$ vs. Abn CBD. DM, DMSO; Veh, vehicle (methylacetate); AbC, Abn CBD; Wort, wortmannin.

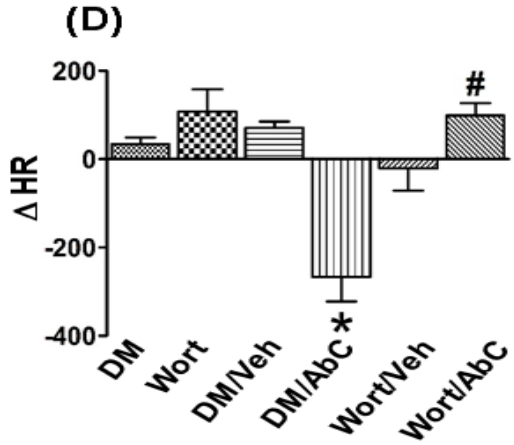
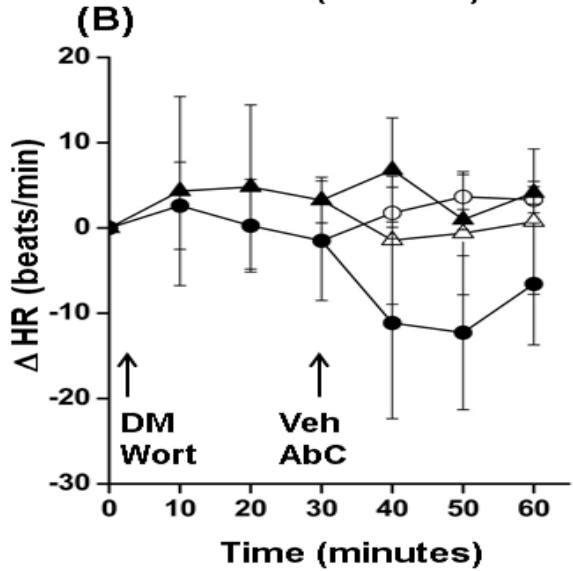
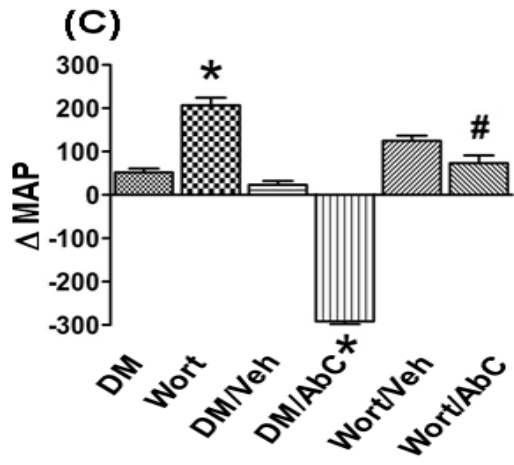
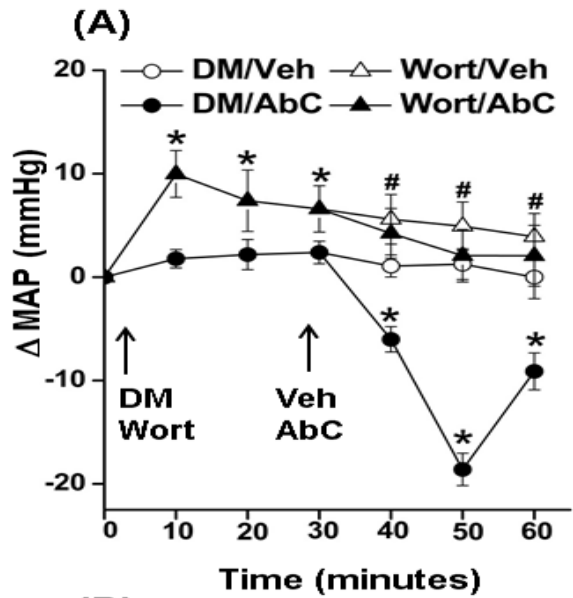


Figure 4.4. Effect of intra-RVLM PD98059 on GPR18 mediated sympathoinhibition

(A) Mean arterial pressure (Δ MAP), and (B) heart rate (Δ HR) changes following intra-RVLM microinjections of either DMSO (diluted 1:16 in ACSF) or PD98059 (50 μ mol) at 0 min and subsequent vehicle (methyl acetate) or Abn CBD (0.4 μ g) microinjection. Pretreatment with PD98059 abrogated the GPR18 (Abn CBD)-mediated hypotensive response. Panels C-D depict the area under the curve (AUC) data generated from the time-course values over the pretreatment (0 to 30 min) and treatment (30-60 min) periods. Compared with vehicle, PD98059 caused significant elevation in BP (Figs. A & C). Abn CBD caused significant reduction in BP, and this response was abrogated in PD98059 pretreated rats (Figs. A & C). All pretreatment groups that received the same drugs were combined for clarity; n = 6 for all groups except DMSO/Vehicle and DMSO/Abn CBD groups (n = 3, each). *P < 0.05 vs. control (vehicle); #P < 0.05 vs. Abn CBD. DM, DMSO; Veh, vehicle (methylacetate); AbC, Abn CBD; PD, PD98059.

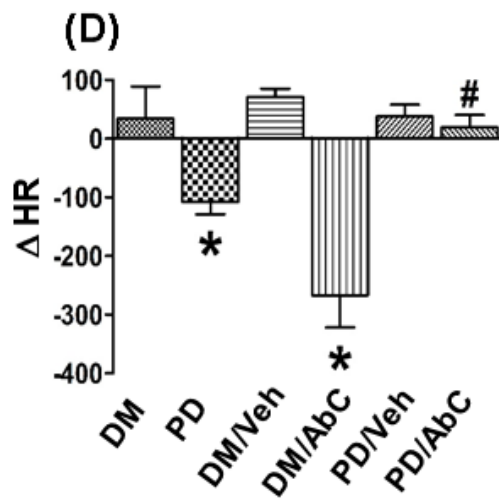
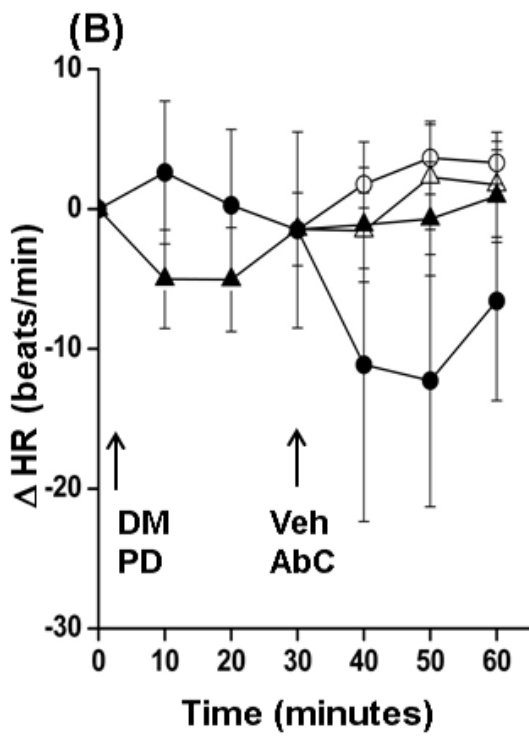
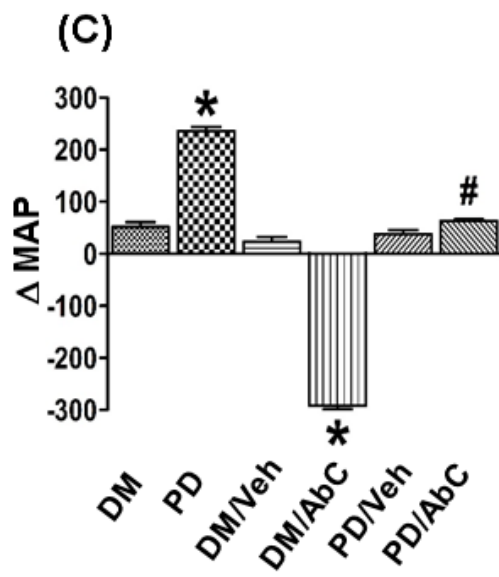
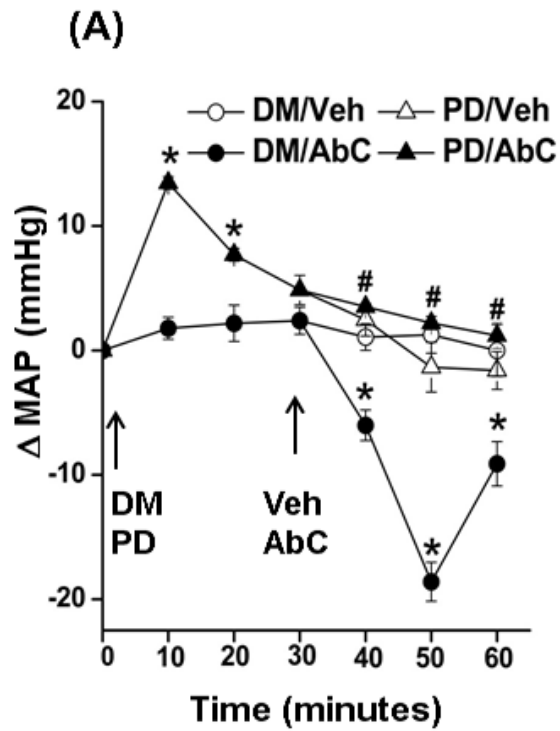


Figure 4.5. Effect of intra-RVLM nNOS and eNOS inhibition on GPR18 mediated hypotension

Changes in **(A)** mean arterial pressure (Δ MAP), and **(B)** heart rate (Δ HR) following intra-RVLM microinjections Abn CBD (0.4 μ g) or equal volume of vehicle in conscious male Sprague-Dawley rats pretreated, 30 min earlier, with L-NIO (selective eNOS inhibitor; 100 pmol) or NPLA (selective nNOS inhibitor; 250 pmol). Pretreatment with NPLA, but not L-NIO, virtually abolished the GPR18 (Abn CBD)-mediated hypotensive response, which rules out eNOS involvement in GPR18 signaling. **C** and **D** depict the area under the curve (AUC) data generated from the time-course values over the pretreatment (0 to 30 min) and treatment (30-60 min) periods. All pretreatment groups that received the same drugs were combined for clarity; $n = 6$ for all groups except Saline/Vehicle and Saline/Abn CBD groups ($n = 3$, each). $*P < 0.05$ vs. control (vehicle); $\#P < 0.05$ vs. Abn CBD. Sal, saline; Veh, vehicle (methylacetate); AbC, Abn CBD.

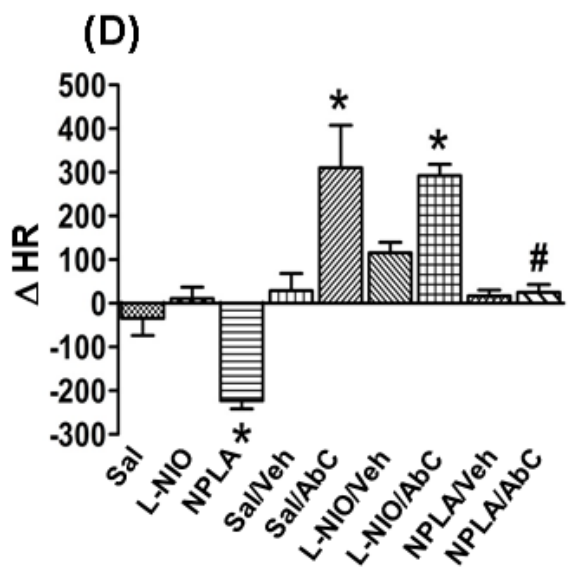
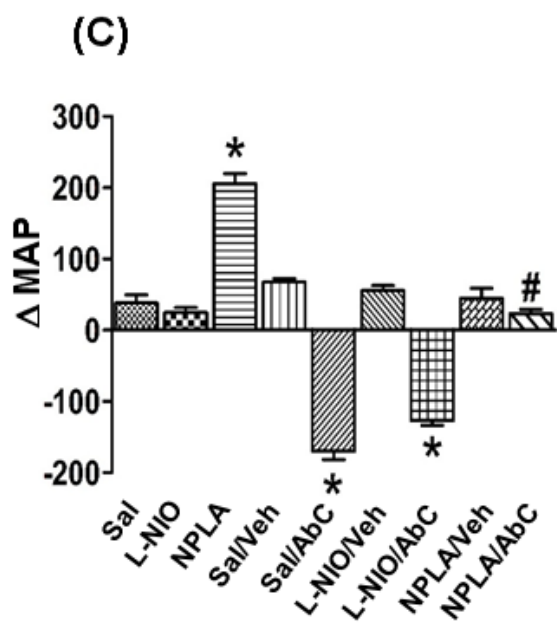
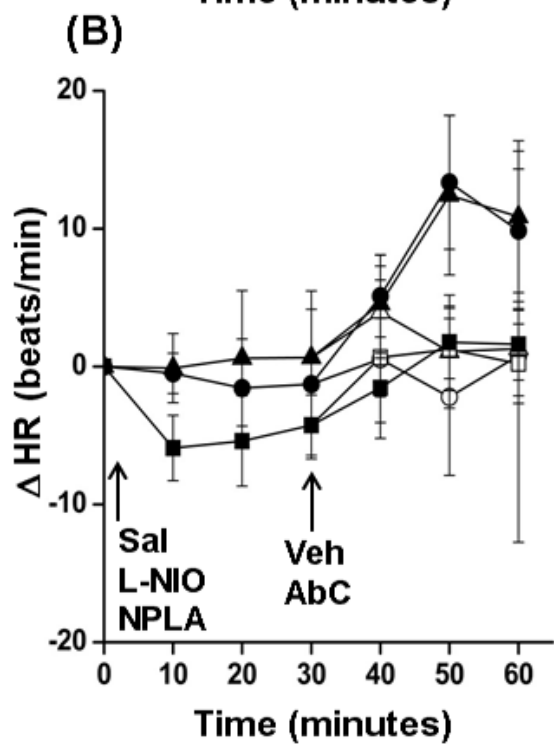
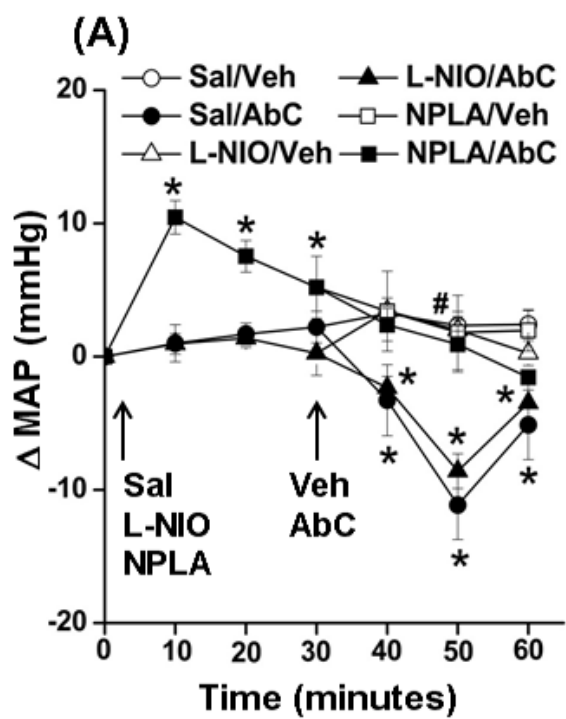


Figure 4.6. Effect of intra-RVLM adenylyl cyclase activation on GPR18 mediated sympathoinhibition

Changes in **(A)** mean arterial pressure (Δ MAP), and **(B)** heart rate (Δ HR) following intra-RVLM microinjections Abn CBD (0.4 μ g) or equal volume of vehicle in conscious male Sprague-Dawley rats pretreated, 30 minutes earlier, with forskolin (cAMP elevation; 50 μ mol). **C** and **D** depict the area under the curve (AUC) data generated from the time-course values over the pretreatment (0 to 30 min) and treatment (30-60 min) periods. All pretreatment groups that received the same drugs were combined for clarity; n = 6 for all groups except DMSO/Vehicle and DMSO/Abn CBD groups (n = 3, each). * $P < 0.05$ vs. control (vehicle); # $P < 0.05$ vs. Abn CBD. DM, DMSO; Veh, vehicle (methylacetate); AbC, Abn CBD; Forsk, forskolin.

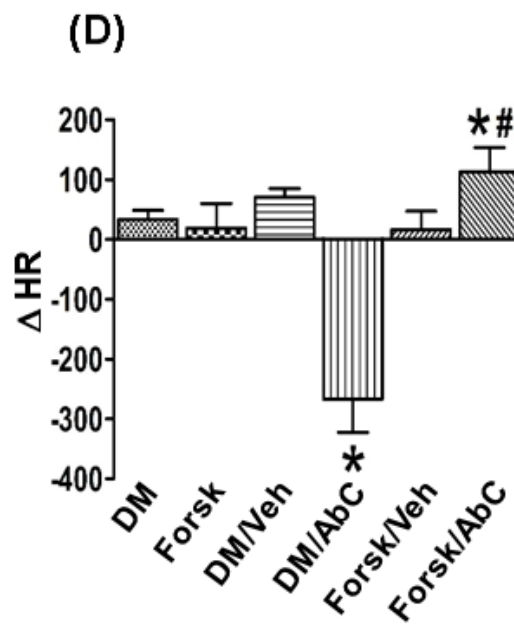
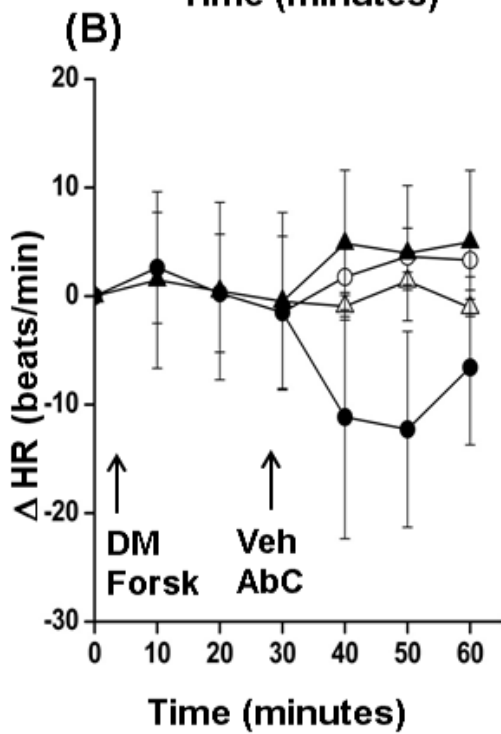
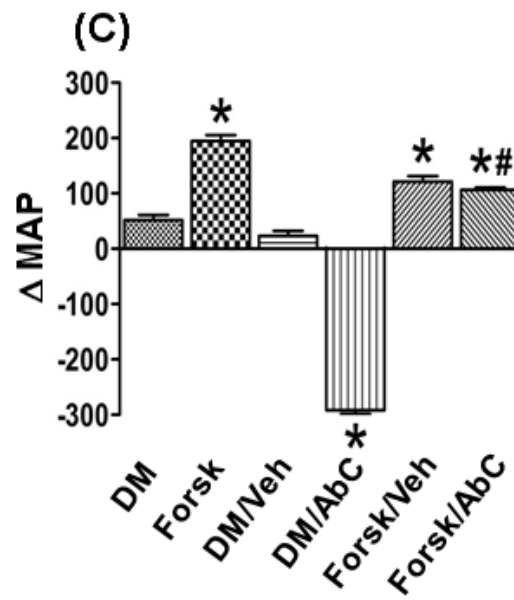
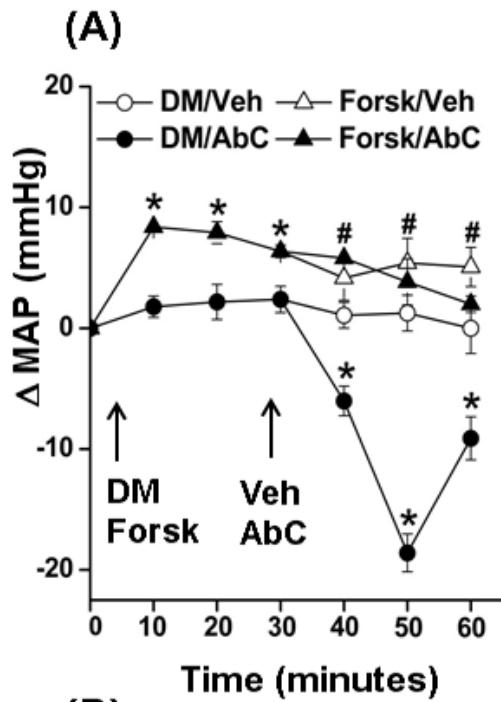


Figure 4.7. Effects of forskolin, NPLA, PD98059 or wortmannin pretreatments on pERK1/2, pAkt, p-nNOS, ADN and ROS levels in the RVLM

Dot blots showing the effects of Abn CBD alone or following pretreatment with forskolin, NPLA, PD98059 or wortmannin on pERK1/2 (**A**), pAkt (**B**), p-nNOS (**C**) and ADN (**D**) levels in the RVLM. Data are presented as integrated density ratio of the phosphorylated protein to its total protein and expressed as percent of control (vehicle). Values are mean \pm S.E.M. of 3-6 observations. * $P < 0.05$ vs. vehicle; # $P < 0.05$ vs. Abn CBD values. (**E**) RVLM ROS levels following treatment with Abn CBD in the absence or presence of forskolin, NPLA, PD98059 or wortmannin. Values are mean \pm S.E.M. of 3-6 observations. * $P < 0.05$ vs. vehicle; # $P < 0.05$ vs. Abn CBD values. Veh, vehicle (methylacetate); AbC, Abn CBD; Wort, wortmannin; PD, PD98059; Forsk, forskolin.

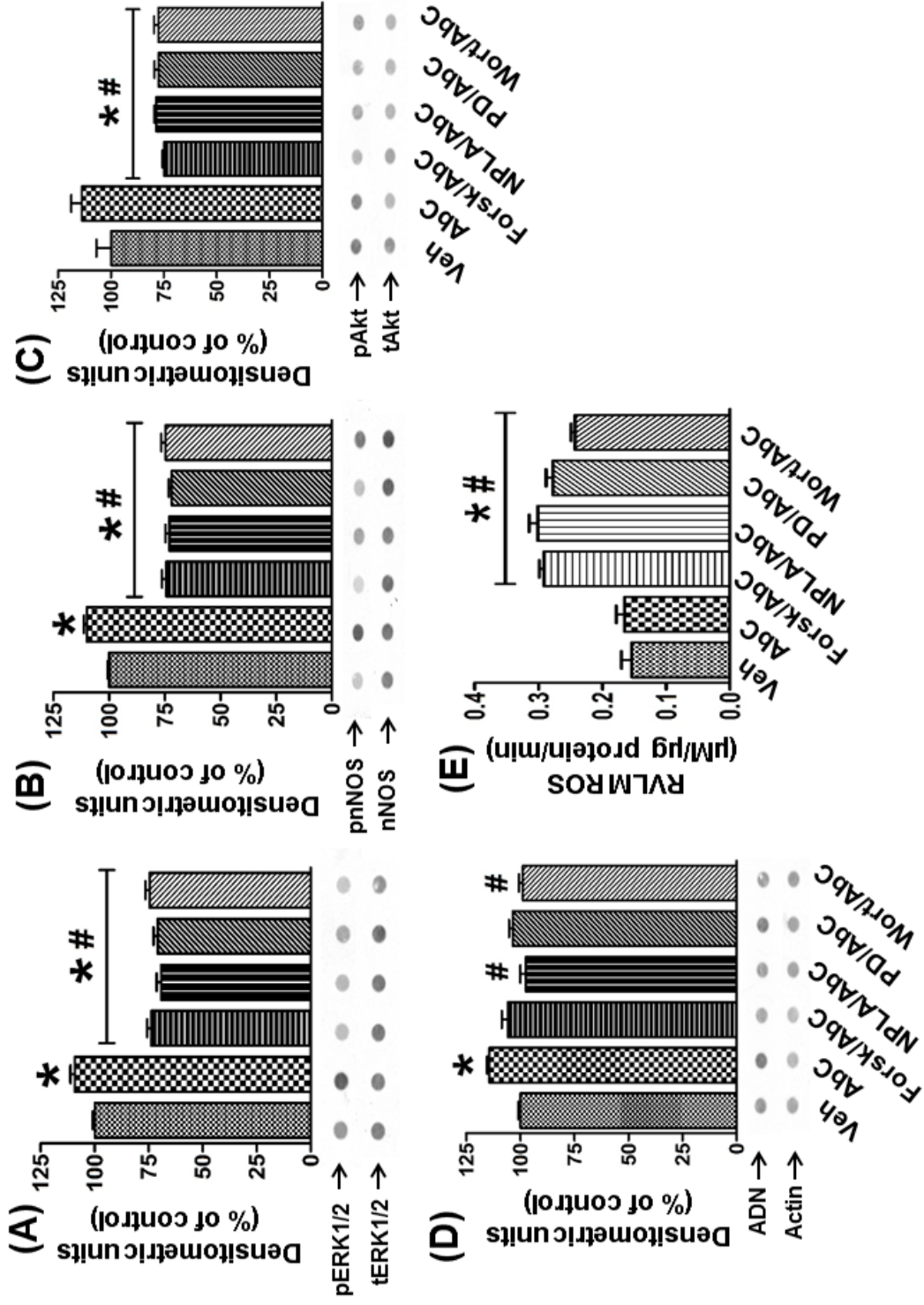
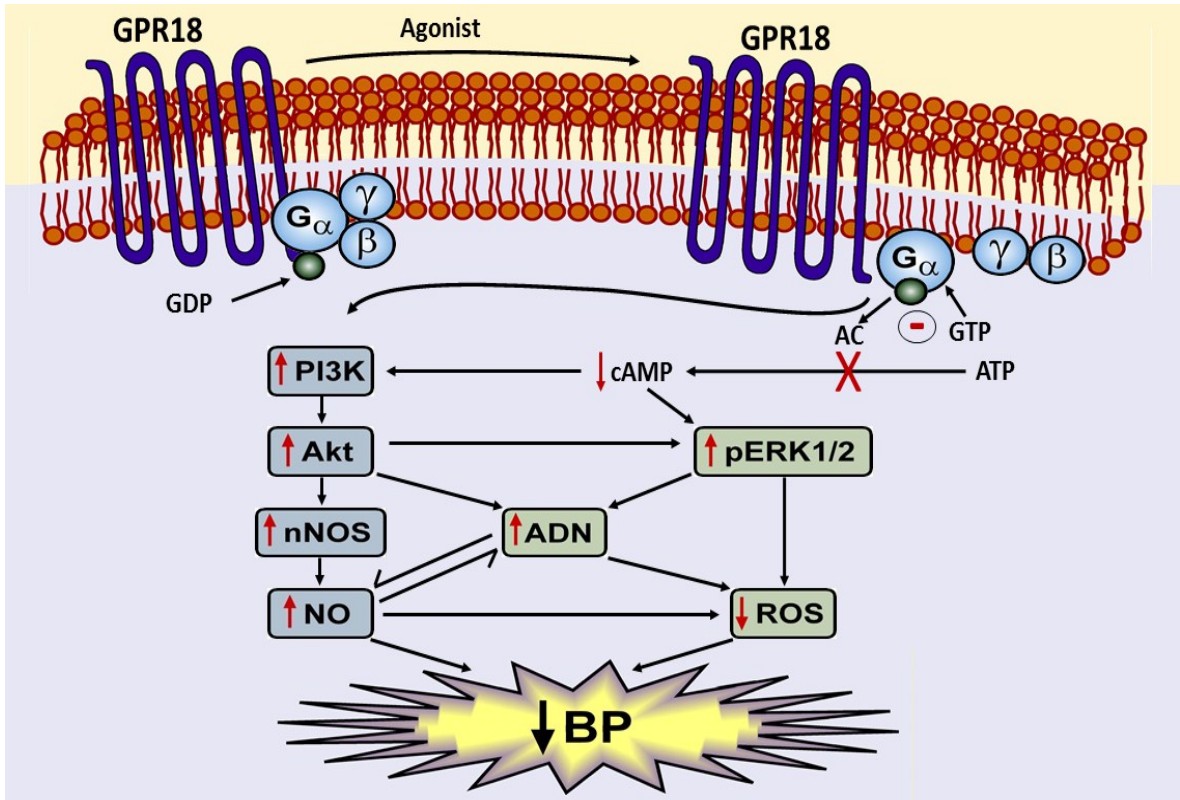


Figure. 4.8. Proposed GPR18 signaling in the RVLM

Schematic presentation of the proposed mechanisms for the neurochemical (RVLM) and blood pressure responses elicited by activating central GPR18. This model is based on the present and our reported findings (Penumarti and Abdel-Rahman, 2014). Activation of intra-RVLM GPR18 inhibits cAMP leading to enhanced ADN, pERK1/2 and pAkt production, which causes increase in p-nNOS and NO production and decrease in ROS generation, eventually leading to hypotension.



4.7. Discussion

We elucidated the molecular mechanisms that underlie the sympathoinhibitory/hypotensive response elicited by RVLM GPR18 activation in conscious rats. The following are the most important findings of the present study: 1) activation of RVLM GPR18 (Abn CBD) increased ADN and pAkt, pERK1/2 and p-nNOS levels in the RVLM; 2) prior blockade of RVLM GPR18 (O-1918) abrogated the GPR18-mediated enhancements of RVLM Akt, ERK1/2 and nNOS phosphorylation; 3) pharmacological inhibition of RVLM PI3K/Akt, ERK1/2 or nNOS or elevation of cAMP increased local ROS level, and attenuated the GPR18-mediated hypotension as well as the increases in ADN level and in Akt, ERK1/2 and nNOS phosphorylation in the RVLM. Together, these findings suggest a pivotal role for the Akt/ERK1/2/nNOS/ADN signaling pathway and inhibition of cAMP as a molecular mechanism for GPR18-mediated reduction in BP in conscious unrestrained rats.

The balance between mediators and suppressors of oxidative stress in the RVLM plays a major role in BP control and hypertension (Fridovich, 1978; Kishi et al., 2004; Chan et al., 2006; Yoshitaka, 2008). While overexpression of some NOS isoforms in NTS and RVLM suppresses sympathetic activity and BP as well as local ROS level (Nassar and Abdel-Rahman, 2008; Kimura et al., 2009; Chan and Chan, 2014), little is known about the role of RVLM ADN in BP control. Notably, ADN confers neuroprotection by reducing oxidative stress (Song et al., 2013). Further, we showed that RVLM GPR18 activation increases local ADN levels and presented the first evidence that intra-RVLM ADN reduces RVLM ROS and BP (Penumarti and Abdel-Rahman, 2014). The present Western blot findings (Fig. 4.2) infer important role for enhanced

Akt, ERK1/2 and nNOS phosphorylation in RVLM GPR18-mediated hypotension. While this link is consistent with findings that implicated RVLM Akt-ERK1/2-nNOS activation in the hypotensive responses (El-Mas et al., 2009; Kastenmayer et al., 2012), it was important to establish a causal role for such neurochemical responses in GPR18-mediated hypotension. Here, we show that inhibition of the Akt-ERK1/2-nNOS pathways or elevation of cAMP production abrogates the GPR18-mediated increase in ADN levels (Fig. 4.7 D) and elevated RVLM ROS levels (Fig. 4.7 E). These neurochemical findings support the contribution of the PI3K/Akt-ERK1/2-nNOS-ADN signaling, acting in conjunction with the adenylyl cyclase/cAMP system, in GPR18 modulation of RVLM redox state and BP (Fig. 4.8). It is important to comment on the limited ability of NAGly, the endogenous GPR18 agonist (McHugh et al., 2010), to reproduce the neurochemical effects of the synthetic agonist Abn CBD (Fig. 4.2). Interestingly, the present findings might lend credence to our hypothesis that concurrent NAGly direct or indirect activation of the physiologically antagonistic CB₁R might explain the inability of intra-RVLM NAGly to lower BP in our recent study (Penumarti and Abdel-Rahman, 2014). Further, the present neurochemical findings might suggest molecular mechanisms for the RVLM GPR18 tonic restraining influence on BP, which manifests as increases in RVLM ROS level and BP following GPR18 blockade (Penumarti and Abdel-Rahman, 2014). Therefore, it was important to elucidate the role of these molecular mechanisms and the type of NOS isoform implicated in GPR18 modulation of RVLM redox state and BP.

We focused on RVLM ERK1/2 and its activator, PI3K/Akt, because their phosphorylation leads to nNOS and eNOS phosphorylation and NO generation (El-Mas et al.,

2009; Kastenmayer et al., 2012), and GPR18 activation increases ERK1/2 phosphorylation in BV-2 microglia and HEK 293 cells (McHugh et al., 2010). It is imperative, however, to discuss the puzzling role of the RVLM ERK1/2-NOS pathway because its activation leads to contradictory redox and BP effects. For example, ERK1/2 phosphorylation in the RVLM via angiotensin II AT₁R (Chan et al., 2007; de Oliveira-Sales et al., 2010) or the classical cannabinoid receptor CB₁R (Ibrahim and Abdel-Rahman, 2012a) activation leads to BP elevation. On the other hand, and in agreement with the present findings (Fig. 4.2 A, and Figs. 4.4-4.5), the activation of another Gi/o-coupled receptor, α_2 -adrenergic receptor in the brainstem increased ERK1/2 phosphorylation and reduced BP (Zhang and Abdel-Rahman, 2005; Nassar and Abdel-Rahman, 2008). Our findings (Fig. 4.2) are consistent with the involvement of pERK1/2, PI3K/Akt, and nNOS in GPR18 signaling in other tissues (Mukhopadhyay et al., 2002; Zhang and Abdel-Rahman, 2005; McCollum et al., 2007; McHugh et al., 2010), and infer their contribution to the GPR18-mediated hypotension.

The second objective of this study was to elucidate the potential causal role of Akt-ERK1/2-nNOS activation in the RVLM in the hypotensive response caused by intra RVLM-GPR18 activation. Since ERK1/2 phosphorylation can be triggered by pAkt (Hong et al., 2012) or can trigger Akt phosphorylation (Ramakrishnan et al., 2012) and both pAkt and pERK1/2 enhance eNOS and nNOS phosphorylation (El-Mas et al., 2009; Kastenmayer et al., 2012), we extended our pharmacological studies to elucidate the roles of pAkt and the NOS isoform implicated in the investigated phenomenon.

We focused on the constitutive NOS isoforms, nNOS and eNOS for two reasons. First, as discussed earlier, eNOS and/or nNOS phosphorylation (activation) is triggered by pAkt and pERK1/2. Second, although overexpression of iNOS in NTS and RVLM decreases BP (Kimura et al., 2005), iNOS is an unlikely contributor to the rapidly developing (10-15 min) GPR18-mediated hypotension here (Fig. 4.3) and in our recent study (Penumarti and Abdel-Rahman, 2014). We showed that activation (Abn CBD) and blockade (O-1918) of RVLM GPR18 enhanced and reduced nNOS phosphorylation (p-nNOS levels) in the RVLM (Fig. 4.2 B). Equally important, selective nNOS (NPLA), but not eNOS (L-NIO), inhibition virtually abolished GPR18-mediated hypotension (Fig. 4.5). Equally important, NPLA abrogated GPR18-mediated nNOS phosphorylation and elevation of ADN level in the RVLM (Fig. 4.7D). These pharmacological (Fig. 4.5) and molecular (Fig. 4.7B) findings support a causal role for p-nNOS in GPR18-mediated hypotension, at least partly, via Akt and ERK1/2 activation. The latter notion is supported by the ability of PI3K/Akt (wortmannin) or ERK1/2 inhibition (PD98059) to abrogate nNOS phosphorylation (Fig. 4.7B) and the hypotensive response (Figs. 4.3 & 4.4) caused by RVLM GPR18 activation.

Finally, we reasoned that a reduction in local cAMP levels, which occurs following activation of the Gi/o coupled receptor GPR18 in BV-2 microglia and HEK 293 cells (McHugh et al., 2010) might contribute to the GPR18-mediated hypotension. This hypothesis is supported by the findings that activation of other Gi/o coupled receptors in the brainstem lowers BP (Zhang and Abdel-Rahman, 2005). We were not able to measure cAMP levels in the limited amounts of tissues collected from the RVLM. An alternate, and reported approach (Mason and Matthews,

2012) for testing our hypothesis, was the use of forskolin to activate AC and generate cAMP (Edwards and Paton, 1999). We show that intra-RVLM forskolin (cAMP elevation) virtually abolished the hypotension (Fig. 4.6) and the increases in phosphorylation of Akt, ERK1/2 and nNOS and in ADN level in RVLM (Fig. 4.7) caused by GPR18 activation (Abn CBD). These neurochemical responses suggest that: (i) cAMP dampens the Akt-ERK1/2-nNOS-ADN signaling in the RVLM, and (ii) reduction in cAMP contributes to the increases in phosphorylation of Akt, ERK1/2 and nNOS and ADN level and ultimately the hypotensive response caused by RVLM GPR18 activation.

In conclusion, the present study yields new insight into the RVLM signaling pathways implicated in GPR18-mediated sympathoinhibition/hypotension. We provide the first evidence that the RVLM PI3K/Akt-ERK1/2-nNOS/ADN signaling and cAMP and ROS levels play key roles in GPR18 modulation of BP in the RVLM (Fig. 4.8). Future studies are warranted to delineate the role of GPR18 in conditions like hypertension to develop novel antihypertensive therapeutics that target the central GPR18 signaling.

CHAPTER FIVE - GPR18 SIGNALING AND ITS INTERACTION WITH LIPID RAFTS IN DIFFERENTIATED PC12 CELLS

5.1. Abstract

Our previous studies demonstrated the expression of the cannabinoid receptor, GPR18, in tyrosine hydroxylase-immunoreactive (TH-ir) neurons in the rostral ventrolateral medulla (RVLM), and suggested an important function for RVLM GPR18 in blood pressure (BP) regulation. The latter is supported by the dose-related reductions and elevations in BP caused by GPR18 activation by the agonist, abnormal cannabidiol (Abn CBD), and blockade by O-1918, respectively, in conscious normotensive rats. Also, activation of the RVLM PI3K/Akt-ERK1/2-nNOS-ADN signaling network and inhibition of cAMP and ROS production play a causal role in GPR18-mediated hypotension. Evidence suggests that lipid rafts (LR) participate in the regulation of GPCRs as well as cannabinoid 1 receptor (CB₁R) binding and signaling. In the present study, we tested the hypothesis that GPR18 signaling is influenced by its interaction with lipid rafts in differentiated PC12 (nPC12) cells. Our studies show that GPR18 is co-expressed with CB₁R in nPC12 cells. Activation of GPR18 by Abn CBD/n-arachidonoyl glycine (NAGly) in nPC12 cells increased pAkt, pERK1/2, pnNOS, NO, ADN levels and decreased cAMP and ROS levels. In contrast, GPR18 blockade (O-1918) produced the opposite effects and culminated in higher cellular oxidative stress. Additionally, confocal imaging findings show that GPR18 is associated with LRs. Activation of GPR18 (Abn CBD or NAGly) dislodged it from the LRs and this response was abrogated by prior GPR18 blockade (O-1918). Furthermore, cholesterol depletion by methyl- β -cyclodextrin (M β CD) enhanced GPR18 signaling and uncovered O-1918-

mediated GPR18 blockade in nPC12 cells. Our findings characterize LR-mediated intracellular mechanisms governing GPR18 signaling in nPC12 cells.

5.2. Introduction

The plasma membrane is a phospholipid bilayer that is highly disorganized and is composed of microdomains called Lipid Rafts (LRs) (Herkenham et al., 1991). These lateral platforms enriched in cholesterol, sphingolipids, plasmenylethanolamine and arachidonic acid are resistant to solubilization with non-ionic detergents (Herkenham et al., 1991; Pike, 2003). Caveolae are funnel shaped invaginations of membrane proteins called caveolins and are a subtype of lipid rafts (Fielding and Fielding, 1997; Czarny et al., 1999). These microdomains participate in a number of cellular functions including cell signaling, cellular protein trafficking and membrane transport (Moffett et al., 2000; Gaus et al., 2003; Wilson et al., 2004) and play a very important role in health and disease (Jin et al., 2011).

Lipid rafts/caveolae are the microdomain regions of localization of several physiologically important GPCRs (Becher et al., 2004; Chini and Parenti, 2004; Insel et al., 2005) and it is well known that the activity of several GPCRs is modulated by LRs (Dainese et al., 2007). LRs and caveolae participate in the regulation of GPCR signaling by affecting both signaling selectivity and coupling efficacy (Chini and Parenti, 2004).

Our previous studies in male normotensive rats demonstrated the expression of GPR18 in the rostral ventrolateral medulla (RVLM) of the brainstem, and indicate that Abn CBD mediated sympathoinhibition is due to enhanced ADN levels, ERK1/2, PI3K/Akt phosphorylation, p-

nNOS-derived NO release and a reduction in ROS generation (Penumarti and Abdel-Rahman, 2013). There is growing evidence suggesting that endocannabinoid uptake and signaling through the cannabinoid receptors are highly dependent on the composition and integrity of lipid rafts (Biswas et al., 2003; Bari et al., 2005b; Bari et al., 2006; Rimmerman et al., 2008b). Anandamide (an endogenous cannabinoid and a precursor of NAGly) and its metabolites accumulate into lipid rafts and these detergent resistant membrane microdomains play an important role in the cellular processing and regulation of AEA function (Sarker and Maruyama, 2003; McFarland et al., 2004; Bari et al., 2005a). NAGly is synthesized from AEA and serves as an endogenous GPR18 ligand (Kohno et al., 2006). Additionally, AEA is a common endocannabinoid for both GPR18 and CB₁R (Bradshaw et al., 2009). There is also evidence that CB₁R binding/signaling, as well as anandamide (AEA) transport is controlled by LRs and caveolin-1 (Dainese et al., 2007; Bari et al., 2008). CB₁R signaling through AC and MAPK is doubled following disruption of LRs indicating the importance of the integrity of LRs in CB₁R signaling (Bari et al., 2005b; Bari et al., 2006). Interestingly in the case of CB₁R, agonist-induced endocytosis is dependent on LRs/caveolae and it is this process that counteracts desensitization of the receptor by facilitating its recycling and reactivation (Wu et al., 2008). In contrast, LR disruption does not influence CB₂R signaling or binding (Potts et al., 2000; Bari et al., 2005a; Bari et al., 2006). One recent publication on the interaction of GPR55 (a putative cannabinoid receptor) with LRs showed that activation of GPR55 leads to localization of the receptor in the LRs and that this association is essential for proper GPR55 signaling (Li et al., 2005). Taken together these findings suggest an important role for LRs in modulating the endocannabinoid system and that the cannabinoid receptor subtypes are differentially modulated by LRs.

Based on these findings, we hypothesized that activation of GPR18 causes receptor dissociation from lipid rafts, which consequently leads to activation of PI3K/AKT-ERK1/2-nNOS-ADN pathway and inhibition of ROS signaling. As the methods of detecting lipid rafts are technically difficult to conduct in tissues, we used nPC12 cells, which are rat pheochromocytoma cells that are capable of differentiating into a neuronal phenotype upon treatment with nerve growth factor (NGF) (Okouchi et al., 2005). Another reason for conducting signaling studies in nPC12 cells is the limited amount of tissue obtained from the RVLM of treated and control rats, which made conducting some neurochemical studies difficult. For example, the GPR18 antagonist, cannabidiol, inhibited catalase activity in the liver (Usami et al., 2008). Such changes in major enzymes that control the oxidative state of the RVLM neurons might explain the expected reduced and enhanced ROS generation in the RVLM neurons following selective GPR18 activation and blockade, respectively. The first objective of the present study was to determine if GPR18 is expressed in differentiated nPC12 cells and to replicate some of the molecular responses observed in RVLM neurons. Thereafter, we conducted molecular and neurochemical studies to elucidate the role of lipid rafts in GPR18 signaling and regulation of the redox state of nPC12 cells.

5.3. Materials and Methods

5.3.1. Cell Culture and Treatment.

Rat pheochromocytoma cells (PC12 cells) (ATCC, Rockville, MD) were cultured, at 37°C with saturated air containing 5% CO₂, on Corning CellBind flasks in ATCC-formulated F-12K medium supplemented with horse serum (15%), fetal bovine serum (2.5%), penicillin (100U/ml) and streptomycin (100U/ml). Cells were incubated with NGF (50ng/ml) for 48 hr to initiate neuronal differentiation, and culture medium was changed every 2 days as in previous studies (Zhang et al., 2001).

Freshly sub-cultured nPC12 cells were incubated with the vehicle (methyl acetate, control) or one of the following treatments: NAGly (1 μM), Abn CBD (1 μM), O-1918 (1 μM), O-1918 (1 μM) + NAGly (1 μM), O-1918 (1 μM) + Abn CBD (1 μM). The concentrations of the GPR18 ligands were based on reported studies in other in vitro model systems (McHugh et al., 2010). In subsequent studies the GPR18 agonists Abn CBD or NAGly were incubated in the absence or presence of reported concentrations of the following pharmacologic interventions: Forskolin (0.1 μM) (Van Sickle et al., 2005), PD98059 (0.1 μM) (Javanmardi et al., 2005), NPLA (0.1 μM), wortmannin (0.1 μM) (Nattie and Li, 1990) for 1 hr at 37°C before scraping the cells for conducting the Western or dot blot studies. For lipid raft disruption studies, the cells were pre-incubated for 30 min at 37°C with 2.5 mM MβCD (dissolved in dH₂O) (Karlsson et al., 2006) before the exposure to GPR18 ligands.

5.3.2. Immunofluorescence.

nPC12 cells were cultured on Lab-Tek Chamber slides coated with poly-L-lysine, washed with cold PBS and fixed with 4% paraformaldehyde for 30 min. The cell membranes were permeabilized with 0.1% triton X-100 and non-specific binding was blocked by 1% bovine serum albumin and 5% normal donkey serum. The cells were incubated for 2.5 hr with the respective primary antibody: goat anti-GPR18 (1:200; Santa Cruz; Dallas, TX) or mouse anti CB₁R (1:200; Santa Cruz; Dallas, TX) mixture diluted in blocking buffer. The cells were then incubated with the corresponding secondary antibody Cy-3 conjugated donkey anti-mouse and fluorescein isothiocyanate-conjugated donkey anti-goat (1:200; Jackson Immunoresearch Laboratories Inc., West Grove, PA) for 1 hr, mounted with Vectashield mounting medium containing DAPI as a counterstain (Vector Laboratories, Burlingame, CA) and left in the dark overnight. Images were acquired using confocal laser microscopy (Carl Zeiss LSM 510, Thornwood, New York). Images were analyzed using the JACoP plugin in ImageJ software.

5.3.3. Western Blotting.

nPC12 cells incubated with the vehicle or the pharmacologic interventions mentioned above were processed for the measurements of phosphorylated ERK1/2 (pERK1/2) or Akt (pAkt) in relation to the corresponding total protein. Homogenized protein extracts were run on 12% SDS-PAGE gel (Invitrogen, Carlsbad, CA) and electro blotted to nitrocellulose membranes. Blots were blocked with Odyssey blocking buffer and incubated overnight at 4°C with goat anti-GPR18 primary antibody (1:200; Santa Cruz; Dallas, TX) or rabbit anti-ERK1/2 or rabbit anti-Akt and mouse anti-pERK1/2 or mouse anti-pAkt (1:500) diluted in blocking solution. The blots

were then washed with rinse buffer and incubated at room temperature with donkey anti-goat or donkey anti-rabbit and donkey anti-mouse IgG secondary antibody (1:10,000). Following additional washes the blots were detected using an Odyssey Infrared Imaging system and analyzed with Odyssey application software v.3 (LICOR Biosciences). All data are presented as mean values of integrated density ratio of phosphorylated protein normalized to its corresponding total protein.

5.3.4. Measurement of ROS (DCFH-DA).

Freshly sub-cultured cells were exposed to 5 μ M DCFH-DA for 30 min after which they were incubated with: methyl acetate (vehicle, control), NAGly (1 μ M), Abn CBD (1 μ M), O-1918 (1 μ M), O-1918 (1 μ M) + NAGly (1 μ M), O-1918 (1 μ M) + Abn CBD (1 μ M) for 2 hr. The cells were washed with PBS, trypsinized and collected in Eppendorf tubes. The fluorescence was measured using a flow cytometer.

5.3.5. Nitrate/Nitrite Assay.

The NO_x content was measured with a colorimetric assay kit in accordance with manufacturer's instructions (Cayman Chemical Company, Ann Arbor, MI). First, 10 μ l enzyme cofactor and 10 μ l nitrate reductase were added to 80 μ l sample mixture, incubated at room temperature for 3 hr. Following incubation, 50 μ l Griess Reagent R1 and R2 (Cayman Chemical Company, Ann Arbor, MI) were added to each well, and read the absorbance at 540 nm.

5.3.6. Measurement of cAMP.

cAMP-Glo Max Assay kit (Promega V1681) was used to measure cAMP in treated nPC12 cells. Cell lysates were subjected to the assay as per the manufacturer's instructions (Promega, Madison, WI) and luminescence was determined with a luminometer and used as a measure of cAMP produced. For each sample: the change in relative luminescence units (Δ RLU) = RLU (untreated sample) – RLU (treated sample). Using this Δ RLU value and the linear equation generated from the standard curve, the cAMP concentration was calculated using the linear formula from the graph as in reported studies (Bari et al., 2005b).

5.3.7. Quantification of Catalase Activity.

Colorimetric measurement of catalase activity was conducted in accordance with manufacturer's instructions (Sigma Aldrich, St. Louis, MO) and as reported in our recent studies (Bari et al., 2006). Briefly, 1 ml of PBS was added to 100 cm² petri dish and the cells were gently scraped and collected into centrifuge tubes after drug treatment for 30 min. The cell suspension was centrifuged at 4°C, 5000 rpm for 5min. The supernatant was collected for measurements of catalase activity and protein using Bio-Rad protein assay (Bio-Rad Laboratories, Hercules, CA). The absorbance of the samples was measured at 520 nm.

5.3.8. Quantification of NADPH Oxidase Activity.

NADPH oxidase activity was measured by a fluorescence assay using Amplex Red (Molecular Probes, OR) dissolved in buffer, pH 7.4 (105 mM K-MES, 30 mM KCl, 10 mM KH₂PO₄, 5 mM MgCl₂-6H₂O, 0.5 g/L BSA), Superoxide dismutase (7500 U/ml), Horseradish

peroxidase (300 U/ml) and addition of NADPH (10 mM). Hydrogen peroxide was used to generate a 7-point standard curve. Quantification was conducted by examining fluorescence intensity using the Fluoromax-3 spectrofluorometer (Horiba Jobin Yvon, Edison, NJ) at excitation (530 nm)/emission (590 nm). Cell suspension samples (50 µg/25 µl) were added to 200 µl Amplex Red, 2 µl Superoxide dismutase and 2 µl horseradish peroxidase. Baseline measurements were taken for five minutes and NADPH (10 µl) was added and readings were recorded for an additional 5 min as in our recent studies (Biswas et al., 2003).

5.3.9. Quantification of ALDH Activity.

Following incubation with the vehicle or the pharmacological interventions, discussed above, nPC12 cells were scraped in 1xPBS and homogenized using a syringe. The cell suspension was centrifuged at 4°C and 5000 rpm for 4 min. The supernatant was collected for protein assay and ALDH activity measurement. The final volume of the assay mixture (200 µl) comprised of 50 µg/25 µl protein or 25 µl of 1xPBS (Blank), 4 µl of 300 µM 6-Methoxy-2-naphthaldehyde in 166.4 µl of 1xPBS. The fluorescence of this mixture was read at excitation 310 nm and emission 360 nm for 7 min before adding 1.3 µl of 11.4 mM NAD. After this addition, the fluorescence of this assay mixture was read at 310 nm/360 nm every 5 min for 45 min and ALDH activity was calculated from the fluorescence values as in our reported studies (El-Mas and Abdel-Rahman, 2011).

5.3.10. Lipid Raft Labeling.

LR labeling studies were conducted in nPC12 cells because such studies were unfeasible in RVLM sections. nPC12 cells were cultured on Lab-Tek Chamber slides coated with poly-L-lysine, washed with cold PBS and fixed with 4% paraformaldehyde for 30 min in the absence or presence of the pharmacological interventions discussed above. The cell membranes were permeabilized with 0.1% triton X-100 and non-specific binding was blocked by 1% bovine serum albumin and 5% normal donkey serum. The cells were incubated for 2.5 hr with goat anti-GPR18 (1:200). The cells were then incubated with fluorescein isothiocyanate-conjugated donkey anti-goat (1:200; Jackson ImmunoResearch Laboratories Inc., West Grove, PA) for 1 hr, mounted with Vectashield mounting medium containing DAPI as counterstain (Vector Laboratories, Burlingame, CA) and left in dark overnight to harden. Vybrant Alexa Fluor 488 lipid raft labeling kit (Molecular Probes, Eugene, OR) was used to label lipid rafts in accordance with the manufacturer's instructions. Images were acquired using confocal laser microscopy (Carl Zeiss LSM 510, Thornwood, New York). Representative images were analyzed using the JACoP plugin in ImageJ software as reported (Sarnataro et al., 2005).

5.3.11. Drugs.

Abn CBD, NAGly and O-1918 were purchased from Cayman Chemical (Ann Arbor, MI). Methyl acetate, methyl beta cyclodextrin, wortmannin, PD98059, forskolin and dimethyl sulfoxide were purchased from Sigma Aldrich (St. Louis, MO). NPLA were purchased from Tocris Biosciences (Ellisville, MO) and dissolved in sterile saline. Sterile saline was purchased

from B. Braun Medical (Irvine, CA). DMSO was used as the vehicle for PD98059, wortmannin and forskolin. Methyl acetate was used as the vehicle for Abn CBD, O-1918 and NAGly.

5.4. Data Analysis and Statistics

All values are expressed as mean \pm S.E.M change from their respective baselines. The dose-response curves were analyzed using repeated measures ANOVA using SPSS 16.0 statistical package for Windows (SPSS Inc., Chicago, IL) for differences in treatment trends. All other statistical analyses were done using a one-way or repeated-measures ANOVA with Bonferroni post hoc test and Student's t test, Prism 5.0 software (GraphPad Software Inc., San Diego, CA) was used to perform statistical analysis and $P < 0.05$ was considered significant.

5.5. Results

5.5.1. Co-expression of GPR18 with CB₁R in nPC12 cell.

Western blot (Fig. 5.1.A) and immunofluorescent (Fig. 5.1.B) findings revealed the expression of GPR18 in differentiated PC12 cells. The GPR18 band was absent in a membrane pre-incubated with the immunizing protein (Fig. 5.1.A). Further, dual labeled immunofluorescence findings revealed the co-expression of GPR18 with CB₁R (Fig. 5.1.C), which was quantified and presented as the Pearson's Correlation Coefficient in the presence and absence of GPR18 primary antibody (Fig.5.1.D).

5.5.2. *GPR18 modulates Akt-ERK1/2-nNOS-ADN signaling and cAMP level in nPC12 cells.*

GPR18 activation (Abn CBD, NAGly) increased ERK1/2, Akt, nNOS phosphorylation and ADN levels in nPC12 cells (Figs. 5.2. A-D). In contrast, GPR18 blockade (O-1918) reduced Akt, ERK1/2, nNOS phosphorylation and ADN levels, and abrogated Abn CBD/NAGly enhancement of pERK1/2, pnNOS and ADN levels (Figs. 5.2. A-D). Compared to the vehicle control, nPC12 GPR18 activation (Abn CBD or NAGly) increased NO and decreased cAMP levels while blockade (O-1918) decreased NO and increased cAMP levels (Figs. 5.2. E & F).

5.5.3. *GPR18 Activation Reduces ROS Generation in nPC12 cells.*

This experiment was conducted to determine the impact of GPR18 activation (NAGly/Abn CBD) or blockade (O-1918) on ROS levels in nPC12 cells. Compared with vehicle, NAGly or Abn CBD significantly ($P < 0.05$) reduced (Fig. 5.3) while O-1918 significantly ($P < 0.05$) increased ROS levels, measured by flow cytometry using DCFH-DA (Fig. 5.3). Further, O-1918 abrogated the reduction in ROS caused by NAGly or Abn CBD (Fig. 5.3). GPR18 activation (Abn CBD or NAGly) caused a significant increase in catalase, (Fig. 5.4. A) ALDH activity (Fig. 5.4. B) and decreased NADPH oxidase activity (Fig. 5.5. A). On the other hand, GPR18 blockade (O-1918) produced the opposite effects (Figs. 5.4.A-B & 5.5.A). Further, pretreatment with O-1918 or inhibition of PI3K/Akt-ERK1/2-nNOS/ADN signaling or increasing cAMP levels abrogated the increases in catalase and ALDH activity (Figs. 5.4. C-E) and decrease in Nox activity (Figs. 5.5. B & C) produced by Abn CBD and/or NAGly. These in vitro findings

paralleled the in vivo responses described in our previous studies (Penumarti and Abdel-Rahman, 2013) and Chapter 3 and 4.

5.5.4. Interaction of GPR18 with Lipid Rafts Following Ligand Binding in nPC12 cells.

There are no reported studies on the cellular localization of GPR18 and how such localization is impacted by GPR18 activation or blockade. This experiment was conducted to study the effect of GPR18 ligands on the intracellular localization of GPR18. Confocal microscopy analysis revealed GPR18 association with lipid rafts under basal conditions, and a reduction in such association following receptor activation (Abn CBD or NAGly) (Fig. 5.6. A-F). We also found that prior GPR18 blockade (O-1918) abolished ($P < 0.05$) the reduction in GPR18 association with LRs caused by the GPR18 agonist (Abn CBD or NAGly). Confocal microscopy analysis of GPR18 association with LR following LR disruption with methyl beta cyclodextrin (M β CD) revealed decreased GPR18-LR association in the presence of vehicle and antagonist treatment whereas association seems to have increased in the presence of the agonist (Fig. 5.7).

5.5.5. Effect of M β CD on GPR18-dependent Signaling Pathways.

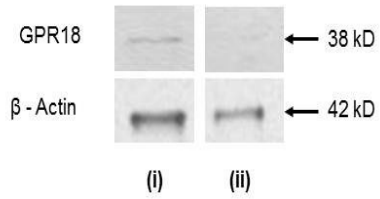
To evaluate the role of lipid raft integrity in GPR18 function, we perturbed the LR composition with M β CD (2.5 mM) and subsequently quantified the effects of GPR18 activation or blockade on the following signaling products in nPC12 cells: pERK1/2, pAkt, pnNOS, ADN, cAMP and ROS after cellular incubation with GPR18 ligands: control (methyl acetate), NAGly (1 μ M), Abn CBD (1 μ M), O-1918 (1 μ M). M β CD depletes membrane cholesterol and is widely

used to disrupt the integrity of lipid rafts (Karlsson et al., 2006). It is noteworthy that the presence of M β CD exacerbated ($P<0.05$) the increase in pERK1/2, pAkt, pnNOS, ADN and decrease in cAMP and ROS levels caused by Abn CBD or NAGly and significantly ($P<0.05$) uncovered the inhibition of pERK1/2-pAkt-pnNOS-ADN pathway and increase in cAMP and ROS levels caused by O-1918 (Fig. 5.8).

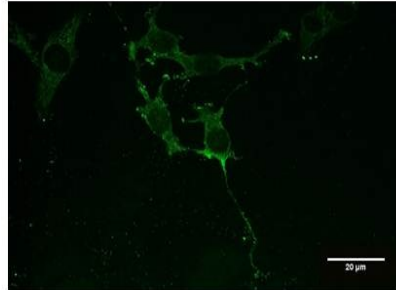
Figure 5.1. GPR18 expression in nPC12 cells

(A) (i) Expression of GPR18 (38kDa) in nPC12 cells. (ii) Absence of GPR18 band in the presence of immunizing peptide (B) Immunofluorescent staining showing the expression of GPR18 in nPC12 cells. (C) Dual labeled immunofluorescence of nPC12 cells showing co-expression of GPR18 and CB₁R. (D) Quantification of degree of co-localization obtained using Pearson's Correlation Coefficient analysis in the presence and absence of GPR18 primary antibody.

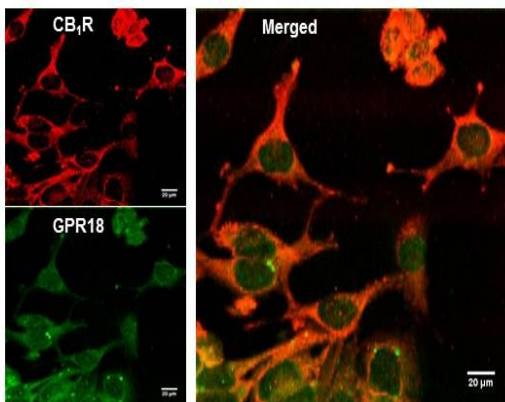
(A)



(B)



(C)



(D)

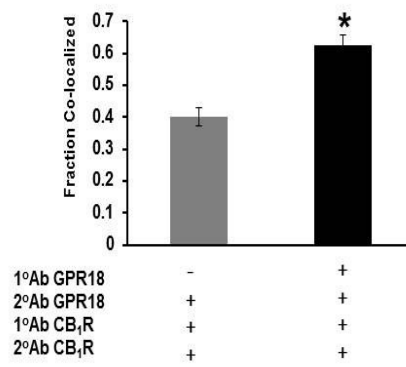


Figure 5.2. Effect of the different ligands on GPR18 signaling in nPC12 cells

Western blots, cAMP and total nitrate/nitrite (NO_x content; index of NO) levels in nPC12 cells showing the effects of NAGly (1μM), Abn CBD (1μM), O-1918 (1μM), O-1918 (1μM) + NAGly (1μM) or O-1918 (1μM) + Abn CBD (1μM) or forskolin (0.1 μM) + NAGly (1μM), PD98059 (0.1 μM) + NAGly (1μM), NPLA (0.1 μM) + NAGly (1μM), wortmannin (0.1 μM) + NAGly (1μM), forskolin (0.1 μM) + Abn CBD (1μM), PD98059 (0.1 μM) + Abn CBD (1μM), NPLA (0.1 μM) + Abn CBD (1μM), wortmannin (0.1 μM) + Abn CBD (1μM) treatment on pERK1/2 (**A**), pAkt (**B**), p-nNOS (**C**), adiponectin (ADN) (**D**), cAMP (**E**) expression and nitrate/nitrite (NO_x) level (F) in nPC12 cells. Values are mean ± S.E.M. of 5-6 observations. **P* < 0.05 vs. vehicle; #*P* < 0.05 vs. Abn CBD; ^*P* < 0.05 vs. NAGly values.

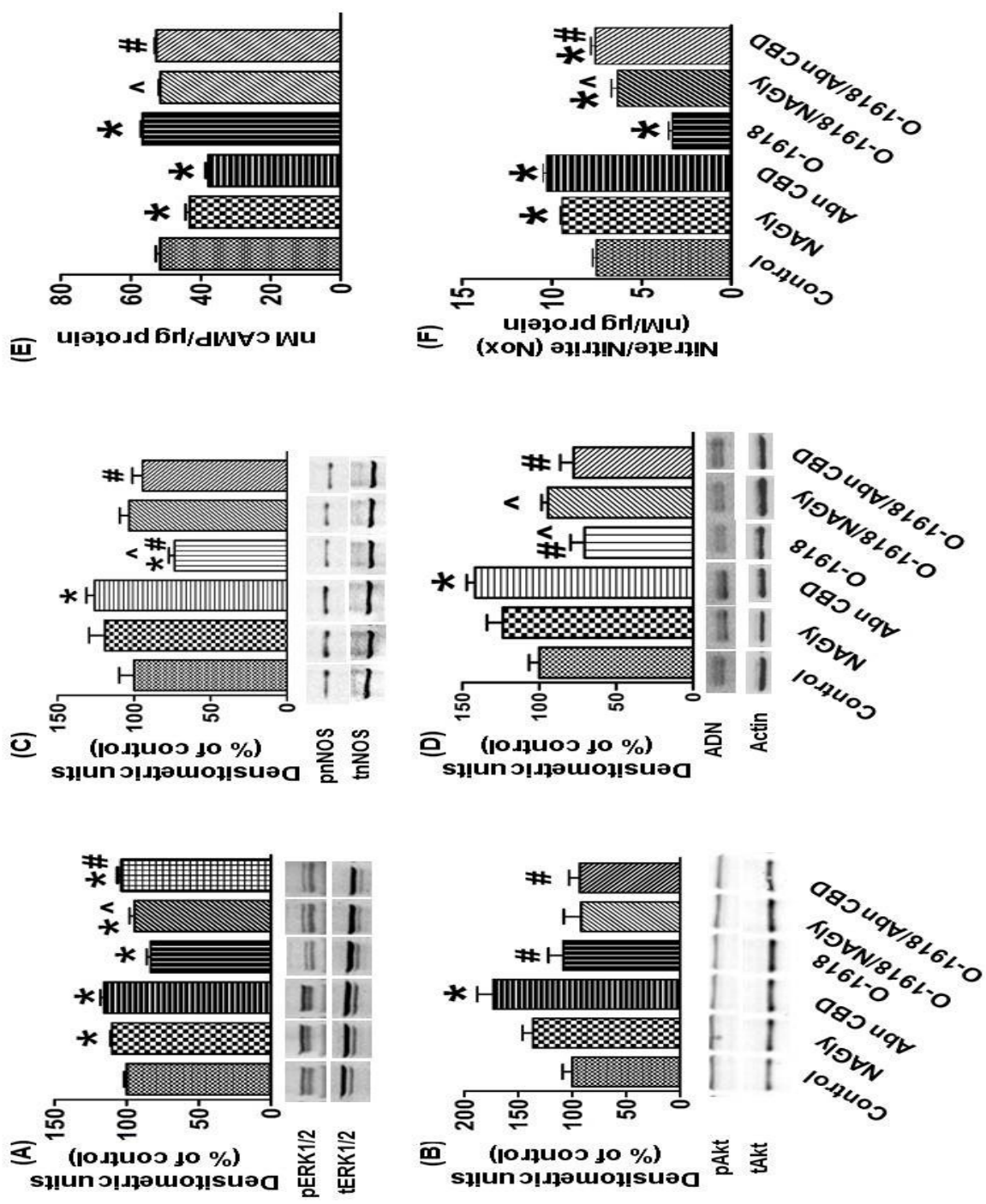


Figure 5.3. Effect of GPR18 activation or blockade on ROS levels in nPC12 cells

DCFH-DA measured ROS levels in terms of mean fluorescence units in nPC12 cells using Flow cytometry following treatment with NAGly (1 μ M), Abn CBD (1 μ M), O-1918 (1 μ M), O-1918 (1 μ M) + NAGly (1 μ M) or O-1918 (1 μ M) + Abn CBD (1 μ M). Values are mean \pm S.E.M (n=5-6 observations). * P < 0.05 vs. vehicle values; # P < 0.05 vs. Abn CBD; ^ P < 0.05 vs. NAGly values.

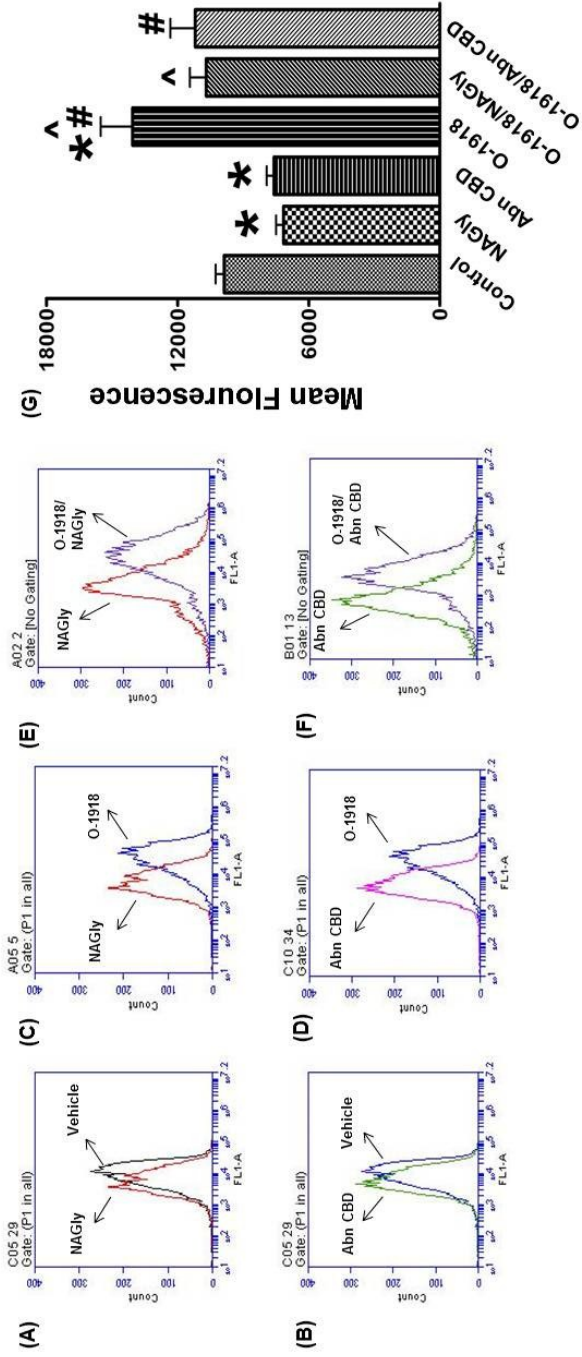


Figure 5.4. Effect of GPR18 activation or blockade on catalase and ALDH activity in nPC12 cells

Measurement of catalase and ALDH enzyme activity in nPC12 cells showing the effects of (A-B) NAGly (1 μ M), Abn CBD (1 μ M), O-1918 (1 μ M), O-1918 (1 μ M) + NAGly (1 μ M) or O-1918 (1 μ M) + Abn CBD (1 μ M) or (C-D) forskolin (0.1 μ M) + NAGly (1 μ M), PD98059 (0.1 μ M) + NAGly (1 μ M), NPLA (0.1 μ M) + NAGly (1 μ M), wortmannin (0.1 μ M) + NAGly (1 μ M), or (E-F) forskolin (0.1 μ M) + Abn CBD (1 μ M), PD98059 (0.1 μ M) + Abn CBD (1 μ M), NPLA (0.1 μ M) + Abn CBD (1 μ M), wortmannin (0.1 μ M) + Abn CBD (1 μ M) treatment. Values are mean \pm S.E.M. of 5-6 observations. * P < 0.05 vs. vehicle; # P < 0.05 vs. Abn CBD; ^ P < 0.05 vs. NAGly values.

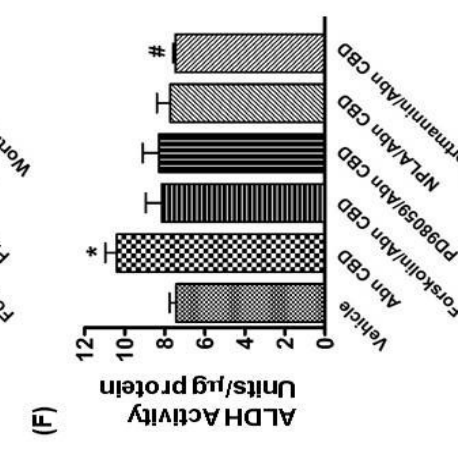
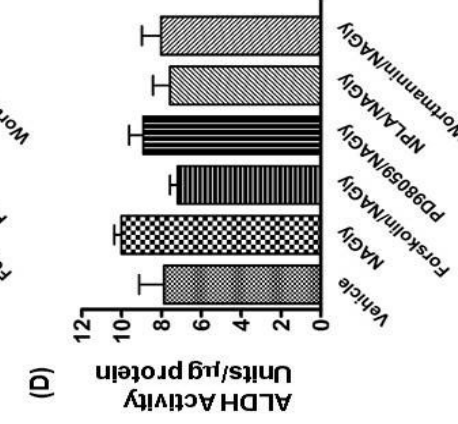
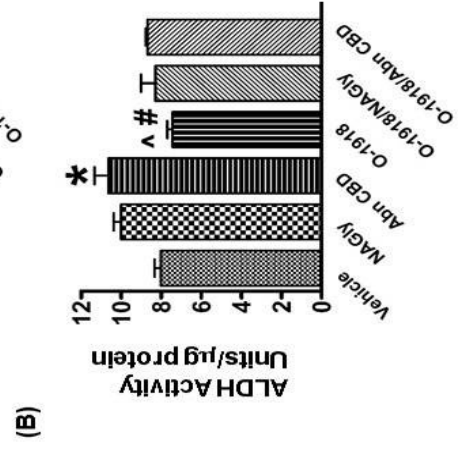
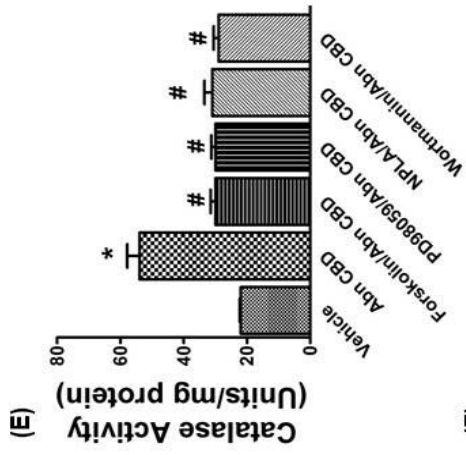
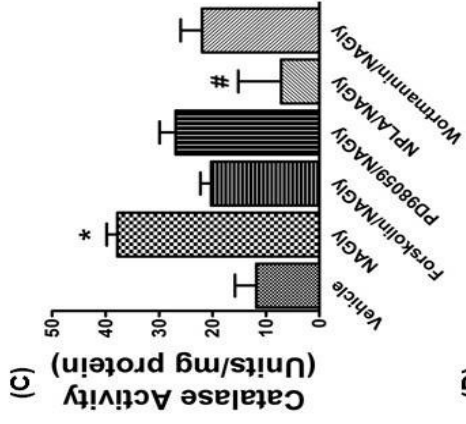
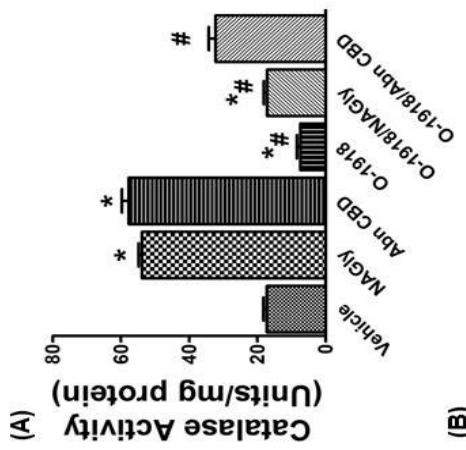


Figure 5.5. Effect of GPR18 activation or blockade on NADPH oxidase activity in nPC12 cells

Measurement of NADPH oxidase activity in nPC12 cells showing the effects of (A) NAGly (1 μ M), Abn CBD (1 μ M), O-1918 (1 μ M), O-1918 (1 μ M) + NAGly (1 μ M) or O-1918 (1 μ M) + Abn CBD (1 μ M) or (B) forskolin (0.1 μ M) + NAGly (1 μ M), PD98059 (0.1 μ M) + NAGly (1 μ M), NPLA (0.1 μ M) + NAGly (1 μ M), wortmannin (0.1 μ M) + NAGly (1 μ M), or (C) forskolin (0.1 μ M) + Abn CBD (1 μ M), PD98059 (0.1 μ M) + Abn CBD (1 μ M), NPLA (0.1 μ M) + Abn CBD (1 μ M), wortmannin (0.1 μ M) + Abn CBD (1 μ M) treatment. Values are mean \pm S.E.M. of 5-6 observations. * P < 0.05 vs. vehicle; # P < 0.05 vs. Abn CBD; ^ P < 0.05 vs. NAGly values.

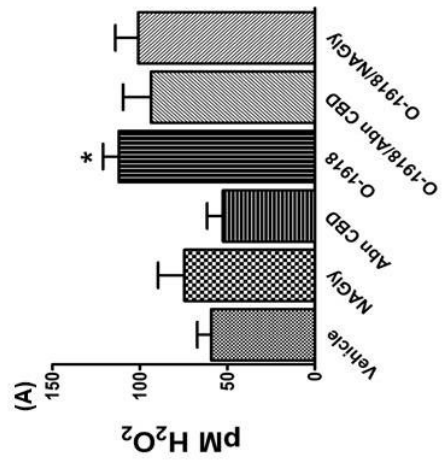
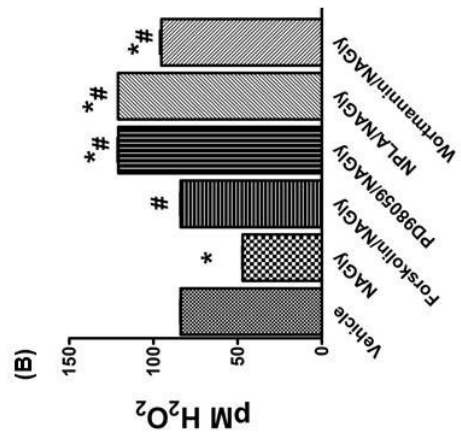
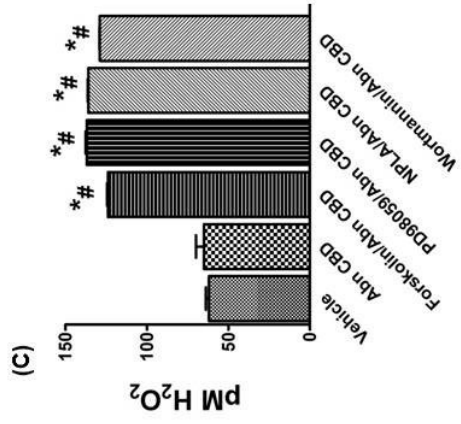


Figure 5.6. Effect of drug treatment on association of GPR18 with lipid rafts in nPC12 cells

Confocal microscopy showing the effect of drug treatment on association of GPR18 with lipid rafts in nPC12 cells. GPR18 exists in rafts at basal conditions (A). Activation of GPR18 (Abn CBD/ NAGly) caused its dissociation from the LR (B-C) and this response was abrogated by prior GPR18 blockade (O-1918) (D-F). Quantification of degree of co-localization obtained using Pearson's Correlation Coefficient analysis (G). Values are mean \pm S.E.M. of 5-6 observations.

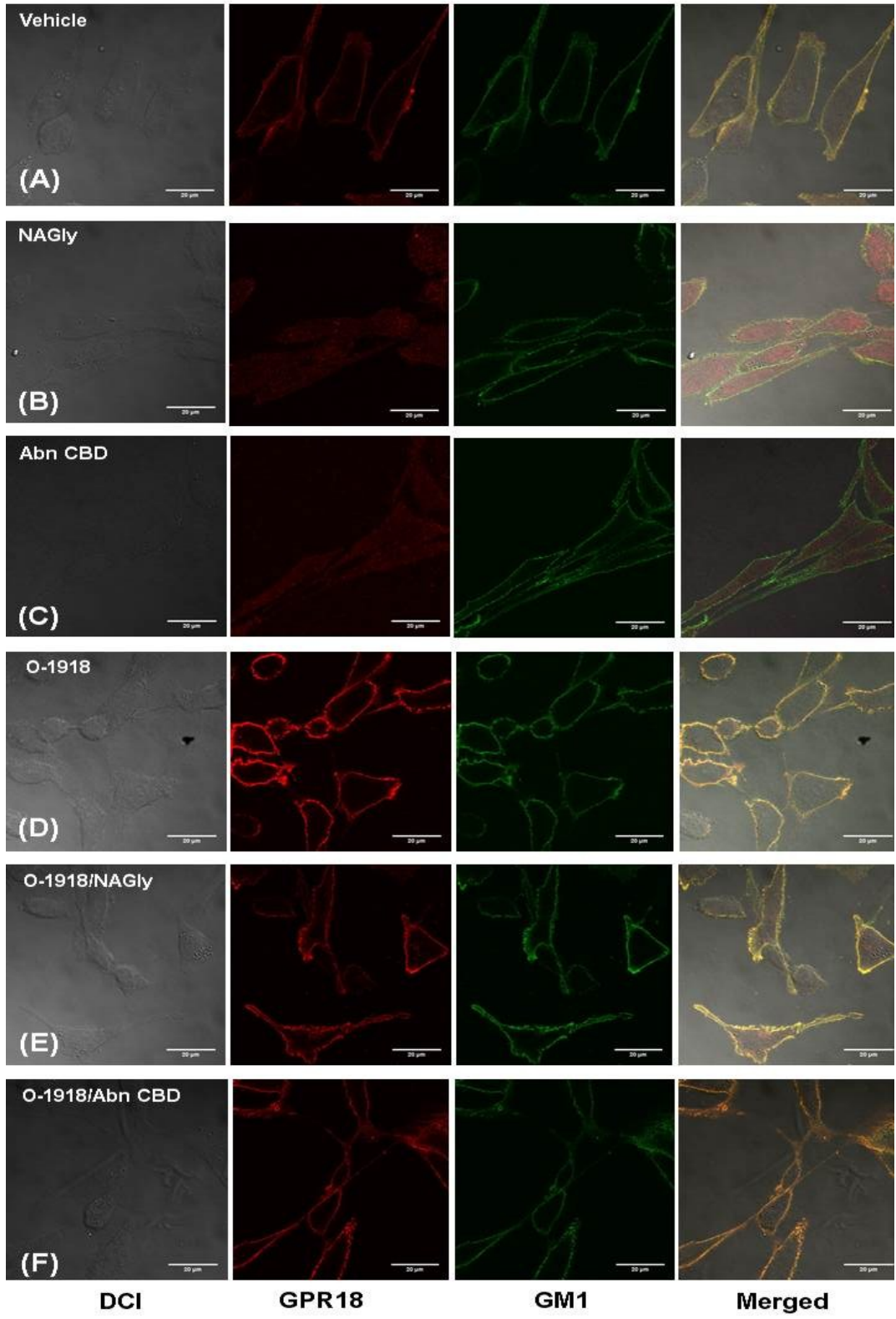


Figure 5.7. Effect of lipid raft disruption and drug treatment on association of GPR18 with lipid rafts in nPC12 cells

Confocal microscopy showing the effect of the LR disrupter methyl beta cyclodextrin (M β CD) and drug treatment on association of GPR18 with lipid rafts in nPC12 cells. GPR18 exists is displaced from the rafts in the presence of M β CD. Quantification of degree of co-localization in the presence and absence of M β CD and different GPR18 ligands obtained using Pearson's Correlation Coefficient analysis (G). Values are mean \pm S.E.M. of 10-12 observations. * $P < 0.05$ vs. control; & $P < 0.05$ vs. Control + M β CD; @ $P < 0.05$ vs. treatment + M β CD values.

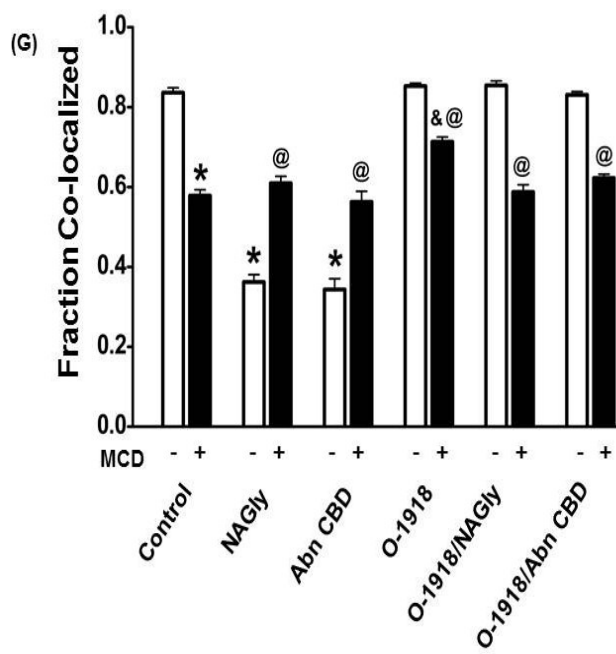
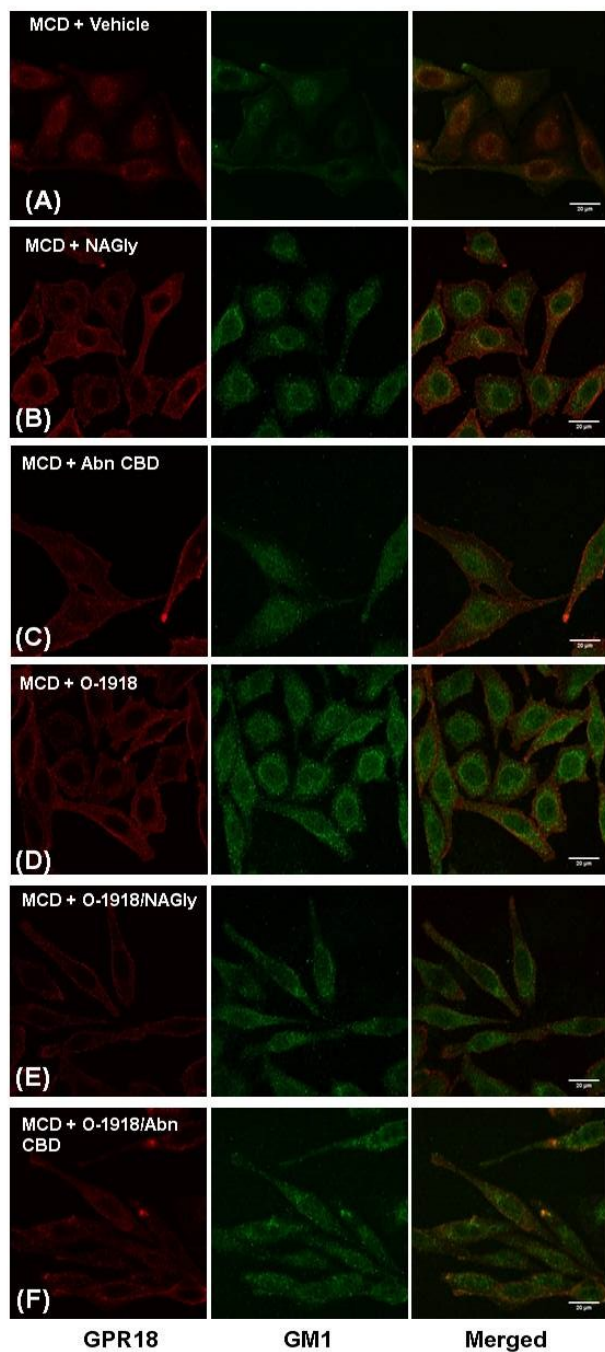


Figure 5.8. Effect of lipid raft disruption on GPR18 signaling in nPC12 cells

Western blots, cAMP and ROS levels in nPC12 cells showing the effects of control (methyl acetate), NAGly (1 μ M), Abn CBD (1 μ M) or O-1918 (1 μ M) treatment on pERK1/2 (A), pAkt (B), p-nNOS (C), adiponectin (ADN) (D), cAMP (E) expression and ROS levels (F) in nPC12 cells in the presence and absence of M β CD (2.5mM). Values are mean \pm S.E.M. of 5-6 observations. * $P < 0.05$ vs. control; & $P < 0.05$ vs. Control + M β CD; @ $P < 0.05$ vs. treatment + M β CD values.

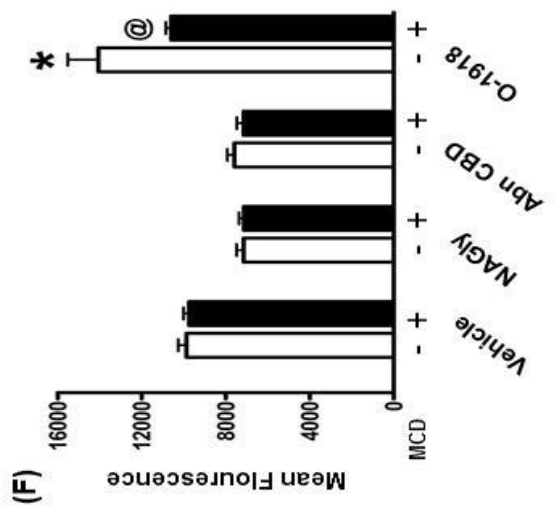
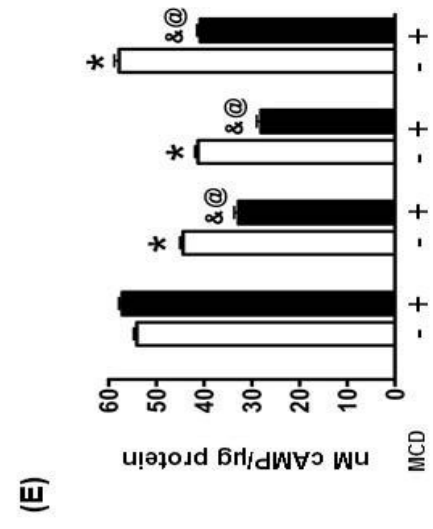
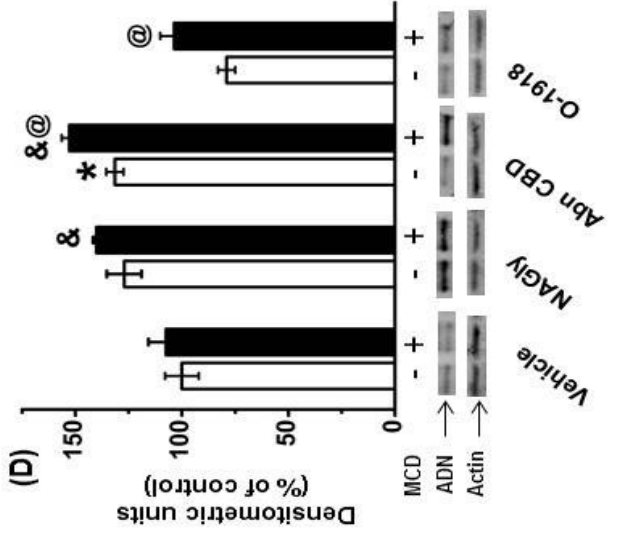
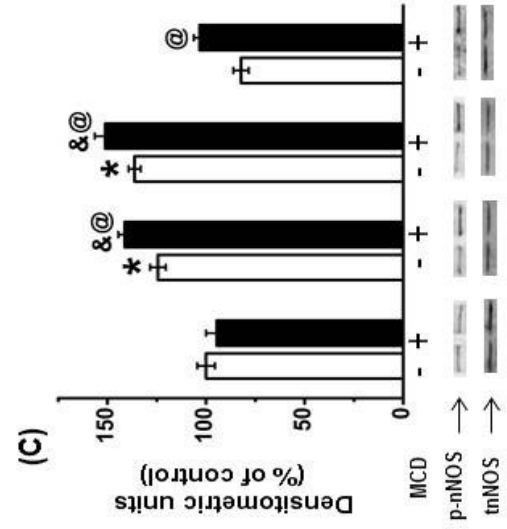
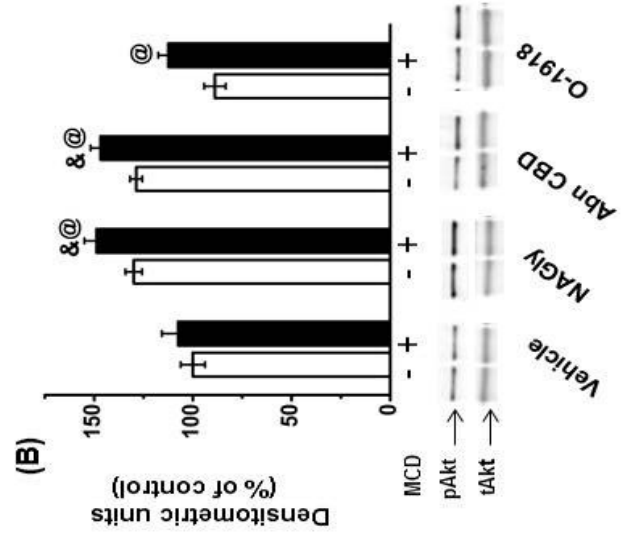
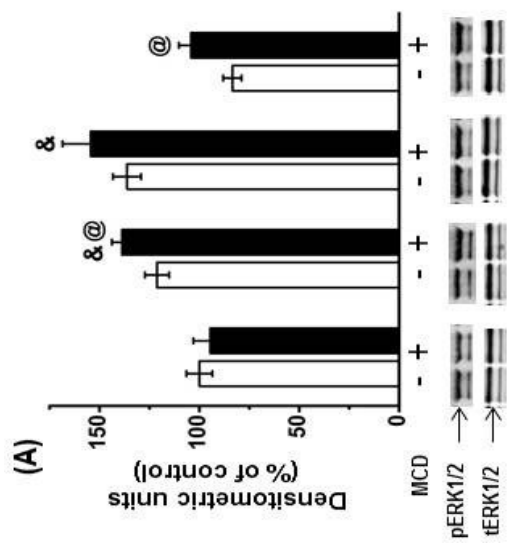
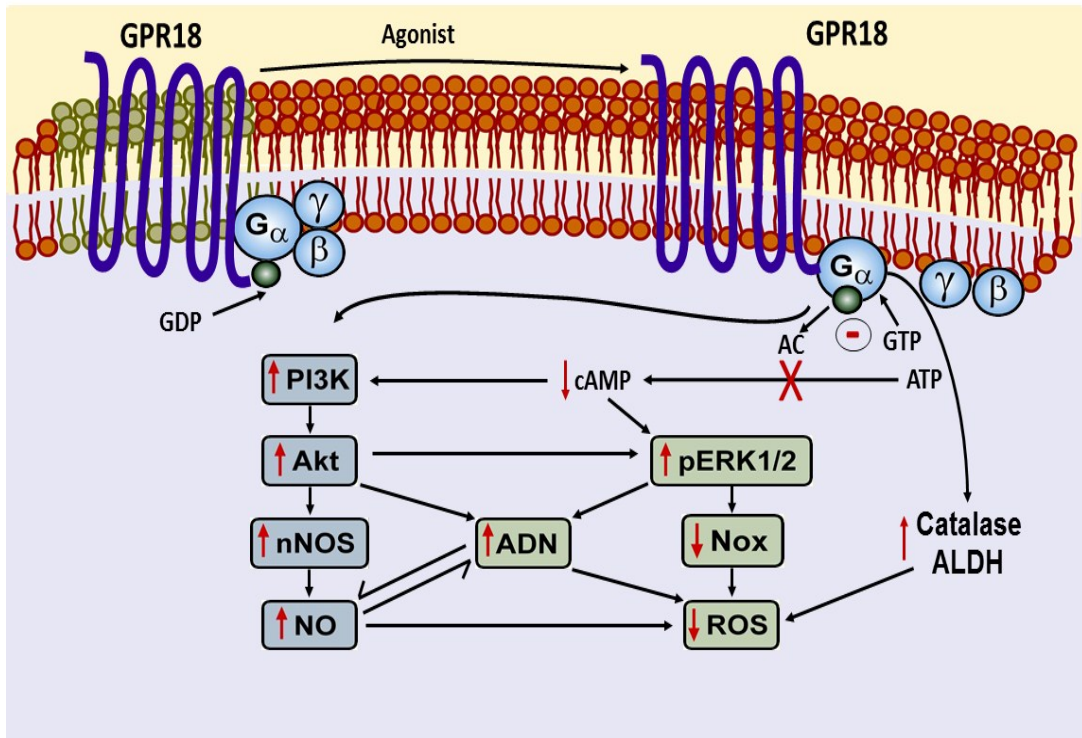


Figure 5.9. Schematic representation of the biochemical responses elicited by activating GPR18 in nPC12 cells

This model is based on the present and our reported findings (Penumarti and Abdel-Rahman, 2013). Activation of GPR18 displaces it from lipid rafts, inhibits cAMP leading to enhanced ADN, pERK1/2 and pAkt production, which causes increase in p-nNOS and NO production and decrease in ROS generation by increasing antioxidant enzymes (ALDH, catalase) and reducing levels of pro-oxidant enzymes (NADPH oxidase).



5.6. Discussion

We investigated the molecular mechanisms that underlie GPR18 activation in differentiated PC12 cells and the intracellular localization of GPR18 and its association with lipid rafts in order to elucidate how the presence of its ligands affect GPR18 trafficking in nPC12 cells. The following are the most important findings of the present study: 1) GPR18 is expressed in and is associated with CB₁R in nPC12 cells; 2) activation of GPR18 in nPC12 cells increased ADN, NO levels and the phosphorylation of Akt, ERK1/2 and nNOS and decreased cAMP levels; 3) activation of GPR18 decreased ROS level possibly through increasing antioxidant enzymes (catalase, ALDH) and decreasing pro-oxidant enzymes (NADPH oxidase); 4) prior blockade of GPR18 (O-1918) abrogated GPR18-mediated enhancements of pAkt, pERK1/2 or pnNOS or ADN levels; 5) GPR18 is associated with LRs in basal conditions and migrates out of LRs upon activation; 6) disrupting the LRs (M β CD) uncovers the effect of O-1918 and causes an increase in pAkt, pERK1/2 or pnNOS or ADN and a decrease in cAMP and ROS levels comparable with agonist treatment. Together, these findings suggest a pivotal role for LRs in GPR18-mediated cAMP-Akt-ERK1/2-nNOS-ADN signaling in nPC12 cells.

While previous studies confirm the expression of GPR18 in several in-vitro model systems (McHugh et al., 2010; Qin et al., 2011), these are the first data to demonstrate the presence of this receptor protein in differentiated PC12 cells (Figs. 5.1. A-B). Our dual labelled immunofluorescence studies show that GPR18 is co-expressed with CB₁R in nPC12 cells (Fig. 5.1. C), which might explain the antagonistic interaction between CB₁R and GPR18 in the RVLM in our recent study (Penumarti and Abdel-Rahman, 2013).

Our previous studies indicated that activation and blockade of intra-RVLM GPR18 caused an increase and decrease in blood pressure (BP), respectively, and that RVLM PI3K/Akt-ERK1/2-nNOS and adenylyl cyclase-cAMP networks play pivotal roles in GPR18 modulation of oxidative stress and BP via local adiponectin (ADN) release (Penumarti and Abdel-Rahman, 2013). Owing to the tissue scarcity in our in vivo model, we selected differentiated PC12 cells to further elucidate the signaling mechanisms of GPR18. Our in vivo studies (Penumarti and Abdel-Rahman, 2013) and other in vitro studies have shown that GPR18 is a Gi/o coupled receptor, activation of which leads to a decrease in adenylyl cyclase activity causing a decrease in cAMP levels and an increase in pERK1/2, pAkt and NO levels (Kishi et al., 2001; Offertáler et al., 2003; Mo et al., 2004). In this study we tested the hypothesis that activation of GPR18 in nPC12 cells triggers a similar signaling pathway. Our biochemical findings show that activation of GPR18 in nPC12 cells enhanced Akt, ERK1/2 and nNOS phosphorylation and increased ADN level while decreasing cAMP levels (Fig. 5.2.) and prior GPR18 blockade (O-1918) abrogated these responses. Our in-vitro studies are in line with our previous in-vivo findings (Penumarti and Abdel-Rahman, 2013) in normotensive rats indicating that GPR18 signals through the PI3K/Akt-ERK1/2-nNOS/ADN pathway.

We have previously shown that reduction in ROS through activation of PI3K/Akt-ERK1/2-nNOS/ADN pathway plays a crucial role in GPR18 mediated hypotension in normotensive rats (Penumarti and Abdel-Rahman, 2013) NAGly (endogenous GPR18 agonist) possesses anti-inflammatory properties (Institute for Laboratory Animal Research, 2011). Further, Δ^9 tetrahydrocannabinol (THC) (GPR18 agonist) exhibits antioxidant properties through

a PPAR γ pathway in models of Parkinson's disease (Carroll et al., 2012), and the GPR18 antagonist, cannabidiol, inhibited catalase activity in the liver (Usami et al., 2008). The link between oxidative stress and the endocannabinoid system is controversial. While, CB₂R and its ligands decrease oxidative stress (Farlow et al., 1984; Dampney et al., 1987), other studies on CB₁R indicate its ability to increase oxidative injury and inflammation in several model systems (Hokfelt T. et al., 1984; Pilowsky et al., 1986; Guyenet et al., 1989). Based on this evidence we sought to investigate the effect of GPR18 activation or blockade on ROS generating in nPC12 cells to further characterize GPR18 signaling in this model system. Our studies revealed that GPR18 activation reduced while its blockade (O-1918) significantly ($P < 0.05$) increased ROS levels (Fig. 5.3.). Further, O-1918 abrogated the reduction in ROS caused by NAGly or Abn CBD (Fig. 5.3.). GPR18 activation (Abn CBD or NAGly) caused a significant increase and decrease in catalase, ALDH and NADPH oxidase activity, respectively. Further, its blockade (O-1918) produced the opposite effects (Figs. 5.4. & 5.5.) and, similar to the inhibition of PI3K/Akt-ERK1/2-nNOS/ADN signaling or increasing cAMP levels, abrogated the increase in catalase, ALDH activity and the decrease in Nox activity caused by Abn CBD or NAGly (Figs. 5.4. & 5.5.). These results suggest a major role for the PI3K/Akt-ERK1/2-nNOS-ADN signaling acting in conjunction with the adenylyl cyclase/cAMP system in GPR18 modulation of redox state.

We have investigated the cellular distribution of GPR18 and its association with lipid rafts in order to elucidate how the presence of GPR18 ligands and the intracellular cholesterol levels affect GPR18 trafficking and signaling in nPC12 cells. Agonist binding and cholesterol depletion reduce CB₁R-LRs association (Potts et al., 2000). Association of GPR18, a putative

cannabinoid receptor with LRs has not been investigated. Thus, we analyzed whether GPR18 exists in lipid rafts at basal conditions or requires receptor activation. Interestingly, incubation with GPR18 agonist significantly decreased the cell surface distribution of GPR18, which assumed a more diffuse cytoplasmic localization, suggesting that the presence of the agonist modifies the interaction of GPR18 with LRs (Fig. 5.6). However the presence of the antagonist, O-1918 did not displace GPR18 from the rafts (Fig. 5.6). Also, this association seems to be dependent on membrane cholesterol as prior M β CD exposure decreased the GPR18-raft association in the presence of the antagonist (Fig.5.7). Further studies are needed to elucidate the enhanced signaling by the agonist in the presence of LR disruption although our confocal findings show an increased association of GPR18 with LR in the cytoplasm. However, it must be noted that that enhanced association is intracellular and not on the cell surface. These findings show for the first time that GPR18 is associated with LRs and agonist interaction displaces it from the raft domain suggesting the role of LRs as cellular devices for intracellular trafficking of GPR18.

Lipid rafts compartmentalize cellular membrane processes and form large platforms involved in protein and lipid processing, transport and signaling (Aicher et al., 2001; El-Mas and Abdel-Rahman, 2004; Drake et al., 2005). Because raft domains play an integral role in CB₁R (Potts et al., 2000; Bari et al., 2008) and GPR55 (another putative cannabinoid receptor) signaling (Li et al., 2005), we sought to elucidate the impact of LR disruption by cholesterol depletion on GPR18 signaling. One of the most important functional and structural components of lipid rafts is cholesterol (Herkenham et al., 1991; Drake et al., 2005) and its depletion alters

raft composition, function and subsequently the signaling of receptors associated with LRs such as CB₁R (Potts et al., 2000; Bari et al., 2008). According to our findings, pretreatment of nPC12 cells with M β CD enhanced the signaling of GPR18 agonist (Abn CBD or NAGly) and uncovered the effect of the antagonist (O-1918) (Fig. 5.8). These findings are consistent with reported findings on the effect of M β CD on CB₁R (Padley et al., 2003), but differ from GPR55 (decreased signaling following raft disruption) (Li et al., 2005) or CB₂R (unaffected by LR disruption) (Potts et al., 2000; Bari et al., 2005a; Bari et al., 2006). Thus, the trafficking and signaling of the different cannabinoid receptors are distinctly controlled by lipid rafts. Here, we show for the first time that lipid rafts serve as favorable platform to regulate GPR18 signaling. Together, these data establish functional significance of GPR18 cholesterol-dependent plasma membrane localization in regulating GPR18 signaling in nPC12 cells.

In conclusion, the present study yields new insight into the intracellular localization of GPR18 and its association with lipid rafts in nPC12 cells. We provide first evidence that Akt-ERK1/2-nNOS/ADN signaling and cAMP and ROS levels play key roles in GPR18 signaling. These studies also support the concept that GPR18 trafficking and signaling by lipid rafts critically depends on the ligand and membrane cholesterol content in nPC12 cells (Fig. 5.9). Further detailed analysis will be necessary to understand the role of lipid rafts in modulating the interaction of GPR18 and CB₁R and the pathophysiological importance of such an interaction.

CHAPTER SIX-GENERAL DISCUSSION AND SUMMARY

The main goal of the current study was to elucidate the role of the novel cannabinoid receptor GPR18 in central regulation of BP. Following demonstration of the expression of GPR18 in RVLM TH-ir neurons, which regulate sympathetic activity, subsequent studies elucidated the mechanisms implicated in the central GPR18-evoked sympathoinhibition/depressor response in SD rats and to investigate the cellular distribution of GPR18 and the role of lipid rafts in GPR18 trafficking and signaling in nPC12 cells. In pursuit of this goal, we characterized the centrally-elicited hemodynamic effects of GPR18 in conscious SD rats. We have also demonstrated the expression of GPR18 (protein) in nPC12 cells by: (i) detecting the band at 38 kDa (Figs. 3.6. & 5.1 A); (ii) immunohisto/cytochemical imaging in the RVLM and nPC12 respectively (Figs. 3.6. & 5.1 B); (iii) dual-labeling immunofluorescence, which revealed its expression in the C1 area within the RVLM (Fig. 3.6 C). Intra-RVLM administration of Abn CBD dose-dependently decreased MAP and increased HR, suggesting a GPR18-mediated inhibition of central sympathetic tone in conscious rats (Fig. 3.7). Notably, the depressor response elicited by central Abn CBD administration is consistent with reported in vitro findings that Abn CBD causes vasodilation in a CB₁/CB₂R independent manner (Jarai et al., 1999). This response was GPR18-mediated because it was abrogated (Fig. 3.11) by O-1918, a selective GPR18 antagonist (McHugh et al., 2010). Further, intra-RVLM blockade of GPR18 (O-1918) elicited dose-dependent increase in MAP and a decrease in HR (Fig. 3.7). The tachycardic response to Abn CBD plateaued and declined before the hypotensive response reached its nadir, which could be due to the offsetting effect of the central inhibitory effect of intra-RVLM Abn CBD on the baroreflex-mediated tachycardia (Figs. 3.7, 3.12). Collectively, these findings suggest that RVLM GPR18 exerts tonic restraining sympathoinhibitory influence on BP, and that

such central effect might contribute to the complexity of the observed HR responses. Cannabinoid-evoked hemodynamic responses are dramatically compromised by the use of anesthesia hence our studies were conducted in conscious rats to circumvent this negative impact (Lake et al., 1997; Gardiner et al., 2001).

In the second part of this study, we provided evidence for the contribution of the PI3K/Akt-ERK1/2-nNOS-ADN signaling, acting in conjunction with the adenylyl cyclase/cAMP system, in GPR18 modulation of redox state in the RVLM of rats as well as in nPC12 cells (Figs. 4.2-4.7). Activation of RVLM GPR18 (Abn CBD) increased ADN and pAkt, pERK1/2 and p-nNOS levels in the RVLM (Fig. 4.2) while prior blockade of RVLM GPR18 (O-1918) abrogated the enhancements of RVLM Akt, ERK1/2 and nNOS phosphorylation (Fig. 4.2). This is consistent with findings that implicated RVLM Akt-ERK1/2-nNOS activation in hypotensive responses (El-Mas et al., 2009; Kastenmayer et al., 2012) and that activation of other Gi/o coupled receptors in the brainstem lowers BP (Zhang and Abdel-Rahman, 2005). Also, GPR18 activation increases Akt and ERK1/2 phosphorylation and decreases cAMP levels in BV-2 microglia and HEK 293 cells (McHugh et al., 2010). Further, pharmacological inhibition of RVLM PI3K/Akt, ERK1/2 or nNOS or elevation of cAMP increased local ROS level, and attenuated the GPR18-mediated hypotension as well as the increases in ADN level and in Akt, ERK1/2 and nNOS phosphorylation in the RVLM (Figs. 4.3-4.6). Together, these findings suggest a pivotal role for the Akt/ERK1/2/nNOS/ADN signaling pathway and inhibition of cAMP as a molecular mechanism for GPR18-mediated reduction in BP in conscious unrestrained rats. Our studies in nPC12 cells are in line with, and extended, our in-vivo findings in

normotensive rats indicating that GPR18 signals through the PI3K/Akt-ERK1/2-nNOS/ADN pathway even in this in-vitro model system (Fig. 5.2). Our findings (Figs. 4.2 & 5.2) are consistent with the involvement of pERK1/2, PI3K/Akt, and nNOS in GPR18 signaling in other tissues (Mukhopadhyay et al., 2002; Zhang and Abdel-Rahman, 2005; McCollum et al., 2007; McHugh et al., 2010), and infer their contribution to the GPR18-mediated signaling.

A common anti-inflammatory role for ADN (Nanayakkara et al., 2012) and GPR18 (Vuong et al., 2008) might infer a role for ADN in modulating central sympathetic tone and in GPR18 signaling. A very recent study (Song et al., 2013) showed that the active (globular) ADN fraction replicates ADN-evoked neuroprotection via a reduction in oxidative stress. Further, CB₁R agonist WIN55,212-2 reduces ADN while blocking the receptor with rimonabant was shown to increase ADN levels in adipocytes (Sarker and Maruyama, 2003; McFarland et al., 2004; Bari et al., 2005a; Rimmerman et al., 2008b). Here we present the first evidence that GPR18 activation in the RVLM as well as in nPC12 cells results in an increase in ADN and a decrease in ROS levels (Figs. 3.8 A & 5.2 D) along with findings that support a functional role for ADN in GPR18 signaling because RVLM GPR18 blockade (O-1918): (i) reduced RVLM ADN (Fig. 3.8 A) and elevated BP; (ii) abrogated the GPR18 (Abn CBD)-mediated BP and neurochemical responses (Figs. 3.8, 3.11). Next, we show, for the first time, that ADN produced dose-dependent reductions in BP (Fig. 3.9A), increased RVLM NO_x (Fig. 3.9C), and reduced RVLM ROS levels (Fig. 3.9D). Together, these findings implicate RVLM ADN in the GPR18-mediated reductions in neuronal oxidative stress (ROS) in the RVLM and BP.

The inability of intra-RVLM NAGly, the endogenous GPR18 ligand, to reproduce the BP and neurochemical effects of the synthetic agonist Abn CBD was puzzling and cast doubt on the physiological role of GPR18. However, it must be remembered that NAGly direct or indirect activation of the physiologically antagonistic CB₁R might explain its inability to lower BP in our model system. In support of this notion are the following findings: (i) GPR18 and CB₁R are co-localized in RVLM neurons (Fig. 3.10A), which partly agrees with our findings that demonstrated CB₁R expression in RVLM TH-ir neurons (Ibrahim and Abdel-Rahman, 2011); (ii) the ability of intra-RVLM SR141716 (CB₁R blockade) to lower BP (Fig. 3.10B) is consistent with a sympathoexcitatory/pressor function for central CB₁R (Ibrahim and Abdel-Rahman, 2011); (iii) while NAGly alone had no effect on ADN, NO_x or ROS levels, prior CB₁R blockade (SR141716) uncovered NAGly ability to increase ADN and NO (Figs. 3.8 A, B), and to reduce ROS level (Fig. 3.13A) in the RVLM along with lowering BP (Fig. 3.10B). These novel findings replicated the redox and BP effects of Abn CBD (Figs. 3.8, 3.13A). Interestingly, in nPC12 cells the effects of NAGly on GPR18 signaling was comparable to that of Abn CBD (Fig. 5.2) and did not seem to be affected by CB₁R signaling although our studies show that GPR18 is also co-expressed with CB₁R in nPC12 cells (Fig. 5.1 C). This may be due to the involvement of an alternate signaling pathway that circumvents the effect of CB₁R in this system. Together, these data support the conclusion that the reductions in RVLM oxidative stress and BP are caused by Abn CBD direct agonism at GPR18 and suggest a functional role for GPR18-CB₁R interaction in the RVLM and nPC12 cells in modulating the local redox state.

Oxidative stress in the RVLM plays a major role in BP control and hypertension (Fridovich, 1978; Kishi et al., 2004; Chan et al., 2006; Yoshitaka, 2008). The link between oxidative stress and the endocannabinoid system is contrasting. While, CB₂R and its ligands decrease oxidative stress (Farlow et al., 1984; Dampney et al., 1987), other studies on CB₁R indicate its ability to increase oxidative injury and inflammation in several model systems (Hokfelt T. et al., 1984; Pilowsky et al., 1986; Guyenet et al., 1989). NAGly (endogenous GPR18 agonist) possesses anti-inflammatory properties (Institute for Laboratory Animal Research, 2011). Further, Δ⁹tetrahydrocannabinol (THC) (GPR18 agonist) exhibits antioxidant properties through a PPARγ pathway in models of Parkinson's disease (Carroll et al., 2012) and the GPR18 antagonist cannabidiol inhibited catalase activity in the liver (Usami et al., 2008). In this study we show that activation of RVLM GPR18 reduced neuronal ROS while its blockade increased neuronal ROS and abrogated the GPR18-mediated ROS reduction (Fig. 3.13). These redox findings, which paralleled the ADN (Fig. 3.8A) and BP (Figs. 3.11A, B) responses, reinforce a well-established role for oxidative stress in RVLM neurons in sympathoexcitation and BP elevation. Further, the findings lend credence to our conclusion that ADN-dependent reduction in RVLM ROS plays a crucial role in GPR18-mediated hypotension. Owing to the tissue scarcity in our in vivo model, we selected differentiated PC12 cells to further elucidate the signaling mechanisms of GPR18. Our studies in nPC12 cells revealed that GPR18 activation reduced while blockade (O-1918) significantly (P<0.05) increased ROS levels (Fig. 5.3.). Further, O-1918 abrogated the reduction in ROS caused by NAGly and Abn CBD (Fig. 5.3.). GPR18 activation (Abn CBD or NAGly) caused a significant increase and decrease in catalase, ALDH and NADPH oxidase activity respectively while its blockade (O-1918) produced the

opposite effect (Figs. 5.4. & 5.5.). Further, pretreatment with O-1918 or inhibition of PI3K/Akt-ERK1/2-nNOS/ADN signaling and increasing cAMP levels abrogated the increase in catalase, ALDH activity and attenuated the decrease in Nox activity produced by Abn CBD and/or NAGly (Figs. 5.4. & 5.5.). These results indicate the contribution of the PI3K/Akt-ERK1/2-nNOS-ADN signaling acting in conjunction with the adenylyl cyclase/cAMP system and pro-/anti-oxidant enzymes in GPR18 modulation of redox state.

We have investigated the cellular distribution of GPR18 and its association with lipid rafts in order to elucidate how the presence of GPR18 ligands and the intracellular cholesterol levels affect GPR18 trafficking and signaling in nPC12 cells. Agonist binding and cholesterol depletion were shown to decrease raft association of CB₁R (an important member of the endocannabinoid system) (Potts et al., 2000). There are no reports on the potential association of GPR18 with lipid rafts. Therefore, we investigated if such association exists in nPC12 cells. Interestingly, GPR18 agonists significantly decreased the cell surface distribution of GPR18, which assumed a more diffuse cytoplasmic localization, indicating that the presence of the agonist modifies the interaction of GPR18 with lipid rafts (Fig. 5.6.). However, the GPR18 antagonist, O-1918, did not displace GPR18 from the rafts (Fig. 5.6.). These findings show for the first time that GPR18 is associated with LRs and agonist interaction displaces it from the raft domain suggesting the role of LRs as cellular devices for intracellular trafficking of GPR18 (Fig. 5.7). Further, prior cholesterol depletion by M β CD decreases the association of GPR18 with rafts in the presence of vehicle and antagonist treatment (Fig. 5.8) indicating the importance of integrity of the raft for GPR18 trafficking.

We further sought to analyze whether disruption of rafts by cholesterol depletion affects GPR18 signaling. One of the most important functional and structural components of lipid rafts is cholesterol (Herkenham et al., 1991; Drake et al., 2005) and its depletion alters raft composition, function and subsequently the signaling of receptors like CB₁R (Potts et al., 2000; Bari et al., 2008). Our studies indicate that pretreatment of nPC12 cells with M β CD enhanced the signaling of GPR18 agonists (Abn CBD/NAGly) and uncovered the effect of the antagonist (O-1918) (Fig. 5.8.). Interestingly, this response is similar to the effect of M β CD on CB₁R (Padley et al., 2003) but differs from GPR55 (decreased signaling following raft disruption) (Li et al., 2005) or CB₂R (unaffected by LR disruption) (Potts et al., 2000; Bari et al., 2005a; Bari et al., 2006). Thus, the trafficking and signaling of the different cannabinoid receptors are distinctly controlled by lipid rafts. Here, we show for the first time that lipid rafts serve as a favorable platform to regulate GPR18 signaling. Together, these data establish functional significance of GPR18 cholesterol-dependent plasma membrane localization in regulating GPR18 signaling in nPC12 cells.

In summary, the present study yields new insight into the role of the novel cannabinoid receptor GPR18 in central (RVLM) control of BP. We present the first evidence that RVLM GPR18 mediates reductions in oxidative stress and BP in conscious rats. In the RVLM, CB₁R serves a counterbalancing role against GPR18, which explains the negligible hypotensive response caused by the endogenous GPR18 ligand NAGly in our model system. The present neurochemical findings provide first evidence that the RVLM PI3K/Akt-ERK1/2-nNOS/ADN signaling and cAMP and ROS levels play key roles in GPR18 modulation of BP in the RVLM

(Fig. 6.1). The results of our in-vitro studies highlight the intracellular localization of GPR18 and its association with lipid rafts in nPC12 cells. We provide first evidence that Akt-ERK1/2-nNOS/ADN signaling and cAMP and ROS levels play key roles in GPR18 signaling. These studies also support the concept that GPR18 trafficking and signaling by lipid rafts critically depends on the ligand and membrane cholesterol content in nPC12 cells (Fig. 5.9.).

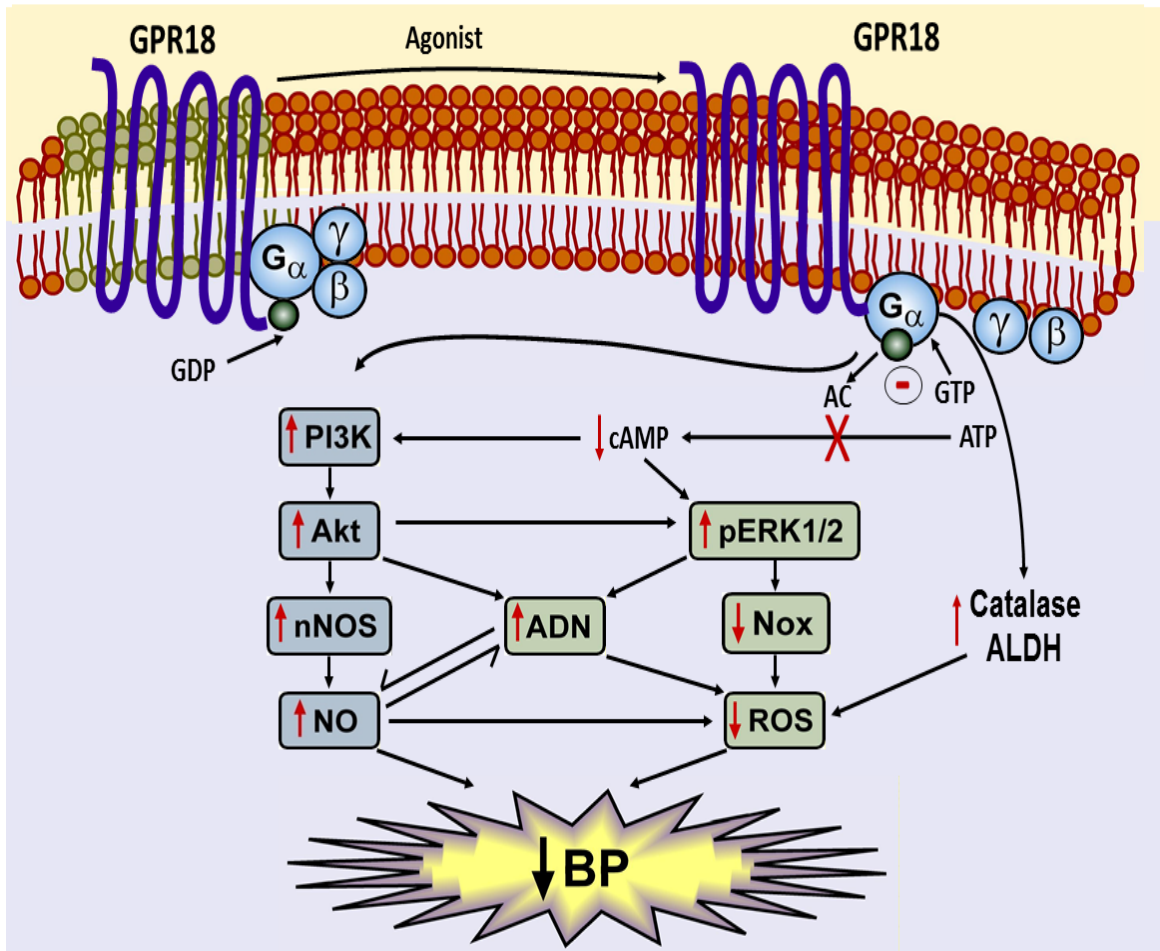
LIMITATIONS

1. Most of the agents that were used as ligands for GPR18 are either lipids or lipid derivatives. Notably the endogenous agonist (NAGly) is highly lipophilic and could be degraded by fatty acid amide hydrolase (FAAH). Accurate dosing can be assured by pretreating the animals with a FAAH (hydrolyses NAGly) (Bezuglov et al., 2006) inhibitor like PF-622 or URB597.
2. The present studies rely heavily on examination of changes in nitric oxide levels and ROS generation with the use of DHE fluorescence assay. However, quantification with intensity histogram alone may be inadequate. Therefore, biochemical approaches such as the nitrite/nitrate colorimetric assay and DCF were implemented to support the data obtained from DHE fluorescence assay.
3. The double labeling co-localization studies might not precisely and conclusively demonstrate the association between the proteins of interest. This limitation could be resolved by using a new technique, fluorescence resonance energy transfer (FRET), which is frequently used to explore protein-protein interaction. Also, the identification of lipid rafts using the cholera toxin-B (CTB) has a drawback of changing the functionality

of the membrane because it works by crosslinking the gangliosides (GM1) inside the membrane. In order to address this question, alternative method of LR identification can be utilized in future studies.

4. The use of M β CD, as a lipid raft disruptor, has the drawback of extracting other membrane components of the cells and subjecting them to a stress situation, which might confound the result. This pitfall can be overcome by replenishing the cells with cholesterol, which should reverse the effects of drug treatment indicating that the results are not artifacts.

Figure. 6. 1. Schematic presentation of the major findings of the study and proposed future studies. See details in the text.



FUTURE DIRECTIONS

The present findings suggest a novel role for brainstem cAMP-PI3K/Akt-ERK1/2-nNOS/ADN signaling in the central GPR18-evoked depressor response. Importantly, the findings established a causal link between suppression of brainstem ROS generation and the sympathoinhibitory/depressor response elicited by central GPR18 activation (Fig.6.1). Notably, in vivo and in vitro findings associated the enhanced PI3K/Akt-ERK1/2-nNOS/ADN signaling with modulation of ROS generation in normotensive rats. Therefore, it will be interesting to determine whether the expression or signaling of GPR18 is altered in hypertensive rats. Since ERK1/2 phosphorylation can be triggered by pAkt (Hong et al., 2012) or can trigger Akt phosphorylation (Ramakrishnan et al., 2012) and both pAkt and pERK1/2 enhance nNOS phosphorylation (El-Mas et al., 2009; Kastenmayer et al., 2012). Further studies are needed to elucidate the signaling pathways between PI3K/Akt and ERK1/2. Further detailed analysis will be necessary to understand the role of lipid rafts in modulating the interaction of GPR18 and CB₁R and the pathophysiological importance of such an interaction in in-vivo models. Also, future studies are warranted to delineate the role of GPR18 in conditions like hypertension to develop novel antihypertensive therapeutics that target the central GPR18 signaling. Such studies will advance our knowledge of the role of endocannabinoids in the neural control of BP and might lead to the development of novel antihypertensive drugs.

Reference List

- Aicher SA, Kraus JA, Sharma S, Patel A and Milner TA (2001) Selective distribution of mu-opioid receptors in C1 adrenergic neurons and their afferents. *Journal of Comparative Neurology* **433**:23-33.
- Akki A, Zhang M, Murdoch C, Brewer A and Shah AM (2009) NADPH oxidase signaling and cardiac myocyte function. *Journal of Molecular and Cellular Cardiology* **47**:15-22.
- Alessi DR, Cuenda A, Cohen P, Dudley DT and Saltiel AR (1995) PD 098059 Is a Specific Inhibitor of the Activation of Mitogen-activated Protein Kinase Kinase in Vitro and in Vivo. *Journal of Biological Chemistry* **270**:27489-27494.
- Alexander SP (2012) So what do we call GPR18 now? *British journal of pharmacology* **165**:2411-2413.
- Bari M, Battista N, Fezza F, Finazzi-Agrò A and Maccarrone M (2005a) Lipid Rafts Control Signaling of Type-1 Cannabinoid Receptors in Neuronal Cells: IMPLICATIONS FOR ANANDAMIDE-INDUCED APOPTOSIS. *Journal of Biological Chemistry* **280**:12212-12220.
- Bari M, Oddi S, De Simone C, Spagnolo P, Gasperi V, Battista N, Centonze D and Maccarrone M (2008) Type-1 cannabinoid receptors colocalize with caveolin-1 in neuronal cells. *Neuropharmacology* **54**:45-50.

- Bari M, Paradisi A, Pasquariello N and Maccarrone M (2005b) Cholesterol-dependent modulation of type 1 cannabinoid receptors in nerve cells. *Journal of Neuroscience Research* **81**:275-283.
- Bari M, Spagnuolo P, Fezza F, Oddi S, Pasquariello N, Finazzi-Agrò A and Maccarrone M (2006) Effect of Lipid Rafts on Cb2 Receptor Signaling and 2-Arachidonoyl-Glycerol Metabolism in Human Immune Cells. *The Journal of Immunology* **177**:4971-4980.
- Becher A, Green A, Ige AO, Wise A, White JH and McIlhinney RA (2004) Ectopically expressed gamma-aminobutyric acid receptor B is functionally down-regulated in isolated lipid raft-enriched membranes. *Biochemical and biophysical research communications* **321**:981-987.
- Bedard K and Krause K-H (2007) The NOX Family of ROS-Generating NADPH Oxidases: Physiology and Pathophysiology. *Physiological Reviews* **87**:245-313.
- Begg M, Pacher P, Bátkai S, Osei-Hyiaman D, Offertáler L, Mo FM, Liu J and Kunos G (2005) Evidence for novel cannabinoid receptors. *Pharmacology & Therapeutics* **106**:133-145.
- Bezuglov VV, Gretskaja NM, Blazhenova AV, Adrianova EL, Akimov AV, Bobrov M, Nazimov IV, Kisel MI, Sharko OL, Novikov AV, Krasnov NV, Shevchenko VP, V'Iunova T V and Miasoedova NF (2006) [Arachidonoyl amino acids and arachidonoyl peptides: synthesis and properties]. *Bioorganicheskaia khimiia* **32**:258-267.

- Biswas KK, Sarker KP, Abeyama K, Kawahara K-i, Iino S, Otsubo Y, Saigo K, Izumi H, Hashiguchi T, Yamakuchi M, Yamaji K, Endo R, Suzuki K, Imaizumi H and Maruyama I (2003) Membrane cholesterol but not putative receptors mediates anandamide-induced hepatocyte apoptosis. *Hepatology* **38**:1167-1177.
- Bradshaw H, Rimmerman N, Hu S, Benton V, Stuart J, Masuda K, Cravatt B, O'Dell D and Walker JM (2009) The endocannabinoid anandamide is a precursor for the signaling lipid N-arachidonoyl glycine by two distinct pathways. *BMC Biochemistry* **10**:14.
- Burstein SH, Huang SM, Petros TJ, Rossetti RG, Walker JM and Zurier RB (2002) Regulation of anandamide tissue levels by N-arachidonoylglycine. *Biochemical Pharmacology* **64**:1147-1150.
- Caldwell MD, Hu SS-J, Viswanathan S, Bradshaw H, Kelly MEM and Straiker A (2013) A GPR18-based signalling system regulates IOP in murine eye. *British journal of pharmacology* **169**:834-843.
- Campese VM, Ye S, Zhong H, Yanamadala V, Ye Z and Chiu J (2004) Reactive oxygen species stimulate central and peripheral sympathetic nervous system activity. *American journal of physiology Heart and circulatory physiology* **287**:H695-703.
- Carbone L (2012) Pain Management Standards in the Eighth Edition of the Guide for the Care and Use of Laboratory Animals. *J Am Assoc Lab Anim* **51**:322-328.

- Carroll CB, Zeissler ML, Hanemann CO and Zajicek JP (2012) Δ 9-tetrahydrocannabinol (Δ 9-THC) exerts a direct neuroprotective effect in a human cell culture model of Parkinson's disease. *Neuropathology and Applied Neurobiology* **38**:535-547.
- Chan SH and Chan JY (2014) Brain Stem NOS and ROS in Neural Mechanisms of Hypertension. *Antioxidants & redox signaling* **20**:146-163.
- Chan SH, Wang LL and Chan JY (2003) Differential engagements of glutamate and GABA receptors in cardiovascular actions of endogenous nNOS or iNOS at rostral ventrolateral medulla of rats. *Br J Pharmacol* **138**:584-593.
- Chan SH, Wang LL, Tseng HL and Chan JY (2007) Upregulation of AT1 receptor gene on activation of protein kinase Cbeta/nicotinamide adenine dinucleotide diphosphate oxidase/ERK1/2/c-fos signaling cascade mediates long-term pressor effect of angiotensin II in rostral ventrolateral medulla. *Journal of hypertension* **25**:1845-1861.
- Chan SHH, Tai M-H, Li C-Y and Chan JYH (2006) Reduction in molecular synthesis or enzyme activity of superoxide dismutases and catalase contributes to oxidative stress and neurogenic hypertension in spontaneously hypertensive rats. *Free Radical Biology and Medicine* **40**:2028-2039.
- Chan SHH, Wang L-L, Wang S-H and Chan JYH (2001) Differential cardiovascular responses to blockade of nNOS or iNOS in rostral ventrolateral medulla of the rat. *British journal of pharmacology* **133**:606-614.

- Chini B and Parenti M (2004) G-protein coupled receptors in lipid rafts and caveolae: how, when and why do they go there? *Journal of Molecular Endocrinology* **32**:325-338.
- Coleman TG (1980) Arterial baroreflex control of heart rate in the conscious rat. *American Journal of Physiology - Heart and Circulatory Physiology* **238**:H515-H520.
- Collin B, Busseuil D, Zeller M, Perrin C, Barthez O, Du villard L, Vergely C, Bardou M, Dumas M, Cottin Y and Rochette L (2007) Increased superoxide anion production is associated with early atherosclerosis and cardiovascular dysfunctions in a rabbit model. *Mol Cell Biochem* **294**:225-235.
- Czarny M, Lavie Y, Fiucci G and Liscovitch M (1999) Localization of Phospholipase D in Detergent-insoluble, Caveolin-rich Membrane Domains: MODULATION BY CAVEOLIN-1 EXPRESSION AND CAVEOLIN-182-101. *Journal of Biological Chemistry* **274**:2717-2724.
- Dainese E, Oddi S, Bari M and Maccarrone M (2007) Modulation of the Endocannabinoid System by Lipid Rafts. *Current Medicinal Chemistry* **14**:2702-2715.
- Dampney RA (1994) Functional organization of central pathways regulating the cardiovascular system. *Physiological Reviews* **74**:323-364.
- Dampney RA, Czachurski J, Dembowski K, Goodchild AK and Seller H (1987) Afferent connections and spinal projections of the pressor region in the rostral ventrolateral medulla of the cat. *Journal of the Autonomic Nervous System* **20**:73-86.

- de Oliveira-Sales EB, Nishi EE, Boim MA, Dolnikoff MS, Bergamaschi CT and Campos RR (2010) Upregulation of AT1R and iNOS in the rostral ventrolateral medulla (RVLM) is essential for the sympathetic hyperactivity and hypertension in the 2K-1C Wistar rat model. *American journal of hypertension* **23**:708-715.
- Drake CT, Aicher SA, Montalmant FL and Milner TA (2005) Redistribution of mu-opioid receptors in C1 adrenergic neurons following chronic administration of morphine. *Experimental Neurology* **196**:365-372.
- Edwards E and Paton JF (1999) 5-HT(4) receptors in nucleus tractus solitarii attenuate cardiopulmonary reflex in anesthetized rats. *The American journal of physiology* **277**:H1914-1923.
- El-Mas MM and Abdel-Rahman AA (2004) Differential modulation by estrogen of alpha2-adrenergic and I1-imidazoline receptor-mediated hypotension in female rats. *Journal of Applied Physiology* **97**:1237-1244.
- El-Mas MM and Abdel-Rahman AA (2011) Enhanced catabolism to acetaldehyde in rostral ventrolateral medullary neurons accounts for the pressor effect of ethanol in spontaneously hypertensive rats. *American Journal of Physiology - Heart and Circulatory Physiology*.
- El-Mas MM, Fan M and Abdel-Rahman AA (2009) Facilitation of Myocardial PI3K/Akt/nNOS Signaling Contributes to Ethanol-Evoked Hypotension in Female Rats. *Alcoholism: Clinical and Experimental Research* **33**:1158-1168.

- Farlow DM, Goodchild AK and Dampney RA (1984) Evidence that vasomotor neurons in the rostral ventrolateral medulla project to the spinal sympathetic outflow via the dorsomedial pressor area. *Brain Research* **298**:313-320.
- Fielding CJ and Fielding PE (1997) Intracellular cholesterol transport. *Journal of Lipid Research* **38**:1503-1521.
- Frey RS, Ushio-Fukai M and Malik AB (2009) NADPH oxidase-dependent signaling in endothelial cells: role in physiology and pathophysiology. *Antioxidants & redox signaling* **11**:791-810.
- Fridovich I (1978) The biology of oxygen radicals. *Science* **201**:875-880.
- Fry M, Smith PM, Hoyda TD, Duncan M, Ahima RS, Sharkey KA and Ferguson AV (2006) Area postrema neurons are modulated by the adipocyte hormone adiponectin. *The Journal of neuroscience : the official journal of the Society for Neuroscience* **26**:9695-9702.
- Gantz I, Muraoka A, Yang YK, Samuelson LC, Zimmerman EM, Cook H and Yamada T (1997) Cloning and chromosomal localization of a gene (GPR18) encoding a novel seven transmembrane receptor highly expressed in spleen and testis. *Genomics* **42**:462-466.
- Gardiner SM, March JE, Kemp PA and Bennett T (2001) Regional haemodynamic responses to the cannabinoid agonist, WIN 55212-2, in conscious, normotensive rats, and in hypertensive, transgenic rats. *British Journal of Pharmacology* **133**:445-453.

- Gardiner SM, March JE, Kemp PA and Bennett T (2002) Complex regional haemodynamic effects of anandamide in conscious rats. *British journal of pharmacology* **135**:1889-1896.
- Gaus K, Gratton E, Kable EPW, Jones AS, Gelissen I, Kritharides L and Jessup W (2003) Visualizing lipid structure and raft domains in living cells with two-photon microscopy. *Proceedings of the National Academy of Sciences* **100**:15554-15559.
- Godlewski G, Offertaler L, Wagner JA and Kunos G (2009) Receptors for acylethanolamides- GPR55 and GPR119. *Prostaglandins Other Lipid Mediat* **89**:105-111.
- Griendling KK, Sorescu D and Ushio-Fukai M (2000) NAD(P)H Oxidase : Role in Cardiovascular Biology and Disease. *Circulation Research* **86**:494-501.
- Guyenet PG (2006) The sympathetic control of blood pressure. *Nat Rev Neurosci* **7**:335-346.
- Guyenet PG, Haselton JR and Sun MK (1989) Sympathoexcitatory neurons of the rostroventrolateral medulla and the origin of the sympathetic vasomotor tone. *Progress in Brain Research* **81**:105-116.
- Herkenham M, Lynn AB, Johnson MR, Melvin LS, de Costa BR and Rice KC (1991) Characterization and localization of cannabinoid receptors in rat brain: a quantitative in vitro autoradiographic study. *Journal of Neuroscience* **11**:563-583.
- Hirooka Y (2008) Role of reactive oxygen species in brainstem in neural mechanisms of hypertension. *Autonomic neuroscience : basic & clinical* **142**:20-24.

- Hohmann AG, Suplita RL, Bolton NM, Neely MH, Fegley D, Mangieri R, Krey JF, Walker JM, Holmes PV, Crystal JD, Duranti A, Tontini A, Mor M, Tarzia G and Piomelli D (2005) An endocannabinoid mechanism for stress-induced analgesia. *Nature* **435**:1108-1112.
- Hokfelt T., Johansson O. and M. G (1984) Central catecholamine neurons as revealed by immunohistochemistry with special reference to adrenaline neurons. *Classical Transmitters in the CNS*:157-276.
- Hong J, Qian T, Le Q, Sun X, Wu J, Chen J, Yu X and Xu J (2012) NGF promotes cell cycle progression by regulating D-type cyclins via PI3K/Akt and MAPK/Erk activation in human corneal epithelial cells. *Molecular vision* **18**:758-764.
- Huang S, Bisogno T, Petros T, Chang S, Zavitsanos P, Zipkin R, Sivakumar R, Coop A, Maeda D and De Petrocellis L (2001) Identification of a new class of molecules, the arachidonyl amino acids, and characterization of one member that inhibits pain. *J Biol Chem* **276**:42639 - 42644.
- Ibrahim BM and Abdel-Rahman AA (2011) Role of brainstem GABAergic signaling in central cannabinoid receptor evoked sympathoexcitation and pressor responses in conscious rats. *Brain Res* **1414**:1-9.
- Ibrahim BM and Abdel-Rahman AA (2012a) Differential modulation of brainstem phosphatidylinositol 3-kinase/Akt and extracellular signal-regulated kinase 1/2 signaling underlies WIN55,212-2 centrally mediated pressor response in conscious rats. *The Journal of pharmacology and experimental therapeutics* **340**:11-18.

- Ibrahim BM and Abdel-Rahman AA (2012b) Enhancement of rostral ventrolateral medulla neuronal nitric-oxide synthase-nitric-oxide signaling mediates the central cannabinoid receptor 1-evoked pressor response in conscious rats. *The Journal of pharmacology and experimental therapeutics* **341**:579-586.
- Ince E, Ciliax BJ and Levey AI (1997) Differential expression of D1 and D2 dopamine and m4 muscarinic acetylcholine receptor proteins in identified striatonigral neurons. *Synapse (New York, NY)* **27**:357-366.
- Insel PA, Head BP, Patel HH, Roth DM, Bunday RA and Swaney JS (2005) Compartmentation of G-protein-coupled receptors and their signalling components in lipid rafts and caveolae. *Biochemical Society transactions* **33**:1131-1134.
- Institute for Laboratory Animal Research (2011) *Guide for the Care and Use of Laboratory Animals 8th ed.* National Research Council, Washington DC.
- Jarai Z, Wagner JA, Varga K, Lake KD, Compton DR, Martin BR, Zimmer AM, Bonner TI, Buckley NE, Mezey E, Razdan RK, Zimmer A and Kunos G (1999) Cannabinoid-induced mesenteric vasodilation through an endothelial site distinct from CB1 or CB2 receptors. *Proceedings of the National Academy of Sciences of the United States of America* **96**:14136-14141.
- Jarbe TU, Gifford RS and Makriyannis A (2010) Antagonism of (9)-THC induced behavioral effects by rimonabant: time course studies in rats. *Eur J Pharmacol* **648**:133-138.

- Javanmardi K, Parviz M, Sadr Ss, Keshavarz M, Minaii B and Dehpour AR (2005) Involvement of N-methyl-D-aspartate Receptors and Nitric Oxide in the Rostra Ventromedial Medulla in Modulating Morphine Pain-Inhibitory Signals From the Periaqueductal Grey Matter in Rats. *Clinical and Experimental Pharmacology and Physiology* **32**:585-589.
- Jeong H-J, Vandenberg RJ and Vaughan CW (2010) N-arachidonyl-glycine modulates synaptic transmission in superficial dorsal horn. *British journal of pharmacology* **161**:925-935.
- Jin S, Zhou F, Katirai F and Li PL (2011) Lipid raft redox signaling: molecular mechanisms in health and disease. *Antioxidants & redox signaling* **15**:1043-1083.
- Johns DG, Behm DJ, Walker DJ, Ao Z, Shapland EM, Daniels DA, Riddick M, Dowell S, Staton PC, Green P, Shabon U, Bao W, Aiyar N, Yue TL, Brown AJ, Morrison AD and Douglas SA (2007) The novel endocannabinoid receptor GPR55 is activated by atypical cannabinoids but does not mediate their vasodilator effects. *British journal of pharmacology* **152**:825-831.
- Karlsson GA, Preuss CV, Chaitoff KA, Maher TJ and Ally A (2006) Medullary monoamines and NMDA-receptor regulation of cardiovascular responses during peripheral nociceptive stimuli. *Neuroscience Research* **55**:316-326.
- Kastenmayer RJ, Moore RM, Bright AL, Torres-Cruz R and Elkins WR (2012) Select Agent and Toxin Regulations: Beyond the Eighth Edition of the Guide for the Care and Use of Laboratory Animals. *J Am Assoc Lab Anim* **51**:333-338.

- Kimura Y, Hirooka Y, Kishi T, Ito K, Sagara Y and Sunagawa K (2009) Role of Inducible Nitric Oxide Synthase in Rostral Ventrolateral Medulla in Blood Pressure Regulation in Spontaneously Hypertensive Rats. *Clinical and Experimental Hypertension* **31**:281-286.
- Kimura Y, Hirooka Y, Sagara Y, Ito K, Kishi T, Shimokawa H, Takeshita A and Sunagawa K (2005) Overexpression of Inducible Nitric Oxide Synthase in Rostral Ventrolateral Medulla Causes Hypertension and Sympathoexcitation via an Increase in Oxidative Stress. *Circulation Research* **96**:252-260.
- Kishi T, Hirooka Y, Ito K, Sakai K, Shimokawa H and Takeshita A (2002) Cardiovascular effects of overexpression of endothelial nitric oxide synthase in the rostral ventrolateral medulla in stroke-prone spontaneously hypertensive rats. *Hypertension* **39**:264-268.
- Kishi T, Hirooka Y, Kimura Y, Ito K, Shimokawa H and Takeshita A (2004) Increased Reactive Oxygen Species in Rostral Ventrolateral Medulla Contribute to Neural Mechanisms of Hypertension in Stroke-Prone Spontaneously Hypertensive Rats. *Circulation* **109**:2357-2362.
- Kishi T, Hirooka Y, Sakai K, Shigematsu H, Shimokawa H and Takeshita A (2001) Overexpression of eNOS in the RVLM Causes Hypotension and Bradycardia Via GABA Release. *Hypertension* **38**:896-901.
- Kohno M, Hasegawa H, Inoue A, Muraoka M, Miyazaki T, Oka K and Yasukawa M (2006) Identification of N-arachidonylglycine as the endogenous ligand for orphan G-protein-

coupled receptor GPR18. *Biochemical and biophysical research communications* **347**:827-832.

Komura N, Maeda N, Mori T, Kihara S, Nakatsuji H, Hirata A, Tochino Y, Funahashi T and Shimomura I (2013) Adiponectin Protein Exists in Aortic Endothelial Cells. *PLoS ONE* **8**:e71271.

Konno S, Hirooka Y, Kishi T and Sunagawa K (2012) Sympathoinhibitory effects of telmisartan through the reduction of oxidative stress in the rostral ventrolateral medulla of obesity-induced hypertensive rats. *J Hypertens* **30**:1992-1999.

Lake KD, Martin BR, Kunos G and Varga K (1997) Cardiovascular effects of anandamide in anesthetized and conscious normotensive and hypertensive rats. *Hypertension* **29**:1204-1210.

Li G, Wang X and Abdel-Rahman AA (2005) Neuronal norepinephrine responses of the rostral ventrolateral medulla and nucleus tractus solitarius neurons distinguish the I1- from the alpha2-receptor-mediated hypotension in conscious SHRs. *Journal of Cardiovascular Pharmacology* **46**:52-62.

Mackie K and Stella N (2006) Cannabinoid receptors and endocannabinoids: evidence for new players. *The AAPS journal* **8**:E298-306.

- Mao L and Abdel-Rahman AA (1994) Inhibition of glutamate uptake in the rostral ventrolateral medulla enhances baroreflex-mediated bradycardia in conscious rats. *Brain Research* **654**:343-348.
- Mao L and Abdel-Rahman AA (1995) Blockade of l-glutamate receptors in the rostral ventrolateral medulla contributes to ethanol-evoked impairment of baroreflexes in conscious rats. *Brain Research Bulletin* **37**:513-521.
- Mason TJ and Matthews M (2012) Aquatic Environment, Housing, and Management in the Eighth Edition of the Guide for the Care and Use of Laboratory Animals: Additional Considerations and Recommendations. *J Am Assoc Lab Anim* **51**:329-332.
- Matias I, Cristino L and Di Marzo V (2008) Endocannabinoids: Some Like it Fat (and Sweet Too). *Journal of Neuroendocrinology* **20**:100-109.
- McCollum L, Howlett AC and Mukhopadhyay S (2007) Anandamide-mediated CB1/CB2 cannabinoid receptor--independent nitric oxide production in rabbit aortic endothelial cells. *The Journal of pharmacology and experimental therapeutics* **321**:930-937.
- McFarland MJ, Porter AC, Rakhshan FR, Rawat DS, Gibbs RA and Barker EL (2004) A Role for Caveolae/Lipid Rafts in the Uptake and Recycling of the Endogenous Cannabinoid Anandamide. *Journal of Biological Chemistry* **279**:41991-41997.
- McGee MA and Abdel-Rahman AA (2012) Enhanced Vascular Neuronal Nitric-Oxide Synthase-Derived Nitric-Oxide Production Underlies the Pressor Response Caused by Peripheral

- N-Methyl-d-Aspartate Receptor Activation in Conscious Rats. *Journal of Pharmacology and Experimental Therapeutics* **342**:461-471.
- McHugh D (2012) GPR18 in microglia: implications for the CNS and endocannabinoid system signalling. *British journal of pharmacology* **167**:1575-1582.
- McHugh D, Hu SS, Rimmerman N, Juknat A, Vogel Z, Walker JM and Bradshaw HB (2010) N-arachidonoyl glycine, an abundant endogenous lipid, potently drives directed cellular migration through GPR18, the putative abnormal cannabidiol receptor. *BMC neuroscience* **11**:44.
- McHugh D, Page J, Dunn E and Bradshaw HB (2011) Delta(9) -THC and N-arachidonoyl glycine are full agonists at GPR18 and cause migration in the human endometrial cell line, HEC-1B. *British journal of pharmacology*.
- McHugh D, Wager-Miller J, Page J and Bradshaw H (2012) siRNA knockdown of GPR18 receptors in BV-2 microglia attenuates N-arachidonoyl glycine-induced cell migration. *Journal of Molecular Signaling* **7**:10.
- Misko TP, Schilling RJ, Salvemini D, Moore WM and Currie MG (1993) A Fluorometric Assay for the Measurement of Nitrite in Biological Samples. *Analytical Biochemistry* **214**:11-16.

- Mo FM, Offertáler L and Kunos G (2004) Atypical cannabinoid stimulates endothelial cell migration via a Gi/Go-coupled receptor distinct from CB1, CB2 or EDG-1. *European Journal of Pharmacology* **489**:21-27.
- Moffett S, Brown DA and Linder ME (2000) Lipid-dependent Targeting of G Proteins into Rafts. *Journal of Biological Chemistry* **275**:2191-2198.
- Mukhopadhyay S, Chapnick BM and Howlett AC (2002) Anandamide-induced vasorelaxation in rabbit aortic rings has two components: G protein dependent and independent. *American journal of physiology Heart and circulatory physiology* **282**:H2046-2054.
- Nanayakkara G, Kariharan T, Wang L, Zhong J and Amin R (2012) The cardio-protective signaling and mechanisms of adiponectin. *American journal of cardiovascular disease* **2**:253-266.
- Nassar N and Abdel-Rahman AA (2008) Brainstem phosphorylated extracellular signal-regulated kinase 1/2-nitric-oxide synthase signaling mediates the adenosine A2A-dependent hypotensive action of clonidine in conscious aortic barodenervated rats. *The Journal of pharmacology and experimental therapeutics* **324**:79-85.
- Nassar NN, Li G, Strat AL and Abdel-Rahman AA (2011) Enhanced hemeoxygenase activity in the rostral ventrolateral medulla mediates exaggerated hemin-evoked hypotension in the spontaneously hypertensive rat. *The Journal of pharmacology and experimental therapeutics* **339**:267-274.

- Nattie EE and Li AH (1990) Fluorescence location of RVLM kainate microinjections that alter the control of breathing. *J Appl Physiol* **68**:1157-1166.
- Offertáler L, Mo F-M, Bátakai S, Liu J, Begg M, Razdan RK, Martin BR, Bukoski RD and Kunos G (2003) Selective Ligands and Cellular Effectors of a G Protein-Coupled Endothelial Cannabinoid Receptor. *Molecular Pharmacology* **63**:699-705.
- Okouchi M, Okayama N and Aw TY (2005) Differential susceptibility of naive and differentiated PC-12 cells to methylglyoxal-induced apoptosis: influence of cellular redox. *Current neurovascular research* **2**:13-22.
- Okuno T and Yokomizo T (2011) What is the natural ligand of GPR55? *Journal of Biochemistry* **149**:495-497.
- Padley JR, Li Q, Pilowsky PM and Goodchild AK (2003) Cannabinoid receptor activation in the rostral ventrolateral medulla oblongata evokes cardiorespiratory effects in anaesthetised rats. *British journal of pharmacology* **140**:384-394.
- Paxinos G and Watson C (2005) *The rat brain in stereotaxic coordinates*. Elsevier Academic Press, Amsterdam ; Boston.
- Penumarti A and Abdel-Rahman AA (2013) Abstract 17612: Central GPR18 Mediates Hypotension via Enhanced PI3K/AKT-ERK1/2-nNOS Signaling and Inhibition of cAMP in the Rostral Ventrolateral Medulla of Conscious Normotensive Rats. *Circulation* **128**:A17612.

- Penumarti A and Abdel-Rahman AA (2014) The Novel Endocannabinoid Receptor GPR18 is Expressed in the Rostral Ventrolateral Medulla and Exerts Tonic Restraining Influence on Blood Pressure. *Journal of Pharmacology and Experimental Therapeutics* **349**:29-38.
- Pike LJ (2003) Lipid rafts: bringing order to chaos. *Journal of Lipid Research* **44**:655-667.
- Pilowsky P, Minson J, Hodgson A, Howe P and Chalmers J (1986) Does substance P coexist with adrenaline in neurones of the rostral ventrolateral medulla in the rat? *Neuroscience Letters* **71**:293-298.
- Pilowsky PM and Goodchild AK (2002) Baroreceptor reflex pathways and neurotransmitters: 10 years on. *Journal of Hypertension* **20**:1675-1688.
- Potts PD, Allen AM, Horiuchi J and Dampney RA (2000) Does angiotensin II have a significant tonic action on cardiovascular neurons in the rostral and caudal VLM? *American Journal of Physiology - Regulatory Integrative & Comparative Physiology* **279**:R1392-1402.
- Pratt PF, Hillard CJ, Edgmond WS and Campbell WB (1998) N-arachidonylethanolamide relaxation of bovine coronary artery is not mediated by CB1 cannabinoid receptor. *American Journal of Physiology - Heart and Circulatory Physiology* **274**:H375-H381.
- Qin Y, Verdegaal EM, Siderius M, Bebelman JP, Smit MJ, Leurs R, Willemze R, Tensen CP and Osanto S (2011) Quantitative expression profiling of G-protein-coupled receptors (GPCRs) in metastatic melanoma: the constitutively active orphan GPCR GPR18 as novel drug target. *Pigment cell & melanoma research* **24**:207-218.

- Ramakrishnan V, Kimlinger T, Haug J, Painuly U, Wellik L, Halling T, Rajkumar SV and Kumar S (2012) Anti-myeloma activity of Akt inhibition is linked to the activation status of PI3K/Akt and MEK/ERK pathway. *PloS one* **7**:e50005.
- Randall MD, Harris D, Kendall DA and Ralevic V (2002) Cardiovascular effects of cannabinoids. *Pharmacology & therapeutics* **95**:191-202.
- Randall MD, Kendall DA and O'Sullivan S (2004) The complexities of the cardiovascular actions of cannabinoids. *British journal of pharmacology* **142**:20-26.
- Ribeiro de Campos R and Bergamaschi CT (2006) Neurotransmission Alterations in Central Cardiovascular Control in Experimental Hypertension. *Current Hypertension Reviews* **2**:193-198.
- Rimmerman N, Bradshaw HB, Hughes HV, Chen JS-C, Hu SS-J, McHugh D, Vefring E, Jahnsen JA, Thompson EL, Masuda K, Cravatt BF, Burstein S, Vasko MR, Prieto AL, O'Dell DK and Walker JM (2008a) N-Palmitoyl Glycine, a Novel Endogenous Lipid That Acts As a Modulator of Calcium Influx and Nitric Oxide Production in Sensory Neurons. *Molecular Pharmacology* **74**:213-224.
- Rimmerman N, Hughes HV, Bradshaw HB, Pazos MX, Mackie K, Prieto AL and Walker JM (2008b) Compartmentalization of endocannabinoids into lipid rafts in a dorsal root ganglion cell line. *British journal of pharmacology* **153**:380-389.

- Sarker KP and Maruyama I (2003) Anandamide induces cell death independently of cannabinoid receptors or vanilloid receptor 1: possible involvement of lipid rafts. *Cellular and molecular life sciences : CMLS* **60**:1200-1208.
- Sarnataro D, Grimaldi C, Pisanti S, Gazzero P, Laezza C, Zurzolo C and Bifulco M (2005) Plasma membrane and lysosomal localization of CB1 cannabinoid receptor are dependent on lipid rafts and regulated by anandamide in human breast cancer cells. *FEBS Lett* **579**:6343-6349.
- Seyedabadi M, Goodchild AK and Pilowsky PM (2001) Differential Role of Kinases in Brain Stem of Hypertensive and Normotensive Rats. *Hypertension* **38**:1087-1092.
- Song W, Huo T, Guo F, Wang H, Wei H, Yang Q, Dong H, Wang Q and Xiong L (2013) Globular adiponectin elicits neuroprotection by inhibiting NADPH oxidase-mediated oxidative damage in ischemic stroke. *Neuroscience* **248C**:136-144.
- Stein EA, Fuller SA, Edgmond WS and Campbell WB (1996) Physiological and behavioural effects of the endogenous cannabinoid, arachidonylethanolamide (anandamide), in the rat. *British journal of pharmacology* **119**:107-114.
- Sved A, Ito S and Sved J (2003) Brainstem mechanisms of hypertension: Role of the rostral ventrolateral medulla. *Current Hypertension Reports* **5**:262-268.

- Usami N, Yamamoto I and Watanabe K (2008) Generation of reactive oxygen species during mouse hepatic microsomal metabolism of cannabidiol and cannabidiol hydroxy-quinone. *Life Sciences* **83**:717-724.
- Van Sickle MD, Duncan M, Kingsley PJ, Mouihate A, Urbani P, Mackie K, Stella N, Makriyannis A, Piomelli D, Davison JS, Marnett LJ, Di Marzo V, Pittman QJ, Patel KD and Sharkey KA (2005) Identification and functional characterization of brainstem cannabinoid CB2 receptors. *Science* **310**:329-332.
- Varga K, Lake K, Martin BR and Kunos G (1995) Novel antagonist implicates the CB1 cannabinoid receptor in the hypotensive action of anandamide. *Eur J Pharmacol* **278**:279-283.
- Vassilatis DK, Hohmann JG, Zeng H, Li F, Ranchalis JE, Mortrud MT, Brown A, Rodriguez SS, Weller JR, Wright AC, Bergmann JE and Gaitanaris GA (2003) The G protein-coupled receptor repertoires of human and mouse. *Proceedings of the National Academy of Sciences of the United States of America* **100**:4903-4908.
- Vuong L, Mitchell V and Vaughan C (2008) Actions of N-arachidonyl-glycine in a rat neuropathic pain model. *Neuropharmacology* **54**:189 - 193.
- Wang X and Abdel-Rahman AA (2005) Effect of chronic ethanol administration on hepatic eNOS activity and its association with caveolin-1 and calmodulin in female rats. *Am J Physiol Gastrointest Liver Physiol* **289**:G579-585.

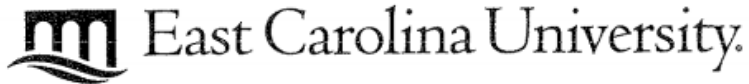
- Wilson BS, Steinberg SL, Liederman K, Pfeiffer JR, Surviladze Z, Zhang J, Samelson LE, Yang L-h, Kotula PG and Oliver JM (2004) Markers for Detergent-resistant Lipid Rafts Occupy Distinct and Dynamic Domains in Native Membranes. *Molecular Biology of the Cell* **15**:2580-2592.
- Worlein JM, Baker K, Bloomsmith M, Coleman K and Koban TL (2011) The Eighth Edition of the Guide for the Care and Use of Laboratory Animals (2011); Implications for Behavioral Management. *Am J Primatol* **73**:98-98.
- Wu DF, Yang LQ, Goschke A, Stumm R, Brandenburg LO, Liang YJ, Hollt V and Koch T (2008) Role of receptor internalization in the agonist-induced desensitization of cannabinoid type 1 receptors. *J Neurochem* **104**:1132-1143.
- Yoshitaka H (2008) Role of reactive oxygen species in brainstem in neural mechanisms of hypertension. *Autonomic Neuroscience* **142**:20-24.
- Zanzinger J and Czachurski J (2000) Chronic oxidative stress in the RVLM modulates sympathetic control of circulation in pigs. *Pflugers Archiv : European journal of physiology* **439**:489-494.
- Zhang J and Abdel-Rahman AA (2002) The Hypotensive Action of Rilmenidine is Dependent on Functional N-Methyl-d-aspartate Receptor in the Rostral Ventrolateral Medulla of Conscious Spontaneously Hypertensive Rats. *Journal of Pharmacology and Experimental Therapeutics* **303**:204-210.

Zhang J and Abdel-Rahman AA (2005) Mitogen-activated protein kinase phosphorylation in the rostral ventrolateral medulla plays a key role in imidazoline (i1)-receptor-mediated hypotension. *The Journal of pharmacology and experimental therapeutics* **314**:945-952.

Zhang J, El-Mas MM and Abdel-Rahman AA (2001) Imidazoline I1 receptor-induced activation of phosphatidylcholine-specific phospholipase C elicits mitogen-activated protein kinase phosphorylation in PC12 cells. *European Journal of Pharmacology* **415**:117-125.

APPENDIX A

ANIMAL CARE AND USE COMMITTEE APPROVAL LETTER



Animal Care and
Use Committee
212 Ed Warren Life
Sciences Building
East Carolina University
Greenville, NC 27834
252-744-2436 office
252-744-2355 fax

November 17, 2010

Abdel Abdel-Rahman, Ph.D.
Department of Pharmacology
Brody 6S-10
ECU Brody School of Medicine

Dear Dr. Abdel-Rahman:

The Amendment to your Animal Use Protocol entitled, "Mechanisms of the Cardiovascular Effects of Alcohol", (AUP #W222) was reviewed by this institution's Animal Care and Use Committee on 11/17/10. The following action was taken by the Committee:

"Approved as amended"

****Please contact Dale Aycock prior to any hazard use**

A copy of the Amendment is enclosed for your laboratory files. Please be reminded that all animal procedures must be conducted as described in the approved Animal Use Protocol. Modifications of these procedures cannot be performed without prior approval of the ACUC. The Animal Welfare Act and Public Health Service Guidelines require the ACUC to suspend activities not in accordance with approved procedures and report such activities to the responsible University Official (Vice Chancellor for Health Sciences or Vice Chancellor for Academic Affairs) and appropriate federal Agencies.

Sincerely yours,

A handwritten signature in black ink that reads 'Robert G. Carroll, Ph.D.'.

Robert G. Carroll, Ph.D.
Chairman, Animal Care and Use Committee

RGC/jd

enclosure